The anti-squat equation (e/d = h/L) defines a locus of points extending from the tire contact point on the ground to the height of the CG over the front axle. Locating the trailing arm pivot at any point on this line will provide 100% anti-squat.

Satisfying the equation with inclusion of the second term implies that the rear suspension will lift to compensate for rebound of the front suspension, thereby keeping the vehicle level. The complete equation may be interpreted as the full anti-pitch relationship. Because the ratio of suspension stiffnesses is nominally 1, the anti-pitch condition is approximately:

$$\frac{e}{d} \approx \frac{h}{L} + \frac{h}{L} = 2\frac{h}{L} \qquad \text{(Full anti-pitch)} \qquad (7\text{-}16)$$

The locus of points for anti-pitch extends from the tire contact point on the ground to the height of the CG at the mid-wheelbase position. Anti-pitch is achieved when the trailing arm pivot point is located on the line from the center of tire contact on the ground to the CG of the vehicle.

Normally some degree of squat and pitch is expected during vehicle acceleration, so full compensation is unusual. Anti-squat performance cannot be designed without considering other performance modes of the vehicle as well. When the trailing arm is short, the rear axle may experience "power hop" during acceleration near the traction limit. The goals for anti-squat may conflict with those for braking or handling. In this latter case, placing the pivot center above the wheel center can produce roll oversteer.

Independent Rear Drive

In the case of an independent rear-drive configuration, the free-body diagram and the analysis is changed slightly from that above. The difference arises from the fact that there is a drive torque reaction acting on the free-body system with a magnitude $T_d = r\,F_x$ (where r is the wheel radius). The differential is mounted on the vehicle body imposing a drive torque on the system of Figure 7.12 through the halfshafts. This alters Eq. (7-10) to the form:

$$\Sigma M_A = W_{rs}\,d + \frac{W}{g}\frac{h}{L}a_x\,d - W_{rs}\,d - \Delta W_r\,d - F_x\,(e - r) = 0 \qquad (7\text{-}17)$$

Carrying this through the analysis alters Eq. (7-14) to the form:

$$\theta_p = \frac{1}{L}\frac{W}{g}a_x\left(\frac{1}{K_r}\frac{h}{L} - \frac{1}{K_r}\frac{e-r}{d} + \frac{1}{K_f}\frac{h}{L}\right) \qquad (7\text{-}18)$$

and it is concluded that full squat compensation is achieved when:

$$\frac{e-r}{d} = \frac{h}{L} + \frac{h}{L}\frac{K_r}{K_f} \qquad (7\text{-}19)$$

Similarly, 100% anti-squat in the rear suspension corresponds to (e-r)/d = h/L.

Front Solid Drive Axle

With a front-drive axle, performing this type of analysis only results in a change of sign on some of the terms. The comparable equations that are obtained are:

$$\theta_p = \frac{1}{L}\frac{W}{g}a_x\left(\frac{1}{K_r}\frac{h}{L} + \frac{1}{K_f}\frac{h}{L} + \frac{1}{K_f}\frac{e}{d}\right) \qquad (7\text{-}20)$$

and

$$\frac{e}{d} = -\frac{h}{L} - \frac{h}{L}\frac{K_f}{K_r} \qquad (7\text{-}21)$$

The first term on the right side of Eq. (7-21) now corresponds to an anti-lift on the front axle, rather than an anti-squat on the rear axle. The negative signs on the right-hand side of the equation imply that the pivot must be behind the axle, corresponding to an effective leading arm arrangement to obtain anti-lift behavior.

Independent Front-Drive Axle

The comparable equations for an independent front-drive axle, as is common on most front-drive cars today, are:

$$\theta_p = \frac{1}{L}\frac{W}{g}a_x\left(\frac{1}{K_r}\frac{h}{L} + \frac{1}{K_f}\frac{h}{L} + \frac{1}{K_f}\frac{e-r}{d}\right) \qquad (7\text{-}22)$$

and

$$\frac{e-r}{d} = -\frac{h}{L} - \frac{h}{L}\frac{K_f}{K_r} \qquad (7\text{-}23)$$

Four-Wheel Drive

The four-wheel-drive case will be considered assuming independent suspensions on both axles. The performance will depend on how the tractive force is distributed between the front and rear axles. Let ξ represent the fraction of the total drive force developed on the front axle. Then:

$$F_{xf} = \xi F_x \quad \text{and} \quad F_{xr} = (1 - \xi) F_x \tag{7-24}$$

The expressions for the change in load on each axle are:

$$\Delta W_r = \frac{W}{g}\frac{h}{L} a_x - (1 - \xi) F_x \frac{e_r - r}{d_r} = K_r \delta_r \tag{7-25}$$

$$\Delta W_f = \frac{W}{g}\frac{h}{L} a_x + \xi F_x \frac{e_f - r}{d_f} = K_f \delta_f \tag{7-26}$$

Then the pitch equation becomes:

$$\theta_p = \frac{1}{L}\frac{W}{g} a_x \left(\frac{1}{K_r}\frac{h}{L} - \frac{(1 - \xi)}{K_r}\frac{e_r - r}{d_r} + \frac{1}{K_f}\frac{h}{L} + \frac{\xi}{K_f}\frac{e_f - r}{d_f} \right) \tag{7-27}$$

This equation indicates that zero pitch will be obtained when the terms in parentheses sum to zero. The terms included here indicate that the anti-squat and anti-pitch performance depends on a combination of vehicle properties—suspension geometry, suspension stiffness and tractive force distribution.

In the event one or both of the axles is a solid axle, the pitch expression can be obtained from the above equation by setting "r" equal to zero in the term of the equation applicable to that axle.

ANTI-DIVE SUSPENSION GEOMETRY

The longitudinal load transfer incidental to braking acts to pitch the vehicle forward producing "brake dive." Just as a suspension can be designed to resist acceleration squat, the same principles apply to generation of anti-dive forces during braking. Because virtually all brakes are mounted on the suspended wheel (the only exception is in-board brakes on independent suspensions), the brake torque acts on the suspension and by proper design can create forces which resist dive.

Using an analysis similar to that developed for the four-wheel-drive anti-squat example given previously, it can be shown that the anti-dive is accomplished when the following relationships hold:

Front suspension:

$$\frac{e_f}{d_f} = \tan \beta_f = -\frac{h}{\xi L} \tag{7-28}$$

Rear suspension:

$$\frac{e_r}{d_r} = \tan \beta_r = \frac{h}{(1 - \xi) L} \tag{7-29}$$

where:

ξ = Fraction of the brake force developed on the front axle

Therefore, to obtain 100% anti-dive on the front and 100% anti-lift on the rear, the pivot for the effective trailing arm must fall on the locus of points defined by these ratios. Figure 7.13 illustrates these conditions. If the pivots are located below the locus, less than 100% anti-dive will be obtained; if above the locus the front will lift and the rear will squat during braking.

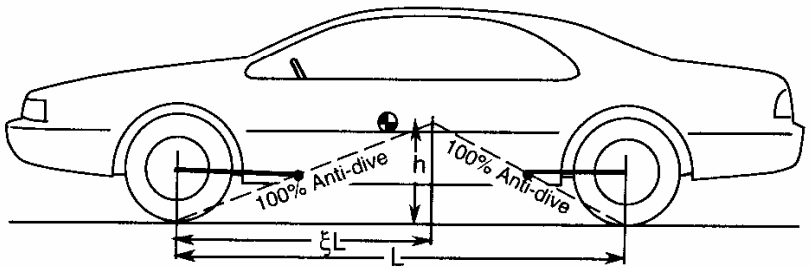

Fig. 7.13 Illustration of the conditions for anti-dive.

In practice, 100% anti-dive is rarely used. The maximum anti-dive seldom exceeds 50%. A number of reasons for this have been cited:

1) Full anti-dive requires that the pivot be located above the point required for full anti-squat. Thus acceleration lift would be produced on solid drive axles.
2) Flat stops are subjectively undesirable.
3) With full anti-dive, front suspension caster angle changes may increase the steering effort substantially during braking.

4) The required steering system geometry may be quite complex.

5) Excessive variation in rotational speed can occur in the drivetrain as the wheels move in jounce and rebound causing rattling and noise in the drive gears.

6) In the rear suspension, oversteer problems may be created by the high location of the pivot.

7) Brake hop may be induced if the effective trailing arm is too short. The propensity for brake hop is reduced by a suspension design with a long effective arm.

8) NVH performance may be compromised.

EXAMPLE PROBLEMS

1) Find the geometry that would be necessary to achieve 100% anti-squat in the rear suspension, and the geometry to achieve full anti-pitch for the solid-axle, rear-wheel-drive vehicle described below. Also, find the pitch rate (degrees pitch/g acceleration) when the geometry is set for 100% anti-squat in the rear suspension.

The front and rear suspension spring rates are 285 and 169 lb/in, respectively (rates are combination of left and right sides). The CG height is 20.5 inches and wheelbase is 108.5.

Solution:

Since the vehicle has a rear-drive solid axle, Eq. (7-15) applies.

$$\frac{e}{d} = \frac{h}{L} + \frac{h}{L}\frac{K_r}{K_f} \qquad (7\text{-}15)$$

$$\frac{e}{d} = \frac{20.5}{108.5} + \frac{20.5}{108.5}\frac{169}{285} = 0.189 + 0.112 = 0.301$$

If the suspension is to achieve 100% anti-squat, then e/d must equal 0.189. Full pitch compensation would be achieved with e/d = 0.301.

The acceleration pitch rate can be calculated using Eq. (7-18).

$$\theta_p = \frac{1}{L}\frac{W}{g} a_x \left(\frac{1}{K_r}\frac{h}{L} - \frac{1}{K_r}\frac{e}{d} + \frac{1}{K_f}\frac{h}{L} \right)$$

$$\frac{\theta_p}{a_x} = \frac{1}{108.5 \text{ in}} \frac{4074 \text{ lb}}{386 \text{ in/sec}^2} \left(\frac{1}{169 \text{ lb/in}} \frac{20.5}{108.5} - \frac{0.189}{169 \text{ lb/in}} + \frac{1}{285 \text{ lb/in}} \frac{20.5}{108.5} \right)$$

$$= 0.0000645 \text{ rad/(in/sec}^2) = 0.0249 \text{ rad/g} = 1.43 \text{ deg/g}$$

2) Determine the acceleration pitch rate for the following front-drive vehicle with no anti-lift in the front suspension, and its value if full anti-lift was designed into the suspension. Essential data are—CG height of 20.5", wheelbase of 108.5", design weight of 4549 lb, and front and rear spring rates of 287 and 174 lb/in, respectively.

Solution:

The pitch equation for a front-wheel drive comes from Eq. (7-22). With no anti-lift the third term on the right side is zero. Thus:

$$\frac{\theta_p}{a_x} = \frac{1}{L}\frac{W}{g} \left(\frac{1}{K_r}\frac{h}{L} + \frac{1}{K_f}\frac{h}{L} \right)$$

$$= \frac{1}{108.5"} \frac{4549 \text{ lb}}{386 \text{ in/sec}^2} \left(\frac{1}{174 \text{ lb/in}} \frac{20.5"}{108.5"} + \frac{1}{287 \text{ lb/in}} \frac{20.5"}{108.5"} \right)$$

$$= 0.0455 + 0.0276 \text{ rad/g} = 4.2 \text{ deg/g}$$

If anti-lift is designed into the suspension it would cancel the second term in this equation, in which case the acceleration pitch rate would be:

$$\frac{\theta_p}{a_x} = 0.0455 \text{ rad/g} = 2.61 \text{ deg/g}$$

ROLL CENTER ANALYSIS

One very important property of a suspension relates to the location at which lateral forces developed by the wheels are transmitted to the sprung mass. This point, which has been referred to as the roll center, affects the behavior of both the sprung and unsprung masses, and thus directly influences cornering.

Each suspension has a suspension roll center, defined as the point in the transverse vertical plane through the wheel centers at which lateral forces may be applied to the sprung mass without producing suspension roll [10]. It derives from the fact that all suspensions possess a roll axis, which is the instantaneous axis about which the unsprung mass rotates with respect to the sprung mass when a pure couple is applied to the unsprung mass. The roll center is the intersection of the suspension roll axis with the vertical plane through the centers of the two wheels. These definitions are illustrated in Figure 7.14. The roll center height is the distance from the ground to the roll center. Once the front and rear suspension roll centers are located, the vehicle roll axis is defined by the line connecting the centers. This axis is the instantaneous axis about which the total vehicle rolls with respect to the ground.

The reference to "instantaneous" axes in these definitions is used to alert the reader to the fact that the location of the axis is only accurate in the absence of roll. As body roll occurs the change in geometry of most suspensions will cause the "center" to migrate, and thus it is not a true center. Nevertheless, the concept is valid for purposes of establishing where the forces are reacted on the sprung mass, which is necessary for analyzing behavior in the lateral plane.

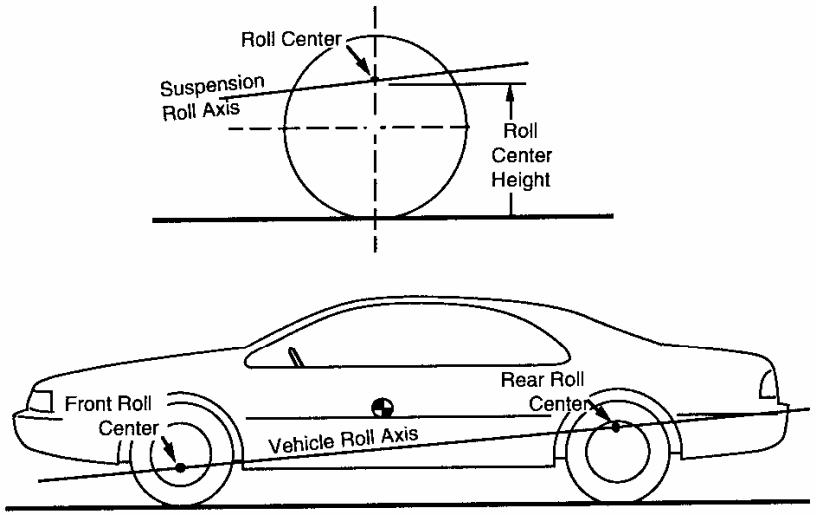

Fig. 7.14 Definitions of suspension roll center and roll axis.

Solid Axle Roll Centers

The suspension roll axis and roll center can be determined from the layouts of the suspension geometry in the plan and elevation views. For the analysis we draw again on the concept of a "virtual reaction point." (The virtual reaction point is analogous to the "instant center" used in kinematic analysis of linkages, but that term is not used here because of implication that it defines a center of motion, when in fact, it does not.) Physically, the virtual reaction point is the intersection of the axes of any pair of suspension control arms. Mechanistically, it is the point where the compression/tension forces in the control arms can be resolved into a single lateral force.

Four-Link Rear Suspension

Consider the case of a four-link suspension with a solid axle, as shown in Figure 7.15. The lateral force acting on the wheel in the top view must react as tension and compression forces in the control arms. The two long arms establish a virtual reaction point ahead of the axle at B, while the two short arms have a virtual reaction point behind the axle at A. In effect, each pair of arms acts like a triangular member pivoting at their respective virtual reaction points with these points establishing the suspension roll axis. Consequently, the lateral force will be distributed between the two points in inverse proportion to the length of the arms in order to achieve moment equilibrium on the axle (i.e., a large force at A and a small force at B).

The two forces at A and B must add up to F_y acting in the transverse vertical plane through the wheel centers. Given that points A and B are at different heights above the ground, their resultant at the axle centerline must be on the line connecting the two. This is the roll center for the axle.

A general procedure for finding roll centers then is as follows:

1) In a plan view of the suspension find the linkages that take the side forces acting on the suspension. Determine the reaction points A and B on the centerline of the vehicle for forces in the links. In the case of paired control arms, this is a virtual reaction point.

2) Locate the points A and B in the side elevation view, thereby identifying the suspension roll axis.

3) The roll center is the point in the side view where the roll axis crosses the vertical centerline of the wheels.

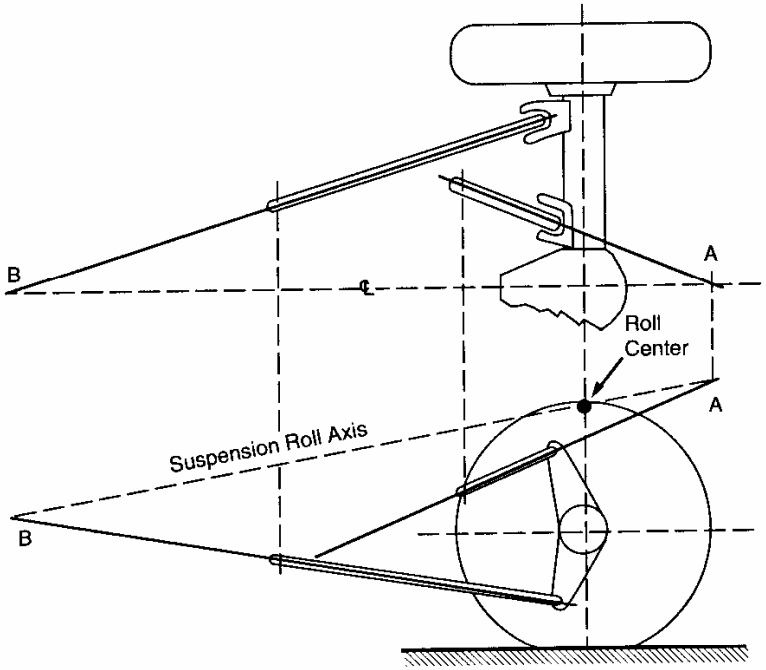

Fig. 7.15 Roll center analysis of a four-link rear suspension.

In the four-link geometry, the change in slope of the roll axis during cornering is often relatively large compared to other live axles. This means considerable change in roll steer and lateral load transfer, which are undesirable effects. Also, the roll center is located relatively high compared to other suspensions, putting excessive roll moment on the rear wheels. On the other hand, the high roll center helps to reduce the tramp and shake of the axle.

Three-Link Rear Suspension

Figure 7.16 shows a three-link suspension consisting of a track bar and two lower control arms. Because the track bar picks up lateral force directly, point A is established at the location where the track bar crosses the centerline of the vehicle. Point B is established as the virtual reaction point for the two lower control arms. Note that the upper link which reacts the axle windup torque does not react lateral forces and is therefore ignored in the analysis.

Due to the location of the track bar, this suspension usually has a roll center that is lower than the four-link geometry. Also, the slope of the roll axis remains relatively unchanged during rolling of the body and with load variations.

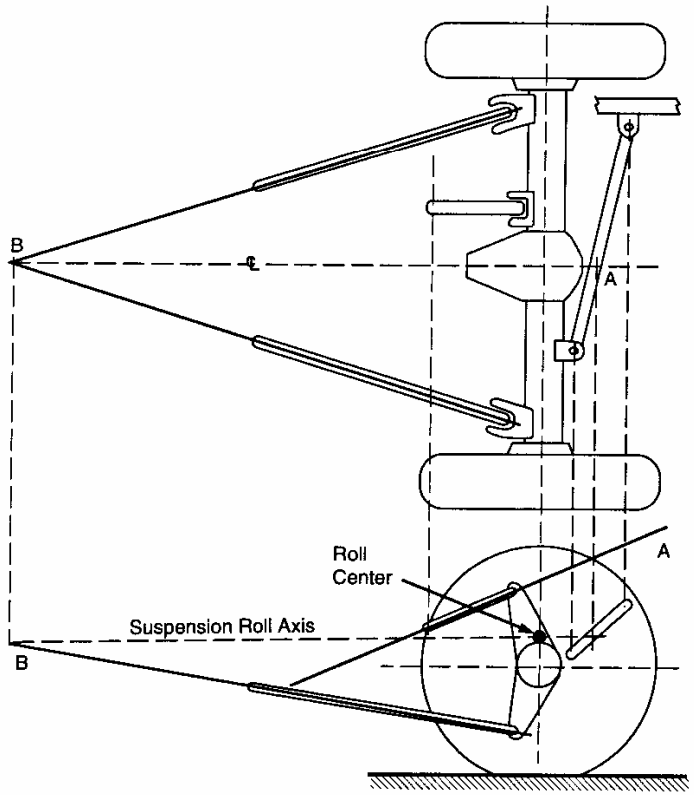

Fig. 7.16 Roll center analysis of a three-link rear suspension.

Four-Link with Parallel Arms

Figure 7.17 shows a four-link rear suspension with lower control arms that are parallel. This geometry is a special case of the four-link suspension discussed previously. In the top view, the virtual reaction point of the upper links is used to find point A in the usual manner. Because the lower arms are parallel, their virtual reaction point is at infinity. Although point B is not defined, we know that this point in the side view must lie on the extended lower

arm centerline somewhere at infinity. Therefore, the roll axis of this geometry (obtained by connecting points A and B in the side view) must be a line parallel to the lower links as indicated in the figure. The slope of the lower arm thus is very important in this type of suspension.

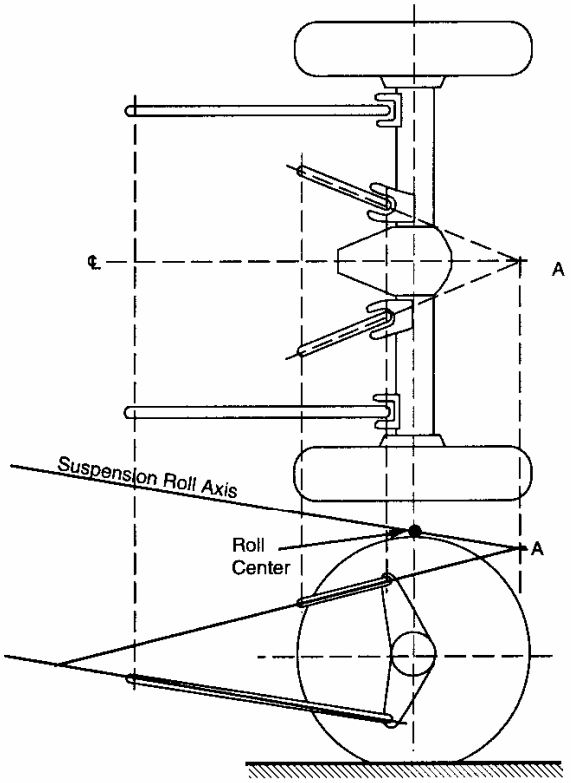

Fig. 7.17 Roll center analysis of a four-link, parallel lower arm rear suspension.

Hotchkiss Suspension

The design of this suspension is quite different from those discussed previously, but the general rules for determining the roll axis and center still apply. Referring to Figure 7.18, it is seen that the leaf springs are the members that react the side thrust. Because they are parallel to the centerline of the vehicle in the top view, the points A and B lie on the centerline of the car, both at infinity.

The lateral forces are applied to the body at the front spring eye and the rear shackle attachment point on the frame. The roll axis of the suspension is established by these points and the roll center is found on the line connecting the points. Although this analysis may seem less obvious than those discussed previously, it should be clear that a side force applied at this point will not roll the body, which is the essential definition of the roll center. Experimental measurements of leaf spring suspensions have generally confirmed the validity of this method in establishing the roll center.

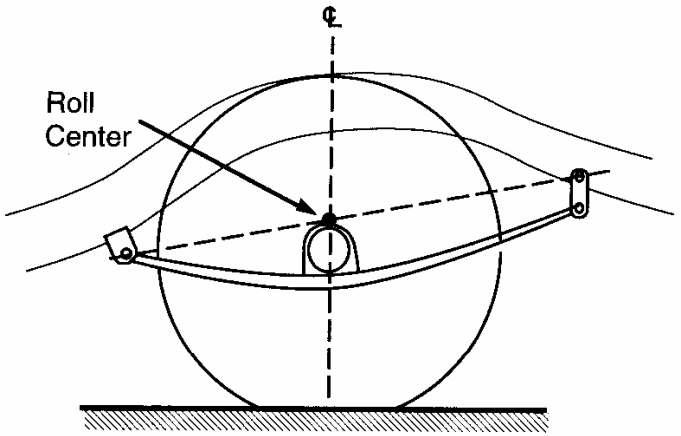

Fig. 7.18 Roll center analysis of a Hotchkiss rear suspension.

Independent Suspension Roll Centers

Determining the roll center of an independent suspension requires a slightly different application of the virtual reaction point concept. Consider the double A-arm suspension shown in Figure 7.19. The virtual reaction point for the A-arms holding the left wheel is located at point A on the right of the vehicle. Mechanistically, the linkage behaves as if the wheel were held by a rigid lateral swing arm pinned to the vehicle body at that point. Understanding the behavior is aided by imagining that the swing arm directly connects the tire contact patch (C) to the pivot point.

A lateral force in the contact patch of the left wheel reacts along the line from the contact patch to the pivot point as illustrated in the left diagram in the figure. Its elevation where it crosses the center plane of the vehicle establishes

the roll center, R. Note that a lateral force from the left-side wheel reacting along that line must have an upward (vertical) force component, thus explaining the source of "jacking" forces inherent to independent suspensions. If the right-hand wheel experiences a lateral force of equal magnitude in the same direction, its reaction will involve a downward force component cancelling the lifting effect from the left wheel. In general, both wheels do not generate equal lateral forces in cornering, so some lifting force is usually present on the suspension.

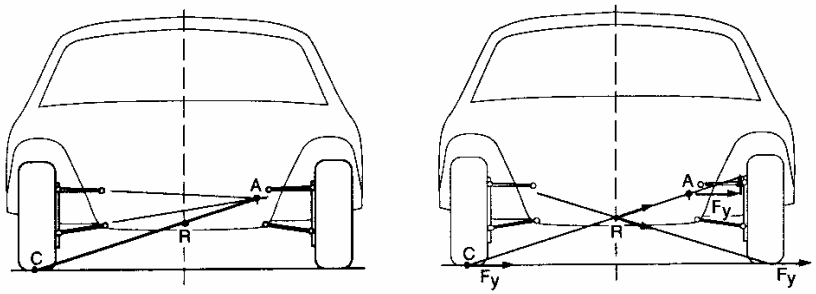

Fig. 7.19 Roll center analysis of an independent suspension.

The procedure for finding the roll center of a symmetric independent suspension is as follows:

1) Find the virtual reaction point of the suspension links (point A).
2) Draw a line from the tire-ground contact patch to the virtual reaction point.
3) The point where this line crosses the centerline of the body is the roll center (R).

Note that this procedure can be used for determining the roll center when the body is rolled; however, the suspensions are no longer symmetrical so both sets must be analyzed.

Positive Swing Arm Geometry

The virtual reaction point of the upper and lower links is first obtained as shown in Figure 7.20. A line is drawn from the tire contact patch to the reaction point. The roll center is established where the line crosses the centerline of the

vehicle. This suspension geometry is referred to as the "positive swing arm" because the roll center is located above the ground.

As the vehicle rolls in cornering, the virtual reaction point of the outside wheel moves downward due to jounce of the wheel, while that of the inside wheel moves upward as it goes into rebound. With the loss of symmetry the roll centers for the two wheels no longer coincide. The lateral force from the outside wheel (which usually dominates cornering forces) moves downward on the body, while weaker force from the inside wheel moves upward. As a consequence, the resultant lateral force reaction on the body moves downward, lowering the effective roll center height.

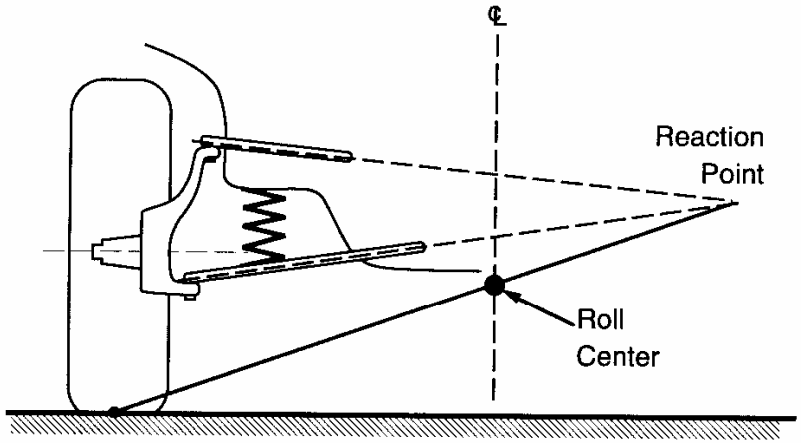

Fig. 7.20 Positive swing arm independent suspension.

Negative Swing Arm Geometry

Negative swing arm geometry is shown in Figure 7.21. The virtual reaction point of the links is first obtained and connected to the tire contact patch as shown. The line is then projected downward to the car centerline below the ground. The roll center is negative; hence, the name "negative swing arm" geometry.

Note that the two independent suspension geometries discussed so far have roll centers either above or below the ground. Consequently, the tread will change during jounce and rebound, and some lateral scrub of the tire contact patch occurs. This scrub introduces friction which (in the past) was considered beneficial for reducing bouncing of the body, but at the expense of tire wear.

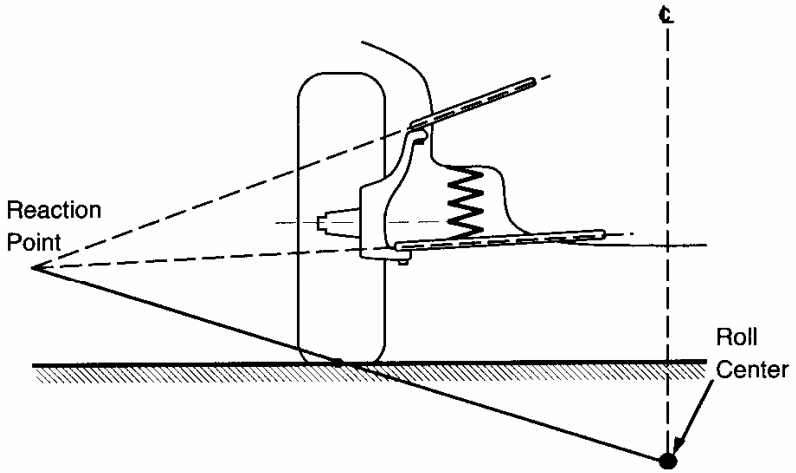

Fig. 7.21 Negative swing arm independent suspension.

Parallel Horizontal Links

A suspension with parallel links that are horizontal (at design load) is shown in Figure 7.22. The virtual reaction point of the two links is therefore at infinity. Drawing a line from the tire contact patch toward infinity places the roll center in the ground plane.

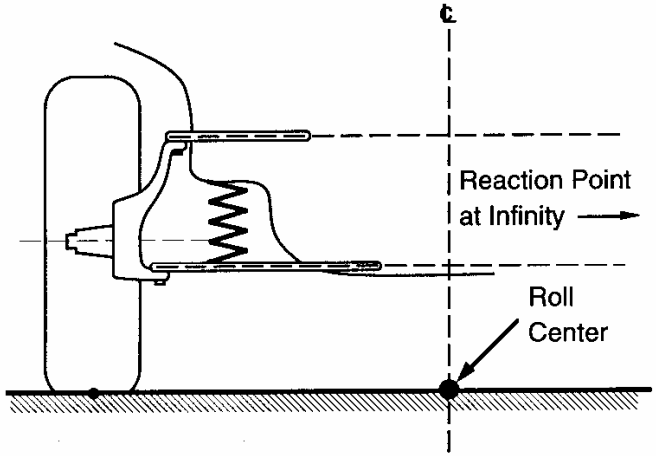

Fig. 7.22 Parallel horizontal link independent suspension.

Inclined Parallel Links

Another possibility is use of parallel links, which are not horizontal at design load as shown in Figure 7.23. The virtual reaction point is at infinity. The line from the tire contact patch to the roll center is inclined at the same angle as the control arms. The roll center is elevated above the ground at the car centerline as shown. In this geometry the roll center moves on the centerline of the car during rolling because the wheels camber with respect to the body. If the links of the suspension are equal there will be no camber change with respect to the body and the roll center will remain stationary.

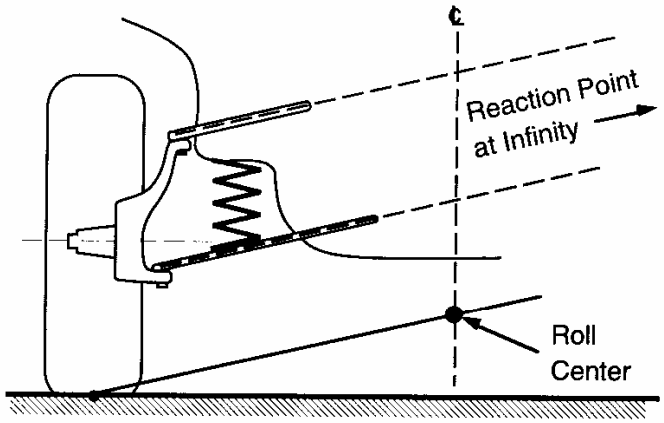

Fig. 7.23 Inclined parallel link independent suspension.

With all of the swing arm geometries the jounce of the outside wheel in cornering lowers the roll center location for that wheel and, consequently, the point at which the lateral force from the wheel is applied to the sprung mass. This reduces the load transfer onto the outside wheel and, with the consequent reduction of cornering force of the wheel, induces an understeer influence on the vehicle.

MacPherson Strut

The MacPherson strut is a combination of a strut with a lower control arm as shown in Figure 7.24. The virtual reaction point must lie at the intersection of the axis of the lower control arm and a line perpendicular to the strut. The

roll center is located on the centerline of the vehicle at the intersection with the line from the center of tire contact to the virtual reaction point.

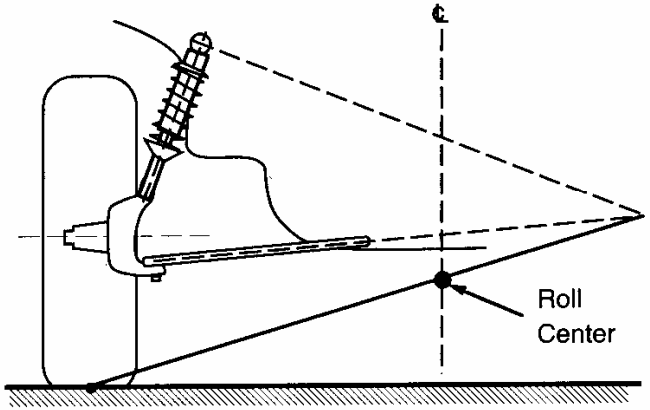

Fig. 7.24 MacPherson strut independent suspension.

Swing Axle

A rear suspension swing axle is generically equivalent to that shown in Figure 7.25. The location of the roll center is easily obtained for this configuration because the virtual reaction point is the actual pivot of the axle. The line from the tire contact passes through the pivot and the roll center is located above the wheel center on the vehicle centerline.

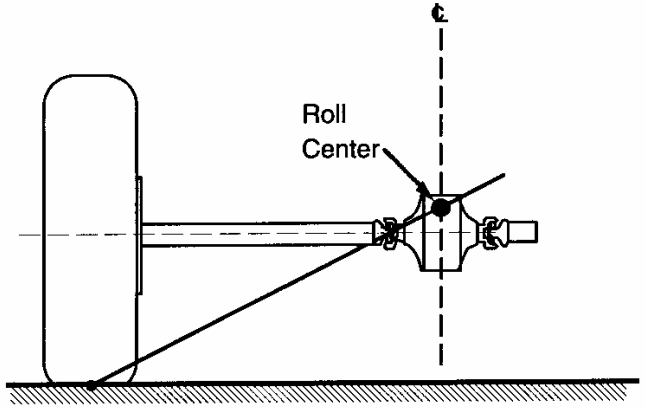

Fig. 7.25 Swing axle independent suspension.

ACTIVE SUSPENSIONS

In the interest of improving the overall performance of automotive vehicles in recent years, suspensions incorporating active components have been developed. The designs may cover a spectrum of performance capabilities [11], but the active components alter only the vertical force reactions of the suspensions, not the kinematics. (Active components that alter kinematic behavior do so to steer the wheels, and would be covered under steering systems.)

Suspension Categories

The various levels of "active" qualities in suspensions may be divided into the categories shown below, listed in order of increasing capabilities.

Passive suspensions consist of conventional components with spring and damping (shock absorber) properties which are time-invariant. Passive elements can only store energy for some portion of a suspension cycle (springs) or dissipate energy (shock absorbers). No external energy is directly supplied to this type of suspension.

Self-leveling suspensions are a variation of the passive suspension in which the primary lift component (usually air springs) can adjust for changes in load. Air suspensions, which are self-leveling, are used on many heavy trucks and on a few luxury passenger cars. A height control valve monitors the suspension deflection, and when its mean position has varied from normal ride height for a designated period of time (typically more than 5 seconds), the air pressure in the spring is adjusted to bring the deflection within the desired range. The most notable feature of an air suspension is that as the pressure changes with load, the spring stiffness changes correspondingly causing the natural frequency of the suspension to remain constant.

Semi-active suspensions contain spring and damping elements, the properties of which can be changed by an external control. A signal or external power is supplied to these systems for purposes of changing the properties. There are several sub-categories of semi-active systems:

- Slow-active—Suspension damping and/or spring rate can be switched between several discrete levels in response to changes in driving conditions. Brake pressure, steering angle or suspension motions are typically used to trigger control changes to higher levels of damping or stiffness. Switching occurs within a fraction of a second giving the system the capability to control pitch, bounce, and roll motions of the

sprung mass under more severe road or maneuvering conditions. However, the switch back to softer settings occurs after a time delay. Thus the system does not adjust continuously during individual cycles of vehicle oscillation. Slow-active systems may also be called "adaptive" suspensions.

- Low-bandwidth—Spring rate and/or damping are modulated continuously in response to the low-frequency sprung mass motions (1-3 Hz).
- High-bandwidth—Spring rate and/or damping are modulated continuously in response to both the low-frequency sprung mass motions (1-3 Hz) and the high-frequency axle motions (10-15 Hz).

Full-Active suspensions incorporate actuators to generate the desired forces in the suspension. The actuators are normally hydraulic cylinders. External power is required to operate the system. Full active systems may be classified as low-bandwidth or high-bandwidth according to the definitions given above.

Functions

The interest in active or semi-active suspensions derives from the potential for improvements to vehicle ride performance with no compromise (and perhaps enhancement) in handling. The modes of performance that can be improved by active control are:

Ride Control—Ride improvements can be obtained by several methods. The system may sense and control pitch and bounce motions of the vehicle body directly. Ride improvements are also obtained indirectly when active control is applied to the modes described below. Suspension properties that optimize ride always degrade performance in other modes, thus necessitating a compromise in design. With active suspensions, however, the control can be applied only during the maneuver, and ride performance need not be compromised during other modes of travel. Specifically, the suspension can be trimmed for optimal ride performance during steady, straight-ahead travel, and ride isolation properties superior to that obtained with purely passive elements can be achieved without compromise of handling behavior.

Height Control—Automatic control of vehicle height offers several advantages in performance. By adjusting to keep height constant despite changes in load or aerodynamic forces the suspension can always operate at the design ride height, providing maximum stroke for negotiating bumps, and eliminating changes in handling that would arise from operation at other than the design

ride height. A height control can lower the vehicle for reduced drag at high speeds or alter the pitch attitude to modify aerodynamic lift. Height can be elevated for increased ground clearance and suspension stroke on bad roads. Height elevation can also be convenient for changing tires and to provide clearance for tire chains.

Roll Control—Roll control in cornering is improved by increasing damping or exerting anti-roll forces in the suspension during cornering. Vehicle speed, steer angle, steer rate and/or lateral acceleration may be sensed to determine when roll control is appropriate. With the use of active force-generating components it is possible to eliminate roll in cornering entirely, and thereby eliminate any roll-induced understeer or oversteer effects from the suspensions. In addition, the roll moments may be selectively applied at either the front or rear axles to alter the understeer gradient by action of the change in cornering stiffness due to lateral load transfer.

Dive Control—Control of dive (forward pitch) during braking can be improved by increasing damping or exerting anti-pitch forces in the suspension during braking. Control may be activated by the brake light signal, brake pressure and/or longitudinal acceleration. Dive control in an active suspension relieves the need to design anti-dive geometry in the suspension linkages.

Squat Control—Control of squat (rearward pitch) during acceleration can be improved by increasing damping or exerting anti-pitch forces in the suspension during acceleration. Control may be activated by the throttle position, gear selection and/or longitudinal acceleration. Squat control in an active suspension relieves the need to design anti-squat geometry in the suspension linkages of drive wheels, and can overcome the squat or lift action on the non-driven wheels.

Road Holding—In addition to control of body motions during maneuvers in the modes described above, active suspensions have the potential to improve road holding by reducing the dynamic variations in wheel loads that are caused from road roughness. Generally, cornering performance is improved when dynamic load variations are minimized. The road damage caused by motor vehicles, particularly heavy trucks, is also reduced by minimizing dynamic wheel loads.

Performance

In general, the semi-active and full-active suspension systems have the greatest capability to achieve optimum performance in the modes described above, but at a penalty in weight, cost, complexity and reliability. Thus the

challenge to vehicle designers is to achieve the benefits of active control with a minimum of hardware. The table below characterizes the relative performance that can be obtained with each level of sophistication in the design.

Performance Potential of Various Types of Suspension Systems

	Performance Mode					
Suspension Type	Ride	Height	Roll	Dive	Squat	Road-holding
Passive	Performance is a compromise between all modes					
Self-leveling	High	High	NA	NA	NA	NA
Semi-active	Medium	NA	Low	Low	Low	Medium
Full-active	High	High	High	High	High	High

With semi-active systems, even slow-active variable damping allows improvement in roll, dive and squat control along with ride and road-holding. Variable stiffness can provide similar benefits, albeit at greater cost due to the need to use air springs or adjustable mechanical springs.

With low-bandwidth stiffness or damping control a more responsive system can be achieved. High-bandwidth control is effective for maintaining the constant wheel loads beneficial to handling, but there is little additional ride benefit from a high-bandwidth control system. Only with a full-active system can the broadest range of improvements be obtained in all performance modes.

The performance of a full-active system optimized for ride contrasts with that of a passive suspension by much better control of the vertical, pitch and roll motions at the sprung mass resonant frequencies [12]. Figure 7.26 compares the response behavior in these three modes for the two types of systems. Whereas the passive system shows sprung mass resonance near 1 Hz in the vertical, pitch and roll directions, a much reduced response occurs with the active system. In effect, the sprung mass motions in these directions (which are sensed by accelerometers) can be heavily damped by control forces developed in the active suspension system.

With control characteristics optimized for ride, there is no significant change in response at the unsprung mass resonant frequency near 10 Hz. This is rationalized by the fact that for the suspension to exert control forces which will reduce unsprung mass motions, those forces must be reacted against the

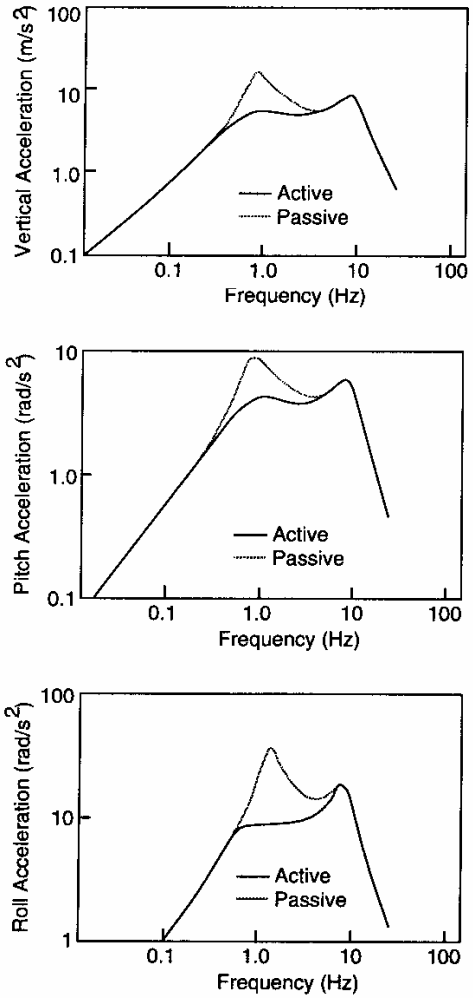

Fig. 7.26 Comparison of responses for active and passive suspension systems [12].

sprung mass, thus increasing the ride vibrations. Handling is affected by system response at the wheel hop frequency because of the associated load variations on the tires. Since the performance of the active and passive systems are identical in this region, little handling benefit is realized. To enhance handling, the control system design should be changed to reduce wheel hop response, although some penalty in ride must be expected.

REFERENCES

1. Bastow, D., Car Suspension and Handling, Second Edition, Pentech Press, London, 1990, 300 p.
2. Kami, Y., and Minikawa, M., "Double-Wishbone Suspension for Honda Prelude," SAE Paper No. 841186, 1984, 7 p.
3. Iijima, Y., and Noguchi, H., "The Development of a High-Performance Suspension for the New Nissan 300ZX," SAE Paper No. 841189, 1984, 9 p.
4. Sorsche, J.H., Encke, K., and Bauer, K., "Some Aspects of Suspension and Steering Design for Modern Compact Cars," SAE Paper No. 741039, 1974, 9 p.
5. Goodsell, D., Dictionary of Automotive Engineering, Butterworths, London, 1989, 182 p.
6. Leggat, J.W., "Steering and Handling of the Automobile," paper delivered before the Case Institute of Technology, October 21, 1953, 29 p.
7. Olley, M., "Independent Wheel Suspensions—Its Whys and Wherefores," *SAE Journal,* Vol. 34, No. 3, 1934, pp. 73-81.
8. Olley, M., "Road Manners of the Modern Car," Institution of Automobile Engineers, 1946, pp. 147-182.
9. Nader, R., Unsafe at any Speed: the Designed-in Dangers of the American Automobile, Grossman Publishers, New York, 1965, 365 p.
10. "Vehicle Dynamics Terminology," SAE J670e, Society of Automotive Engineers, Warrendale, PA (see Appendix A).
11. Sharp, R.S., and Crolla, D.A., "Road Vehicle Suspension System Design - A Review," *Vehicle Systems Dynamics,* Vol. 16, No. 3, 1987, pp. 167-192.
12. Chalasani, R.M.,"Ride Performance Potential of Active Suspension Systems — Part II: Comprehensive Analysis Based on a Full-Car Model," Proceedings, Symposium on Simulation and Control of Ground Vehicles and Transportation Systems, AMD-Vol. 80, DSC-Vol 2, American Society of Mechanical Engineers, pp. 205-226.

CHAPTER 8
THE STEERING SYSTEM

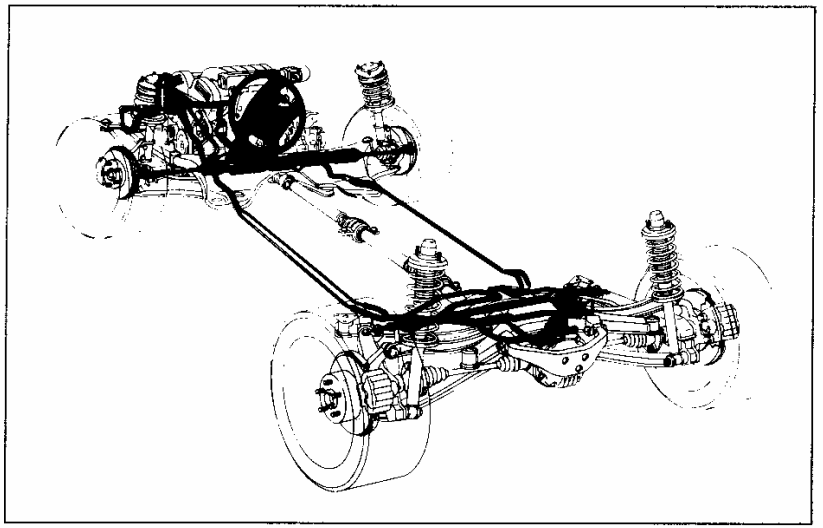

Stealth four-wheel steering system. (Courtesy of Chrysler Corp.)

INTRODUCTION

The design of the steering system has an influence on the directional response behavior of a motor vehicle that is often not fully appreciated. The function of the steering system is to steer the front wheels in response to driver command inputs in order to provide overall directional control of the vehicle. However, the actual steer angles achieved are modified by the geometry of the suspension system, the geometry and reactions within the steering system, and in the case of front-wheel drive (FWD), the geometry and reactions from the drivetrain. These phenomena will be examined in this section first as a general analysis of a steering system and then by considering the influences of front-wheel drive.

THE STEERING LINKAGES

The steering systems used on motor vehicles vary widely in design [1, 2, 3] , but are functionally quite similar. Figure 8.1 illustrates some of these.

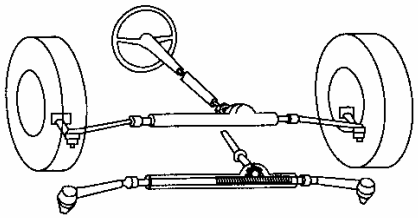

Rack-and-pinion linkage

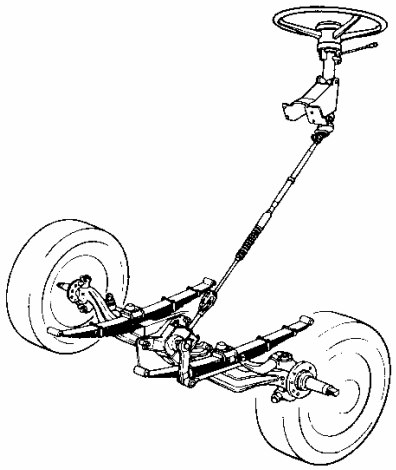

Truck steering system

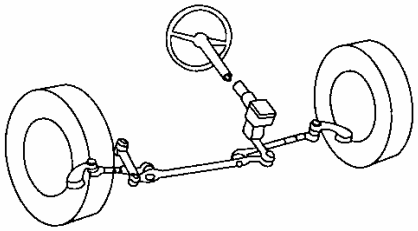

Steering gearbox

Fig. 8.1 Illustration of typical steering systems.

The steering wheel connects by shafts, universal joints, and vibration isolators to the steering gearbox whose purpose is to transform the rotary motion of the steering wheel to a translational motion appropriate for steering the wheels. The rack-and-pinion system consists of a linearly moving rack and pinion, mounted on the firewall or a forward crossmember, which steers the left and right wheels directly by a tie-rod connection. The tie-rod linkage connects to steering arms on the wheels, thereby controlling the steer angle. With the tie rod located ahead of the wheel center, as shown in Figure 8.1, it is a forward-steer configuration.

The steering gearbox is an alternative design used on passenger cars and light trucks. It differs from the rack-and-pinion in that a frame-mounted steering gearbox rotates a pitman arm which controls the steer angle of the left and right wheels through a series of relay linkages and tie rods, the specific

configuration of which varies from vehicle to vehicle. A rear-steer configuration is shown in the figure, identified by the fact that the tie-rod linkage connects to the steering arm behind the wheel center.

Between these two, the rack-and-pinion system has been growing in popularity for passenger cars because of the obvious advantages of reduced complexity, easier accommodation of front-wheel-drive systems, and adaptability to vehicles without frames. The primary functional difference in the steering systems used on heavy trucks is the fact that the frame-mounted steering gearbox steers the left road wheel through a longitudinal drag line, and the right wheel is steered from the left wheel via a tie-rod linkage [1].

The gearbox is the primary means for numerical reduction between the rotational input from the steering wheel and the rotational output about the steer axis. The steering wheel to road wheel angle ratios normally vary with angle, but have nominal values on the order of 15 to 1 in passenger cars, and up to as much as 36 to 1 with some heavy trucks. Initially all rack-and-pinion gearboxes had a fixed gear ratio, in which case any variation in ratio with steer angle was achieved through the geometry of the linkages. Today, rack-and-pinion systems are available that vary their gear ratio directly with steer angle.

The lateral translation produced by the gearbox is relayed through linkages to steering arms on the left and right wheels. The kinematic geometry of the relay linkages and steering arms is usually not a parallelogram (which would produce equal left and right steer angles), but rather a trapezoid to more closely approximate "Ackerman" geometry which steers the inside wheel to a greater angle than the outside wheel. Ackerman geometry is illustrated in Figure 8.2. From analysis of the triangles it can be readily shown that correct Ackerman geometry requires that:

$$\delta_o = \tan^{-1}\frac{L}{(R + t/2)} \cong \frac{L}{(R + t/2)} \tag{8-1}$$

$$\delta_i = \tan^{-1}\frac{L}{(R - t/2)} \cong \frac{L}{(R - t/2)} \tag{8-2}$$

For small angles, as are typical of most turning, the arctangent of the angle is very nearly equal to the angle itself (in radians), justifying the approximations shown on the right side of the equations.

Perfect Ackerman is difficult to achieve with practical linkage designs, but is closely approximated by a trapezoidal arrangement as shown in Figure 8.3. When the wheels steer right or left, the asymmetry in the geometry causes the

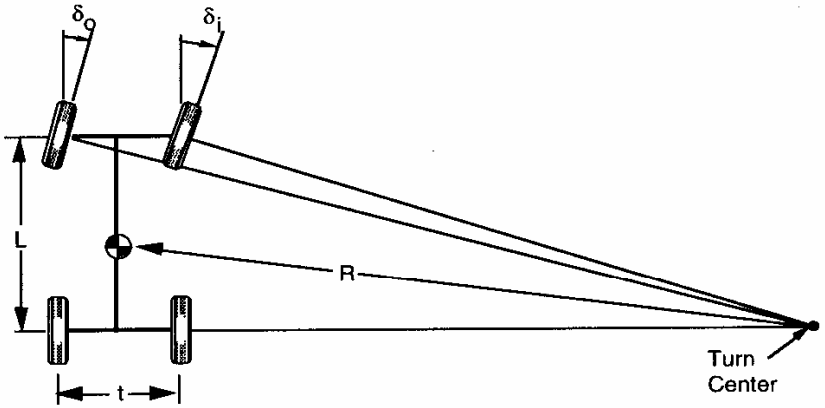

Fig. 8.2 Ackerman turning geometry.

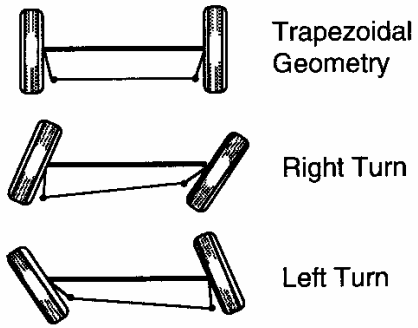

Fig. 8.3 Differential steer from a trapezoidal tie-rod arrangement.

inside wheel to steer to a greater angle than the outside wheel. When the tie rods are located behind the wheel centers, as shown, the steering arm ball joints are located inboard of the steer axis and provide good wheel clearances. If the steering is designed with the tie rods forward of the wheel centers, the steering arm ball joints must be outboard of the steer rotation axis at the wheels in order to get close to Ackerman geometry. Interference with the wheel usually prevents design for good Ackerman in this case. Proper design of the Ackerman geometry is a function of the vehicle wheelbase and front axle tread. Design methods are straightforward and are available in the literature [1]. The

degree to which the Ackerman geometry is achieved on a vehicle has little influence on high-speed directional response behavior, but does have an influence on the self-centering torque during low-speed maneuvers [4]. With Ackerman, the steer resisting torque will grow consistently with steer angle. However, with parallel steer (zero Ackerman), the torque will initially grow with angle, but may then diminish (and even become negative) at sufficiently large angles.

STEERING GEOMETRY ERROR

In the typical steering system the relay linkages transfer the steering action from the gearbox on the body of the vehicle to the steering arms on the wheels. The steering action is achieved by translational displacement of the relay linkage in the presence of arbitrary suspension motions. There is obvious potential for steering actions to arise from suspension motions, which are known as steering geometry errors.

For an ideal steering system the relay linkage is designed such that the arc described by its ball connection to the steering arm exactly follows the arc of the steering arm during suspension deflections. In that case, no steer action results during the normal ride and handling motions of the suspension. In practice, it is not always possible to achieve this ideal because of packaging problems, nonlinearities in the motion of the suspension, and because of geometry changes when the wheels are steered. Consequently, errors will occur that may result in a change in toe angle with suspension deflections, a systematic steer at both wheels, or a combination of both.

The geometry to achieve the "ideal" of no interaction on an independent front suspension is illustrated in Figure 8.4. Regardless of the suspension type used, for the vertical wheel motion around the normal ride point, the motion will be defined by some linkage constraints. For the upper and lower control arm configuration shown, relative to the vehicle body the outboard end of each arm will follow an arc centered at the pivot point on the body. This defines the motion of the upper and lower ends of the steering knuckle and, ultimately, the motion of the steering arm ball at its intermediate location on the knuckle. If the steering arm ball is located in close proximity to one of the control arms, its ideal center will be close to the inboard pivot point of that arm. If located at some intermediate position on the knuckle, its ideal center will be found at a point that is intermediate between the inboard pivots of the two arms. Although the ideal center can be estimated by eye, a geometric study is needed

to precisely determine its location. Many of the computer-aided-design (CAD) programs have the capability to identify this point. Alternatively, various geometrical methods (inflection circle, Hartmann's Construction or Bobillier's Construction) may be used to locate the center [5, 6].

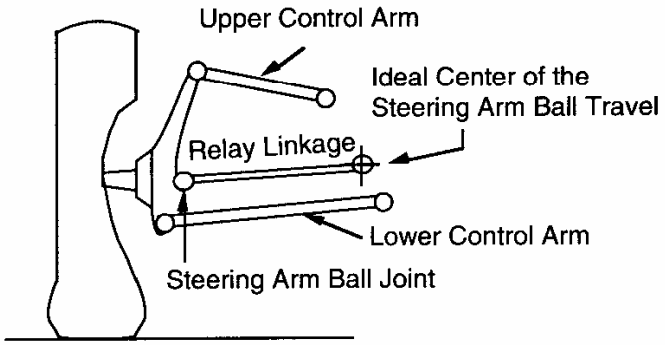

Fig. 8.4 Ideal steering geometry for an independent front suspension.

It should be noted here that the ideal center for the steering arm ball is determined by the kinematic (motion) behavior of the suspension linkages, the analysis for which is subtly different from that used to model anti-dive and anti-squat behavior. In the analysis of anti-dive and anti-squat, the objective is to determine suspension response to force and torque inputs. The conclusion in that case is that the linkages behave like a single arm pivoted at the virtual center of the upper and lower control arms, located at the intersection of the projections of the control arm axes. However, analysis of the motion of the linkages results in a different center because of the angular changes in the linkages as a result of the motion.

Toe Change

The arc that will be followed by the tie-rod end at the wheel is established by the inboard joint of the relay linkage (tie rod)—the joint being the center of the arc. If the linkage joint is either inboard or outboard of this point, the steering geometry error will cause a steer action as the wheel moves into jounce or rebound. Consider the case illustrated in Figure 8.5 which shows the inboard joint of the tie rod located outboard of the ideal center.

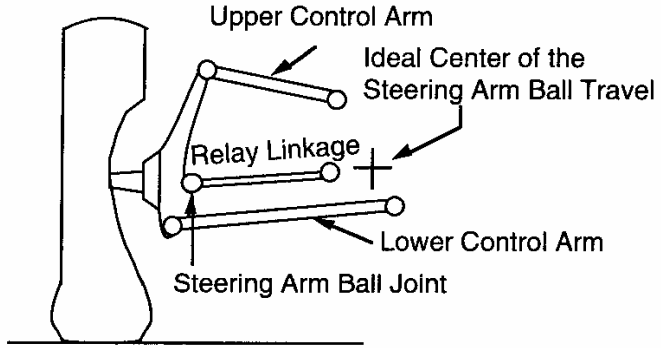

Fig. 8.5 Geometry error causing toe changes.

When the left wheel moves into either jounce or rebound, the end of the relay linkage follows an arc which pulls the steering arm to the right as viewed in Figure 8.5. This produces a left-hand steer when the linkage is located behind the wheel centers. By a similar argument it can be seen that the right wheel will steer to the right in jounce and rebound. Thus, a toe-out error occurs when the wheels are at any position other than the design ride height, and proper toe will be difficult to maintain due to its dependence on front-wheel load condition.

When the relay linkage joint is located too far inboard, the wheels will steer in the opposite direction during jounce and rebound and a toe-in error will occur. Because of the nature of this error, the toe-out or toe-in conditions will also be experienced when the body rolls in cornering. Inasmuch as these are undesirable effects, these may legitimately be considered as steering geometry errors.

Roll Steer

A second type of steering geometry error, which may be used intentionally to alter handling behavior, is to locate the inboard joint of the relay linkage either above or below the ideal center. Figure 8.6 illustrates this case, showing a rear view of a left-hand wheel with the inboard joint located below the ideal center. For the case where the linkage is located aft of the wheel, the arc followed by the relay linkage end will produce a left-hand steer on the wheel as it goes into jounce and a right-hand steer when it goes into rebound. Steer in the opposite directions will be produced on the right-side wheel. Thus, toe-in and toe-out will occur with each cycle of bouncing when the vehicle travels down the road.

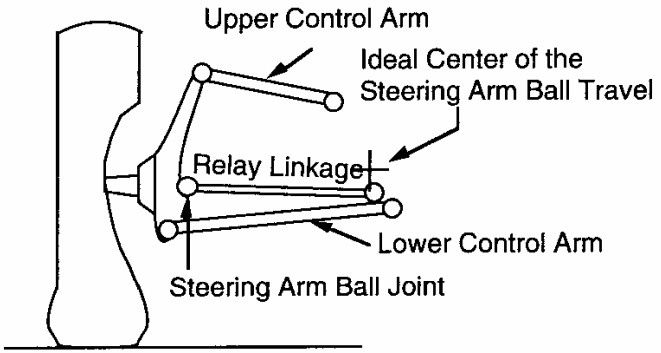

Fig. 8.6 Steering geometry error to add understeer.

Because of the symmetry of this case, both wheels will steer in the same direction when the body rolls. For example, in a turn to the right (positive steer by the SAE convention) the body rolls to the left inducing jounce on the left wheel and rebound on the right. Thus both wheels steer to the left (out of the turn) adding an understeer effect to the vehicle's directional response. Locating the inboard joint of the tie rod above the ideal center produces an oversteer effect.

Figure 8.7 shows the roll steer behavior experimentally measured on a vehicle. Lines sloping upward to the right reflect a roll steer which is understeer in direction (i.e., in a left-hand turn, as the vehicle body rolls to the right, the wheels steer to the right reducing the severity of turn). At any steer angle the slope of the curve is the roll steer coefficient, ε. The understeer gradient is then given by:

$$K_{\text{roll steer}} = \varepsilon \frac{d\,\phi}{d\,a_y} \tag{8-3}$$

Before leaving this subject, it should be noted that most suspensions swing in a plane that is skewed with respect the the vehicle longitudinal axis. The analysis, as illustrated above, should actually be made in the swing plane and transferred to the transverse plane.

FRONT WHEEL GEOMETRY

The important elements of a steering system consist not only of the visible linkages just described, but also the geometry associated with the steer rotation axis at the road wheel. This geometry determines the force and moment

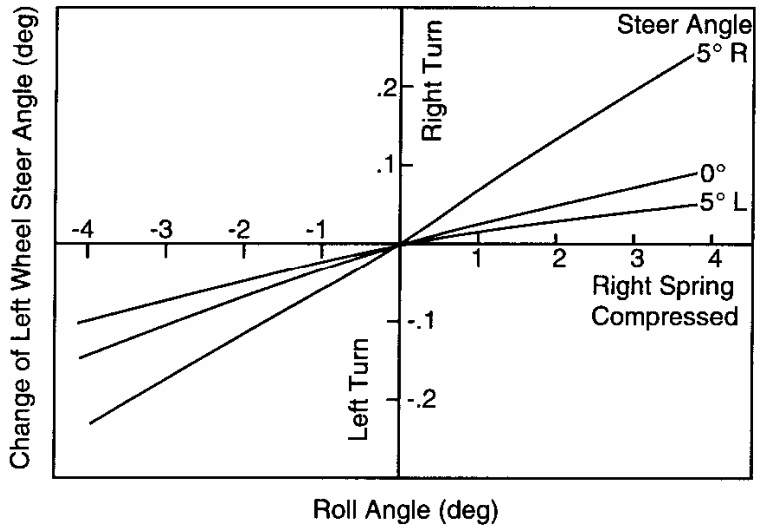

Fig. 8.7 Roll steer behavior experimentally measured on a vehicle.

reactions in the steering system, affecting its overall performance. The important features of the geometry are shown in Figure 8.8.

The steer angle is achieved by rotation of the wheel about a steer rotation axis. Historically, this axis has the name "kingpin" axis, although it may be established by ball joints or the upper mounting bearing on a strut. The axis is normally not vertical, but may be tipped outward at the bottom, producing a lateral inclination angle (kingpin inclination angle) in the range of 0-5 degrees for trucks and 10-15 degrees on passenger cars.

It is common for the wheel to be offset laterally from the point where the steer rotation axis intersects the ground. The lateral distance from the ground intercept to the wheel centerline is the offset at the ground (sometimes called "scrub") and is considered positive when the wheel is outboard of the ground intercept. Offset may be necessary to obtain packaging space for brakes, suspension, and steering components. At the same time, it adds "feel of the road" and reduces static steering efforts by allowing the tire to roll around an arc when it is turned [7].

Caster angle results when the steer rotation axis is inclined in the longitudinal plane. Positive caster places the ground intercept of the steer axis ahead of the center of tire contact. A similar effect is created by including a

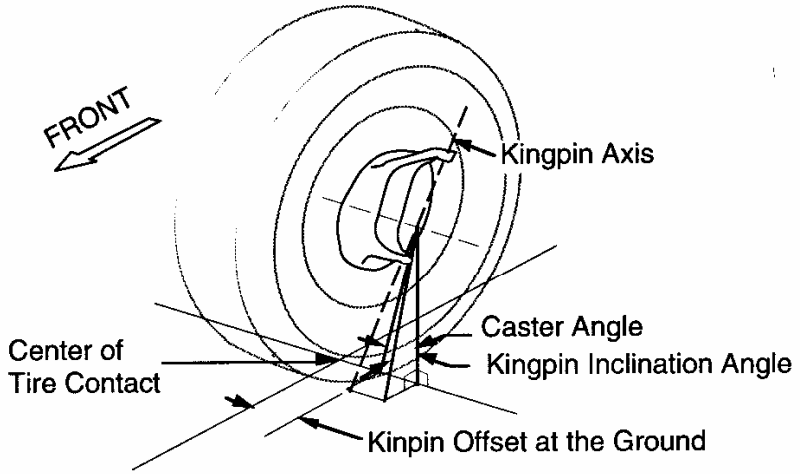

Fig 8.8 Steer rotation geometry at the road wheel.

longitudinal offset between the steer axis and the spin axis of the wheel (spindle), although this is only infrequently used. Caster angle normally ranges from 0 to 5 degrees and may vary with suspension deflection.

Wheel camber angles and toe-in normally have only secondary effects on steering behavior and high-speed directional response. The typical fractional angles specified for camber are selected to achieve near-zero camber angle for the most common load conditions of the vehicle. The small static toe angles are normally selected to achieve zero angle when driving forces and/or rolling resistance forces are present on the road. The selection of these angles is normally dominated by considerations of front tire wear rather than handling [8, 9].

STEERING SYSTEM FORCES AND MOMENTS

The forces and moments imposed on the steering system emanate from those generated at the tire-road interface. The SAE has selected a convention by which to describe the forces on a tire, as shown in Figure 8.9. The forces are measured at the center of the contact with the ground and provide a convenient basis by which to analyze steering reactions.

The ground reactions on the tire are described by three forces and moments, as follows:

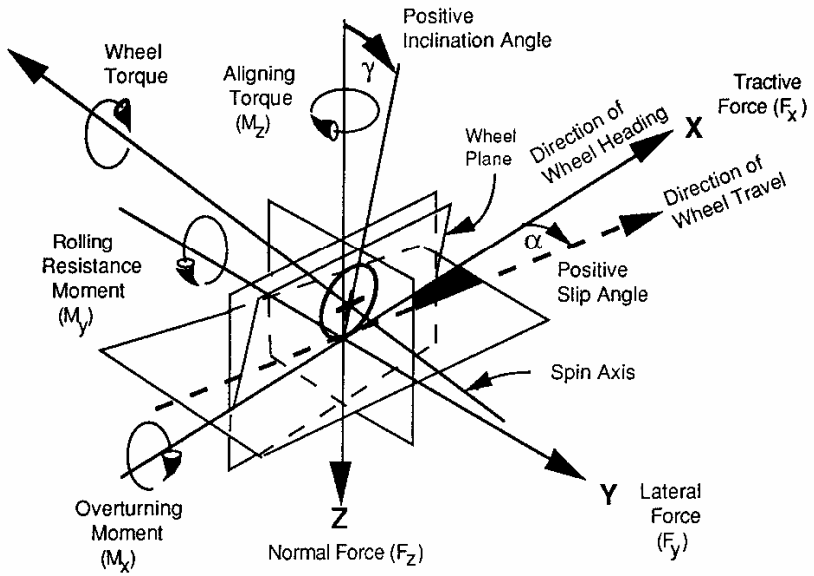

Fig. 8.9 SAE tire force and moment axis system.

Normal force	Aligning torque
Tractive force	Rolling resistance moment
Lateral force	Overturning moment

On front-wheel-drive cars, an additional moment is imposed by the drive torque. This will be discussed separately, along with other factors unique to front-wheel-drive cars that affect handling behavior.

The reaction in the steering system is described by the moment produced on the steer axis, which must be resisted to control the wheel steer angle. Ultimately, the sum of moments from the left and right wheels acting through the steering linkages with their associated ratios and efficiencies account for the steering-wheel torque feedback to the driver.

Figure 8.10 shows the three forces and moments acting on a right-hand road wheel. Each will be examined separately to illustrate its effect on the steering system.

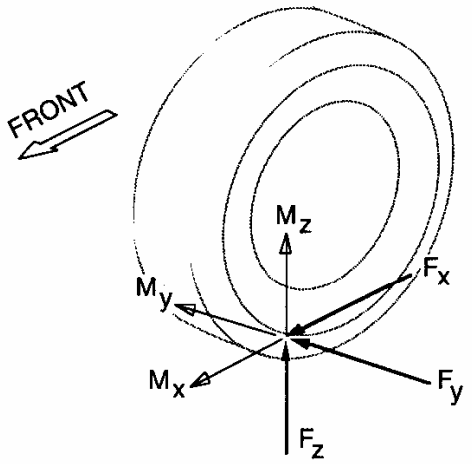

Fig. 8.10 Forces and moments acting on a right-hand road wheel.

Vertical Force

The vertical load, F_z, acts vertically upward on the wheel and by SAE convention is considered a positive force. Because the steering axis is inclined, F_z has a component acting to produce a moment attempting to steer the wheel. The moment arises from both the caster and lateral inclination angles. Assuming small angles and neglecting camber of the wheel as it steers, the total moment from the two can be approximated by:

$$M_V = -(F_{zl}+F_{zr})\, d \sin\lambda \sin\delta + (F_{z1} - F_{zr})\, d \sin\nu \cos\delta \qquad (8\text{-}4)$$

where:

M_V = Total moment from left and right wheels
F_{zl}, F_{zr} = Vertical load on left and right wheels
d = Lateral offset at the ground
λ = Lateral inclination angle
δ = Steer angle
ν = Caster angle

The first expression on the right side of the above equation arises from lateral inclination angle, and the last from caster angle. The source of each of these moments is most easily visualized by considering the effects of lateral inclination angle and caster angle separately.

The vertical force acting on lateral inclination angle, illustrated in Figure 8.11, results in a sine angle force component, $F_{zr} \sin\lambda$, which nominally acts laterally on the moment arm "d sin δ" when the wheel is steered. The moment is zero at zero steer angle. With a steer angle, the moments on both the left and right wheels act together producing a centering moment, as shown in Figure 8.12. The net moment is proportional to the load but independent of left and right load imbalance. When steering, both sides of the vehicle lift, an effect which is often described as the source of the centering moment.

The caster angle results in a sine angle force component, $F_{zr} \sin\nu$, which nominally acts forward on the moment arm "d cos δ" as shown in Figure 8.13. The moments on the left and right wheels are opposite in direction, as shown in Figure 8.14, and tend to balance through the relay linkages. The balance depends on equal right and left wheel loads. Hence, load and caster angle may affect wheel toe-in, and imbalances due to load or geometric asymmetry may result in steering pull. With steer angle, one side of the axle lifts and the other drops, so that the net moment produced depends also on the roll stiffness of the front suspension as it influences the left and right wheel loads.

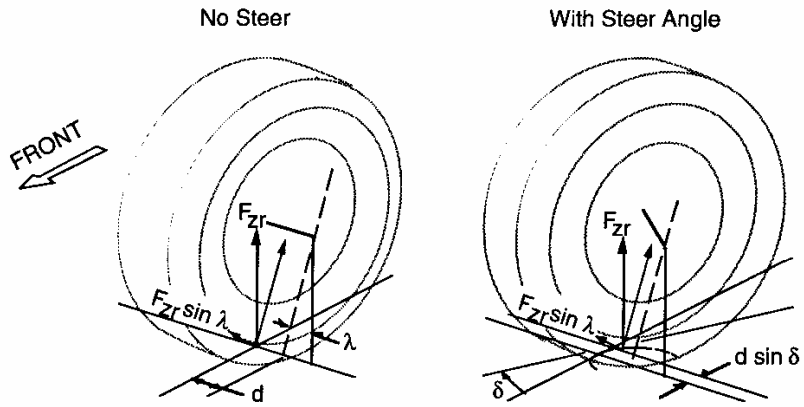

Fig. 8.11 Moment produced by vertical force acting on lateral inclination angle.

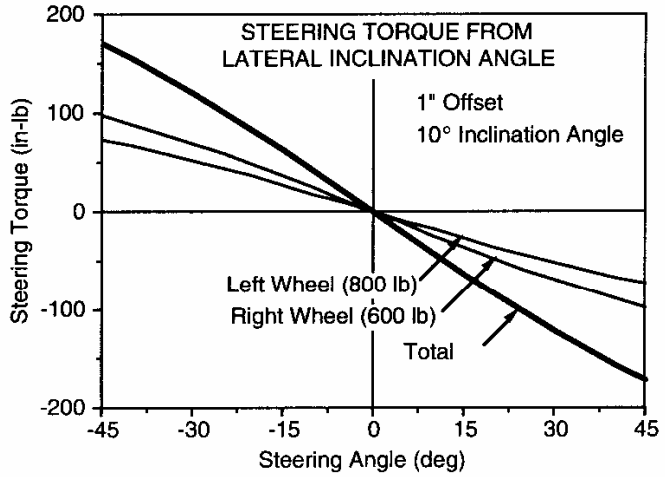

- Torque = - $(F_{zl}+F_{zr})$ d sin λ sin δ
- Axle lifts when steered
- Unaffected by left-right load differences
- Torque gradient depends on:
  - — wheel offset at the ground
  - — inclination angle
  - — axle load

Fig. 8.12 Steering torques arising from lateral inclination angle.

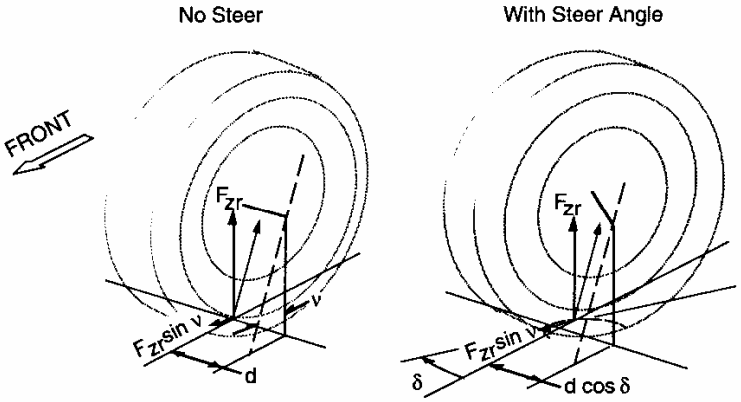

Fig. 8.13 Moment produced by vertical force acting on caster angle.

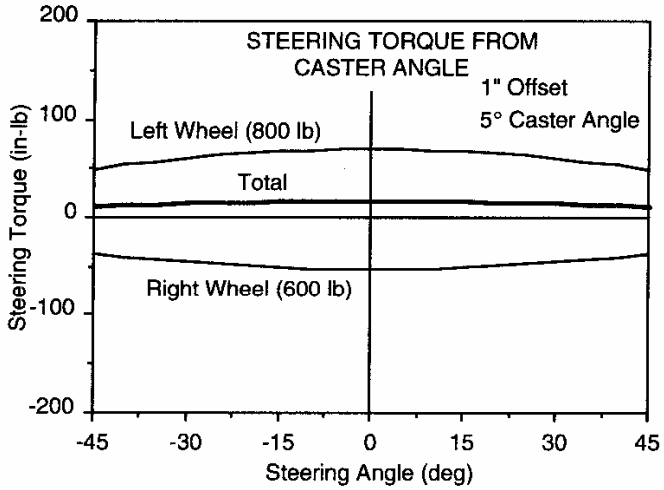

- Torque = $(F_{zl} - F_{zr})$ d sin ν cos δ
- Axle rolls when steered
- Sensitive to left-right load imbalance (load or spring asymmetry)
- Torque gradient depends on
  - — wheel offset at the ground
  - — caster angle
  - — left-right load difference in cornering
    - ·front and rear suspensions roll stiffnesses
    - ·suspension roll center height
    - ·center of gravity height
    - ·lateral acceleration level

Fig. 8.14 Steering torques due to caster angle.

Lateral Force

The lateral force, F_y, acting at the tire center produces a moment through the longitudinal offset resulting from caster angle, as shown in Figure 8.15. The net moment produced is:

$$M_L = (F_{yl}+F_{yr})\, r \tan \nu \qquad (8\text{-}5)$$

where:

F_{yl}, F_{yr} = Lateral forces at left and right wheels (positive to the right)

r = Tire radius

The lateral force is generally dependent on the steer angle and cornering condition, and with positive caster produces a moment attempting to steer the vehicle out of the turn. Hence, it is a major contributor to understeer.

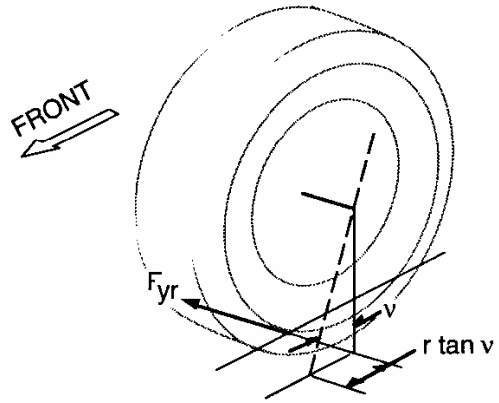

Fig. 8.15 Steering moment produced by lateral force.

Tractive Force

The tractive force, F_x, acts on the kingpin offset to produce a moment as shown in Figure 8.16.

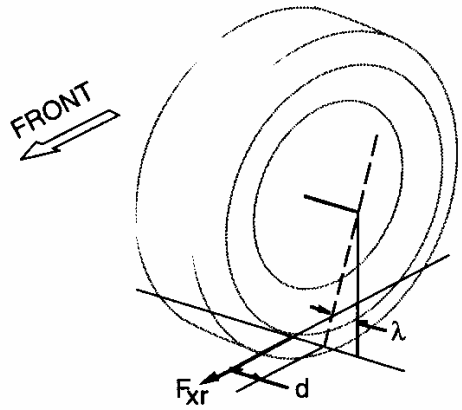

Fig. 8.16 Steering moment produced by tractive force.

Then net moment is:

$$M_T = (F_{xl}-F_{xr})\, d \tag{8-6}$$

where:

F_{xl}, F_{xr} = Tractive forces on left and right wheels (positive forward)

The left and right moments are opposite in direction and tend to balance through the relay linkage. Imbalances, such as may occur with a tire blowout, brake malfunction, or split coefficient surfaces, will tend to produce a steering moment which is dependent on the lateral offset dimension.

Aligning Torque

The aligning torque, M_z, acts vertically and may be resolved into a component acting parallel to the steering axis. Since moments may be translated without a change in magnitude, the equation for the net moment is:

$$M_{AT} = (M_{Zl} + M_{Zr}) \cos \sqrt{\lambda^2 + \nu^2} \tag{8-7}$$

where:

M_{Zl},M_{Zr} = Aligning torques on the left and right wheels

Under normal driving conditions, the aligning torques always act to resist any turning motion, thus their effect is understeer. Only under high braking conditions do they act in a contrary fashion.

Rolling Resistance and Overturning Moments

These moments at most only have a sine angle component acting about the steer axis. They are second-order effects and are usually neglected in analysis of steering system torques.

STEERING SYSTEM MODELS

Equations (8-4) through (8-7) from the preceding discussion describe the moments input to the steer axis of each road wheel coming from the forces and moments acting on the tires. The reactions can be summed directly to

determine the torque feedback to the steering wheel if desired. To quantify the influence on open-loop directional response, however, a model of the steering compliances is required [2]. Figure 8.17 shows the simplest model that is suitable for describing low-frequency behavior. The significant properties of the linkages are the stiffnesses shown here as the composite values between the gearbox and the road wheels. For various reasons, the front suspensions will also exhibit compliance in the lateral direction that adds to the effective compliance interacting with the steering displacements. These effects can be taken into account by appropriately increasing the "lumped" compliance values of the linkages.

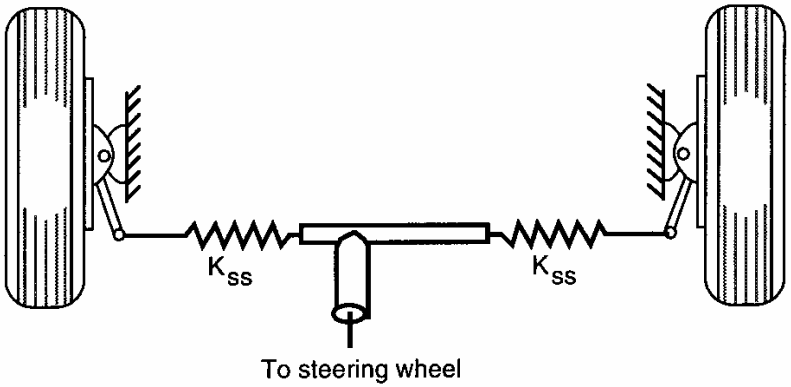

Fig. 8.17 Steering linkages model.

Depending on the purpose of the analysis, the steering gearbox might be represented by the effective steering ratio and by the appropriate input/output torque relationships and efficiencies. Similarly, the model may be expanded by the addition of Ackerman steer angle relationships between the road wheels with nonlinearities when desired. The properties of integral power-steering systems might also be introduced at this point.

The modeling equations are not developed here, but are simple to formulate from the geometric relationships [10] and the application of Hooke's Law to relate forces and displacements across the compliances. Models of steering systems have proved most useful when combined with existing vehicle simulation models, such as the ADAMS models. The directional response simulations compute the vehicle dynamic motions and the associated force and moment conditions imposed on each tire, needed as input to the steering system

model. These are used as input to the model then to determine the incremental steer angles produced, which in turn alter the turning behavior of the vehicle. This makes it possible to examine the precise influences of steering system properties on overall handling behavior.

EXAMPLES OF STEERING SYSTEM EFFECTS

The specific design of a steering system geometry has a well-recognized influence on steering performance measures such as center feel, returnability, and steering efforts as normally evaluated by vehicle manufacturers. Additionally, in the systematic study of directional response, other phenomena are observed, ranging from simple influences on steering ratio to cornering and even braking.

Steering Ratio

The steering ratio is defined as the ratio of steering wheel rotation angle to steer angle at the road wheels. Normally these range from 15 or 20 to 1 on passenger cars, and 20-36 to 1 on trucks. Because of the compliance and steer torque gradients with increasing steer angles, the actual steering ratio may be as much as twice the designed ratio. Figure 8.18 shows experimental measure-

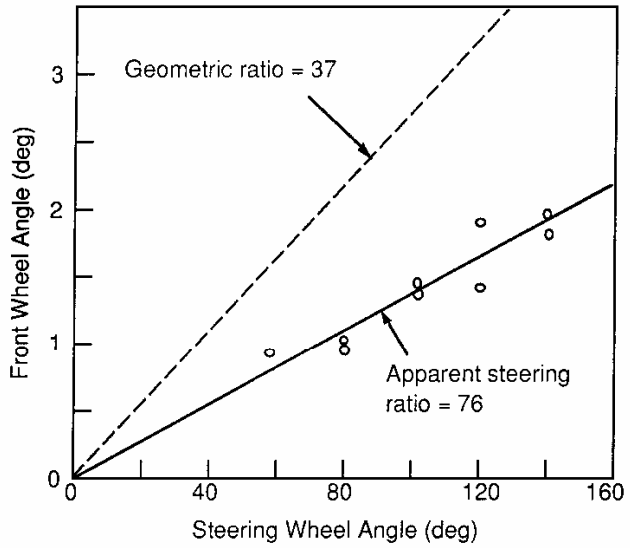

Fig. 8.18 Experimental measurement of steering ratio on a truck.

ments on a truck which illustrate the phenomenon. While the compliance property is constant on a vehicle, the torque gradient will vary with load on the front tires, tire type, pressure, coefficient of friction, etc. Hence, the actual steering ratio may vary (always exceeding the design value) and influencing the low-speed maneuverability of the vehicle.

Understeer

The steady-state cornering performance of a vehicle is frequently characterized by the understeer gradient measured at the steering wheel. Because compliance in the steering system allows the road wheels to deviate from the steering wheel input, the results obtained are influenced by the steering system properties. Figure 8.19 shows the steer angle gradient measured at the steering wheel and the left road wheel of a loaded truck with manual steering [11].

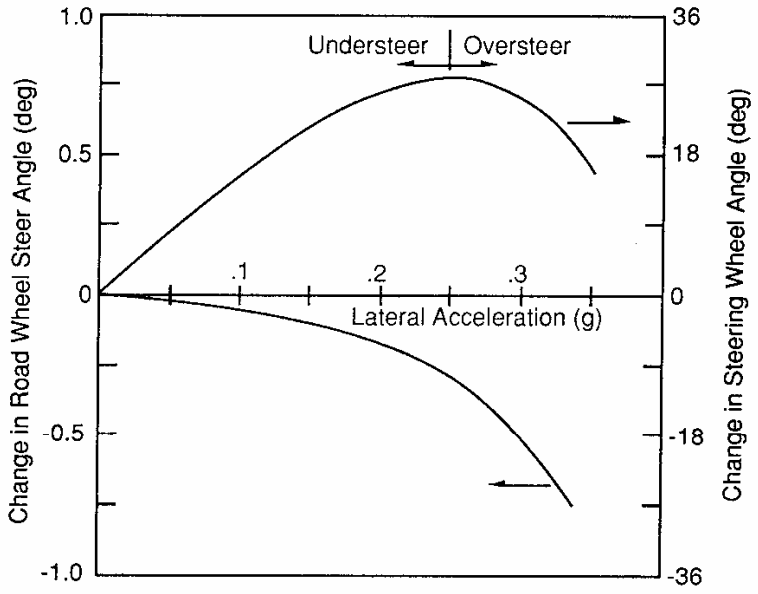

Fig. 8.19 Understeer gradient measured at the steering wheel and road wheel of a truck.

The vehicle has a very high understeer gradient at the steering wheel equal to approximately 150 degrees/g (the initial slope of the steering wheel gradient on the plot). Corrected for the ratio of the steering system (36 to 1) it is equivalent to an apparent gradient of 4 degrees/g at the road wheel. However, independent measurements of the road wheel angle indicated an initial slope that is nearly horizontal—equivalent to neutral steer at the road wheel. The difference arises from deflections in the steering linkage as the reactions on the road wheels act against the steering compliances.

The magnitude of the steering system contribution is dependent on the front-wheel load and caster angle. From a simple analysis for the understeer influences in which the lateral forces and aligning torques are dominant (neglecting vertical force effects), it can be shown that the understeer gradient is:

$$K_{strg} = \frac{W_f(r\,\nu + p)}{K_{ss}} \tag{8-8}$$

where:

K_{strg} = Understeer increment (deg/g) due to steering system
W_f = Front wheel load (lb)
r = Wheel radius (in)
p = Pneumatic trail associated with aligning torque (in)
ν = Caster angle (rad)
K_{ss} = Steering stiffness (in-lb/deg) between road wheel and steering wheel

As seen here, caster angle and aligning torque effects add to the understeer in the presence of a compliant steering system. For typical values of the above parameters, Eq. (8-8) would account for understeer increments on the order of 4-6 deg/g.

Braking Stability

Braking is a special case in which steering system design plays an important role in directional response [2]. Specifically, the design has a direct influence on stability and resistance to brake imbalance effects. It was shown that caster angle influences stability by way of its action to resist steering deviations caused by front brake imbalance. Yet, the benefits of caster angle are particularly vulnerable during braking conditions. Vehicle pitch and front suspension windup may overcome the few degrees of caster angle designed

into the system at normal trim conditions. Further, the tire aligning torques which effectively act like 4-8 degrees of caster angle under free-rolling conditions can also reverse in direction during braking. This tire effect is illustrated in Figure 8.20 by measurements from a truck tire. The tire caster effect in this plot is obtained by dividing the aligning torque by the lateral force to determine the pneumatic trail at each data point. The pneumatic trail normalized by the tire radius then yields the effective angle at which the lateral force acts under the tire, which is the tire caster effect. At low braking coefficients the aligning torque acts in the direction to steer the tire in its direction of travel, which on the steered wheels attempts to steer the vehicle out of the turn (an understeer influence). But at high braking coefficient, the aligning torque reverses direction and may reach elevated negative levels, which will attempt to steer the tire into the direction of turn (an oversteer influence). As a result, the normal stabilizing effects of positive caster and tire aligning torque may be substantially reduced or eliminated during high-level braking.

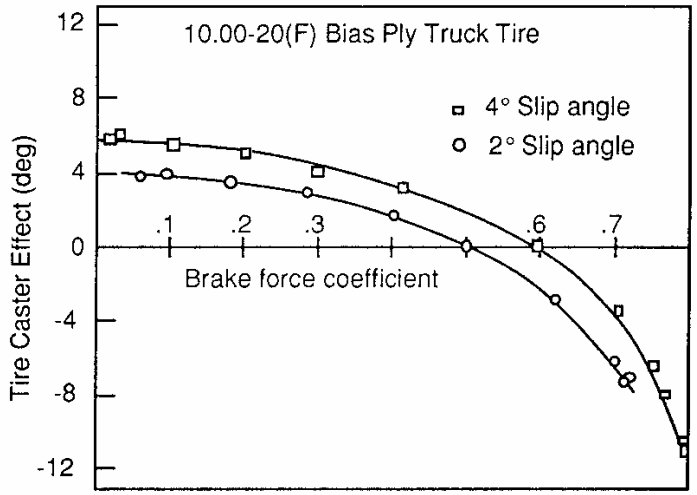

Fig. 8.20 Change of tire aligning torques with braking coefficient.

Brake force imbalance (due to brake malfunction or a split-coefficient surface) will also act on the compliant steering system, attempting to steer the vehicle. Using the split coefficient surface as an example, the higher brake

forces on the high-coefficient surface will attempt to rotate the vehicle onto that surface by virtue of the moment produced on the vehicle. With a positive lateral offset, the dominant front wheel brake force on the high-coefficient surface will also attempt to steer the vehicle onto that surface. The brake force "steering" effect may be as much as 2 to 3 times greater than the direct moment on the vehicle in causing the vehicle to veer onto the high-coefficient surface. Negative offsets have been used on certain cars to counteract this mechanism on split coefficient braking, and when diagonal-split brake failure modes are employed.

INFLUENCE OF FRONT-WHEEL DRIVE

It is generally recognized that with front-wheel-drive (FWD) vehicles, the turning behavior varies with the application of engine power. In most cases, throttle-on produces understeer, and throttle-off produces oversteer. The turning equation developed in Chapter 6 for FWD vehicles would suggest just the opposite behavior. Obviously, other mechanisms must be at work. Three have been identified and will be discussed here. The discussion focuses on handling influences unique to front-wheel drive. All the other influences considered in earlier sections will still be present and acting on the vehicle.

Driveline Torque About the Steer Axis

Even in straight-ahead driving, the torque in the driveline produces a moment about the steer axis. This comes out of the model shown in Figure 8.21. In it a constant-velocity joint connects the halfshaft to the wheel spindle. The front wheel is in the straight-ahead position.

Neglecting the rolling resistance moment and the moments deriving from the normal force between the tire and road, the net moment about the steer axis of one wheel is:

$$M_{SA} = F_x\, d \cos \nu \cos \lambda + T_d \sin (\lambda+\zeta) \qquad (8\text{-}9)$$

Since

$$T_d = F_x\, r \qquad (8\text{-}10)$$

equation (8-9) can be rewritten:

$$M_{SA} = F_x\, [d \cos \nu \cos \lambda + r \sin (\lambda+\zeta)] \qquad (8\text{-}11)$$

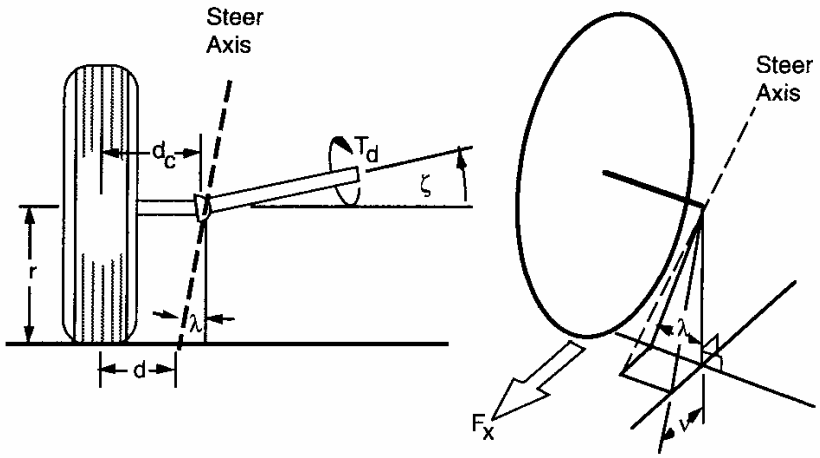

Fig. 8.21 Drive forces and moments acting on a front wheel.

Normally, the lateral inclination and caster angles (λ and ν) are small enough that the cosine function can be assumed unity, in which case:

$$M_{SA} = F_X [d + r \sin (\lambda+\zeta)] \qquad (8\text{-}12)$$

In effect, the arm about which the drive force acts to create a moment on the steering axis is [d + r sin (λ+ζ)]. Now d is the lateral offset at the ground. The term "r sin (λ+ζ)" is the additional distance out to the perpendicular from the halfshaft at the constant-velocity joint. That is, envision a plane through the constant-velocity joint which is perpendicular to the halfshaft. The offset determining the moment arm extends from the tire contact patch to that plane.

When the halfshaft is horizontal (most often the case in straight-ahead driving), ζ is zero. Then the moment arm is d + r sin λ which is the same as the offset at the wheel center, d_c. Hence, the expression "the drive force acts at the wheel center." (Note, because the brake torque acts through the suspension, it can be shown that the brake force moment arm is simply the lateral offset at the ground, d. When inboard brakes are used, the moment arm is again d + r sin λ.)

When a vehicle goes into a turn, body roll causes the halfshaft on the outside wheel to reduce its inclination angle, ζ (going negative if it were already zero), while the angle on the inside wheel increases. Thus the moment arm about which the drive force acts gets smaller on the outside wheel and larger on the inside wheel. With a drive force (in the forward direction) this imbalance

introduces a moment in the steering system which opposes the steer angle, trying to steer the vehicle out of the turn (understeer). The magnitude of the moment is dependent on: the degree of body roll, and how much difference in halfshaft angles is created; the difference between kingpin inclination angles on the left and right side during body roll; caster angles; and any geometric differences between the left- and right-hand sides (tire radius, etc.).

The understeer influence is proportional to the magnitude of the moment divided by the stiffness of the steering system. Thus minimizing body roll and stiffening the steering system minimizes the effect. Although the influence is specific to each vehicle, the understeer change from throttle-on to throttle-off is estimated to be on the order of 1 degree/g for a typical vehicle [12].

Influence of Tractive Force on Tire Cornering Stiffness

It is well known that a tire loses cornering force when a tractive force is present as well. Figure 8.22 shows typical behavior of lateral force as a function of tractive force. The effect is most pronounced with bias-ply tires, and less so with radial tires. The application of throttle (a demand for drive force) causes the front tires to lose cornering force, and the tires must seek a higher slip angle. This, of course, produces understeer.

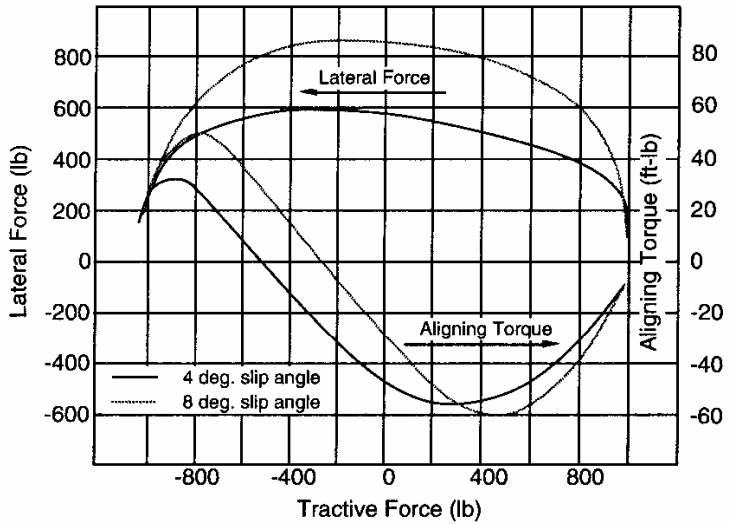

Fig. 8.22 Effect of tractive force on tire lateral force and aligning moment.

The magnitude will be proportional to the tractive force level. It is estimated [13] that the understeer change will be in the range of 0 to 2 degrees/g for the throttle change going from 0.2 g acceleration to 0.05 g deceleration. The influence is lowest with radial-ply tires.

Influence of Tractive Force on Aligning Moment

As seen in Figure 8.22, tractive force demand tends to increase the aligning moment produced by a tire (again less significantly with radial-ply tires). The additional aligning moment tends to steer the vehicle out of the turn, and is thus understeer. The magnitude of the understeer depends on the change in aligning moment divided by the stiffness of the steering system. It has been estimated that this mechanism contributes on the order of 0.5 to 1 degree/g of understeer [12].

Fore/Aft Load Transfer

Understeer is normally characterized only in steady speed turns. Yet it has been necessary to consider the difference between accelerating and decelerating conditions for purposes of describing the influence of FWD on understeer. When the vehicle accelerates, load is transferred to the rear wheels dynamically. This causes the rear wheels to achieve a higher cornering stiffness, while the front wheels lose cornering stiffness (causing understeer). It is worthwhile to estimate this effect for comparison purposes (to see to what degree it accounts for the understeer change that we ascribe to the FWD car because it would also be present on RWD cars, if they were tested in the same fashion). For a typical car, the understeer influence for the throttle changes described above is on the order of 1 degree/g [12].

Summary of FWD Understeer Influences

In summary, the primary mechanisms responsible for throttle on/off changes in understeer of a FWD vehicle are:

1) The lateral component of drive thrust—While this mechanism is relatively weak (<0.5 deg/g), it is oversteer in direction.

2) Drive torque acting about the steer axis—Highly dependent on driveline geometry and the degree of body roll in cornering, this mechanism is understeer in direction (about 1 deg/g).

3) Loss of lateral force—A tire property which causes understeer (about 1-1.5 deg/g).

4) Increase in aligning moment—A tire property which causes understeer (about 0.5-1 deg/g).

5) Fore/aft load transfer—Although present on FWD and RWD vehicles, it is always understeer in direction (about 1 deg/g).

The total understeer due to above effects is approximately 4-5 deg/g. The mechanisms present in items 2-4 generate torques that feed back into the steering system and are the primary sources of "torque steer" often noted with FWD vehicles. Finally, it should be noted that friction in a differential can be significant (10 to 15%) when a driveline is under load. Although not treated here, under certain circumstances it could be an additional mechanism contributing to throttle-on understeer in FWD vehicles.

FOUR-WHEEL STEER

Vehicle performance in turning can be enhanced by actively steering the rear wheels as well as the front wheels (4WS). Active steering is accomplished by steering action applied directly to the rear wheels, in contrast to passive steering in which compliances are purposely designed into the suspension to provide incremental steer deviations that improve cornering [14]. Four-wheel steering may be used to improve low-speed maneuverability and/or high-speed cornering.

Low-Speed Turning

Low-speed turning performance is improved by steering the rear wheels out-of-phase with the front wheels to reduce the turn radius, thus improving maneuverability as shown in Figure 8.23. Rear-wheel steer is accomplished by mechanical, hydraulic or electronic means [14-18]. Normally, the rear-wheel steer angles are a fraction of that at the front (typically limited to about 5 degrees of steer), and may only be applied at low speeds [17] or at high steer angles typical of low-speed turns [15]. Analysis of the turning performance is simplified by assuming average angles for the front and rear wheels, analogous to the bicycle model approximation.

With the rear-wheel steer angle proportional to the front-wheel angle, the turning equations are as follows:

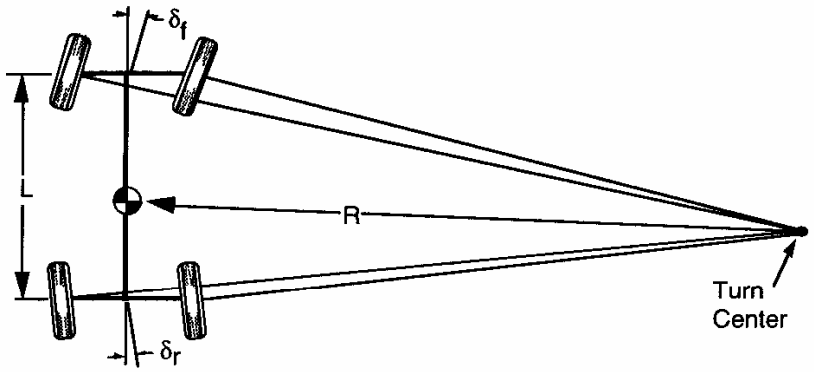

Fig. 8.23 Turning geometry of a four-wheel-steer vehicle.

$$\delta_r = \xi\,\delta_f \tag{8-13}$$

$$\delta_f + \delta_r = \delta_f + \xi\,\delta_f = \delta_f\,(1 + \xi) = L/R \tag{8-14}$$

Then the turn radius is:

$$R = \frac{L}{\delta_f(1 + \xi)} \tag{8-15}$$

Equation (8-15) gives the explicit expression for the way in which the turn radius is reduced by the use of rear steer. At 50 percent rear steer, a one-third reduction in turn radius (1/1.5) is achieved. At 100 percent rear steer (steering the rear wheels to the same magnitude as the front wheels), a 50 percent reduction in turn radius (1/2) occurs.

The expression for off-tracking with four-wheel steer is somewhat more complicated than that for two-wheel steer. Recognizing that the front and rear turn radii, R_f and R_r, respectively, are related by the expression:

$$R_f \cos\delta_f = R_r \cos\delta_r = R_r \cos(\xi\,\delta_f) \tag{8-16}$$

it is possible to obtain an equation in the following form as an approximation of the off-tracking distance:

$$\Delta \cong \frac{L^2}{2R}\,\frac{(1 - \xi^2)}{(1 + \xi^2)} \tag{8-17}$$

With no rear steer ($\xi = 0$) the off-tracking is the same as developed earlier in Eq. (6-4). With the rear wheels steered to the same angle as the front (100 percent), the off-tracking distance becomes zero.

High-Speed Cornering

The out-of-phase rear steer used for low-speed maneuverability would be inappropriate for high-speed turning because the outward movement of the rear wheels would constitute an oversteer influence. Thus an in-phase rear steer is used at high speed (e.g., 20 mph and above), although limited to a few degrees of steer. The transition between out-of-phase and in-phase steering is accomplished by sensing vehicle speed and changing the steering control algorithm in electronically controlled systems [17], or in mechanical systems by a mechanism that produces in-phase steer at small front wheel angles (0 to 250 degrees at the steering wheel) typical of high-speed driving [15].

The primary advantages of four-wheel steer are derived from the better control of transient behavior in cornering [19-24]. In general, 4WS systems yield a quicker response with better damping of the yaw oscillation that occurs with initiation of a turn. This can be seen in the lateral acceleration response to a step steer as shown in Figure 8.24 when the behavior of a "proportional" 4WS is compared to two-wheel steer. Other schemes for improving performance such as adding advances or delays into the steering action at front or rear wheels can provide additional options for tailoring the performance on 4WS vehicles.

Another picture of the advantages of 4WS can be obtained by examining the response in sideslip angle as a turn is initiated. Figure 8.25 compares the behavior of a two-wheel-steer system to various implementations of four-wheel steer. Depending on the amount of rear-wheel-steer action, the body sideslip angle can be arbitrarily reduced in cornering. The reduced amount of oscillation in sideslip angle with 4WS, as seen in Figure 8.25, adds the general feeling of better stability during transient maneuvers.

Overall, a properly implemented four-wheel steer can result in a vehicle which is more maneuverable at low speeds, and more responsive and stable in high-speed transient maneuvers. In other high-speed driving, however, its presence is imperceptible.

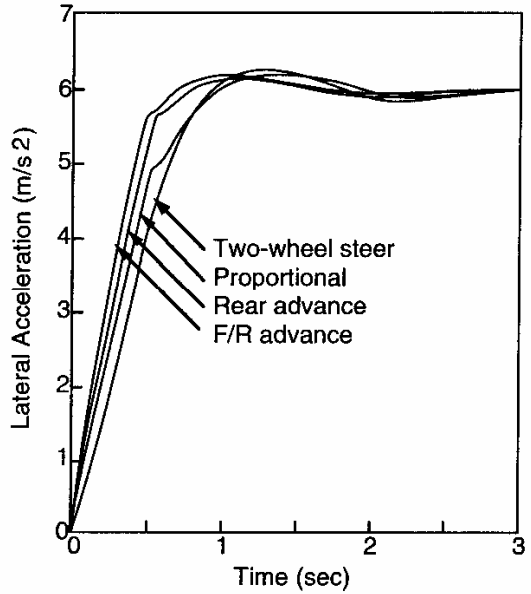

Fig. 8.24 Lateral acceleration response with different 4WS systems [20].

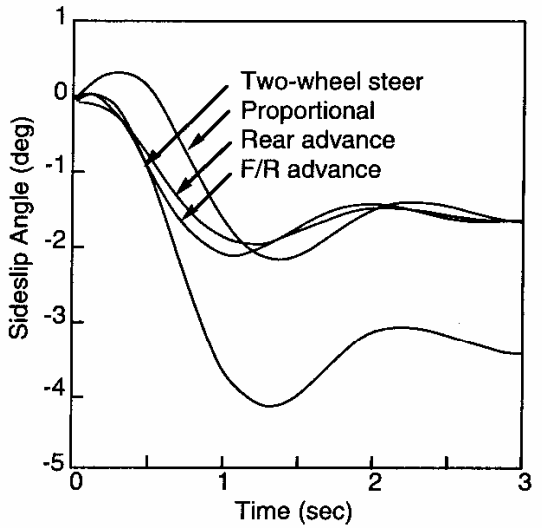

Fig. 8.25 Body sideslip angle with different 4WS systems [20].

REFERENCES

1. Durstine, J.W., The Truck Steering System from Hand Wheel to Road Wheel, SAE SP-374, January 1974, 76 p.
2. Gillespie, T.D., "Front Brake Interactions with Heavy Vehicle Steering and Handling during Braking," SAE Paper No. 760025, 1976, 16 p.
3. Dwiggins, B.H., Automotive Steering Systems, Delmar Publisher, Albany, NY, 1968, 248 p.
4. Pitts, S., and Wildig, A.W., "Effect of Steering Geometry on Self-Centering Torque and 'Feel' During Low-Speed Maneuvers," *Automotive Engineer,* Inst. of Mech. Engr., July-July 1978.
5. Hall, A.S., Jr., Kinematics and Linkage Design, Prentice Hall, Inc., Englewood Cliffs, NJ, 1961.
6. Dijksman, E.A., Motion Geometry of Mechanisms, Cambridge University Press, Cambridge, England, 1976.
7. Taborek, J.J., Mechanics of Vehicles, Towmotor Corporation, Cleveland, OH, 1957, 93 p.
8. Lugner, P., and Springer, H., "Uber den Enfluss der Lenkgeometrie auf die stationare Kurvenfahrt eines LKW," (Influence of Steering Geometry on the Stationary Cornering of a Truck), *Automobil-Industrie*, April 1974, 5 p.
9. Wheel Alignment—Modern Setting for Modern Vehicles, SAE SP-249, December 1963, 13 p.
10. MacAdam, C.C., *et al.*, "A Computerized Model for Simulating the Braking and Steering Dynamics of Trucks, Tractor-Semitrailers, Doubles, and Triples Combinations—User's Manual, Phase 4," Highway Safety Research Institute, University of Michigan, Report No. UM-HSRI-80-58, September 1980, 355 p.
11. Gillespie, T.D., "Validation of the MVMA/HSRI Phase II Straight Truck Directional Response Simulation," Highway Safety Research Institute, University of Michigan, Report No. UM-HSRI-78-46, October 1978, 58 p.
12. Gillespie, T.D., and Segel, L., "Influence of Front-Wheel Drive on Vehicle Handling at Low Levels of Lateral Acceleration," Road

Vehicle Handling, Mechanical Engineering Publications Ltd., London, 1983, pp. 61-68.

13. Braess, H.H., "Contributions to the Driving Behavior of Motor Vehicles with Front Wheel Drive Throttle Change During Cornering," Institute of Internal Combustion Machines and Motor Vehicles, Munich (Germany), 1970, 15 p.

14. Sharp, R.S., and Crolla, D.A., "Controlled Rear Steering for Cars - A Review," Proceedings of the Institution of Mechanical Engineers, International Conference on Advanced Suspensions, 1988, pp. 149-163.

15. Sano, S., *et al.*, "Operational and Design Features of the Steer Angle Dependent Four Wheel Steering System," 11th International Conference on Experimental Safety Vehicles, Washington, D.C., 1988, 5 p.

16. Nakaya, H., and Oguchi, Y., "Characteristics of the Four-Wheel Steering Vehicle and Its Future Prospects," *Vehicle System Dynamics,* Vol. 8, No. 3, 1987, p. 314-325.

17. Takiguchi, T., *et al.*, "Improvement of Vehicle Dynamics by Vehicle-Speed-Sensing Four-Wheel Steering System," SAE Paper No. 860624, 1986, 12 p.

18. Eguchi, T., *et al.*, "'Super HICAS' - A New Rear Wheel Steering System with Phasereversal Control," SAE Paper No. 891978, 1989, 10 p.

19. Fukui, K., *et al.*, "Analysis of Driver and a 'Four Wheel Steering Vehicle' System Using a Driving Simulator," SAE Paper No. 880641, 1988, 13 p.

20. Nalecz, A.G., and Bindemann, A.C., "Analysis of the Dynamic Response of Four Wheel Steering Vehicles at High Speed," *International Journal of Vehicle Design,* Vol. 9, No. 2, 1988, pp. 179-202.

21. Nalecz, A.G., and Bindemann, A.C., "Investigation into the Stability of Four Wheel Steering Vehicles," *International Journal of Vehicle Design,* Vol. 9, No. 2, 1988, pp. 159-179.

22. Ohnuma, A., and Metz, L.D., "Controllability and Stability Aspects of Actively Controlled 4WS Vehicles," SAE Paper No. 891977, 1989, 14 p.

23. Whitehead, J.C., "Four Wheel Steering: Maneuverability and High Speed Stabilization," SAE Paper No. 880642, 1988, 14 p.

24. Whitehead, J.C., "Rear Wheel Steering Dynamics Compared to Front Steering," *Journal of Dynamic Systems, Measurement and Control,* Vol. 112, No. 1, March 1990, pp. 88-93.

CHAPTER 9
ROLLOVER

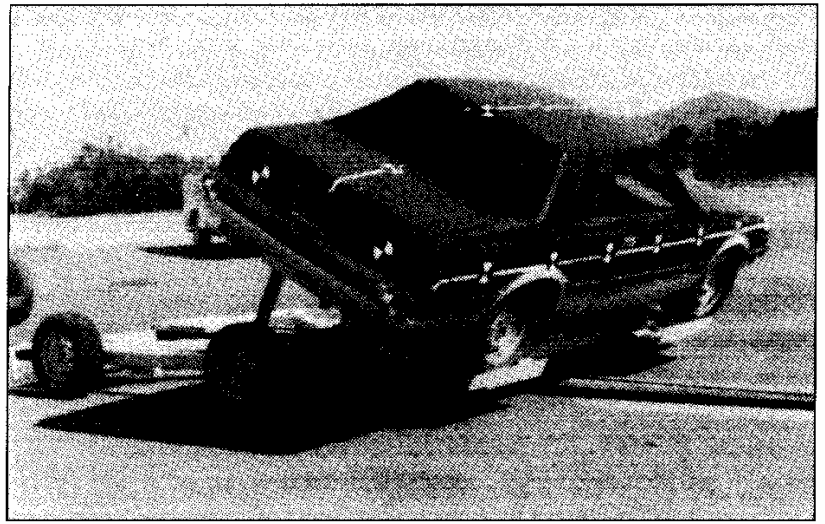

Dolly rollover test. (SAE Paper No. 900366.)

Among the dynamic maneuvers a motor vehicle can experience, rollover is one of the most serious and threatening to the vehicle occupants. Rollover may be defined as any maneuver in which the vehicle rotates 90 degrees or more about its longitudinal axis such that the body makes contact with the ground. Rollover may be precipitated from one or a combination of factors. It may occur on flat and level surfaces when the lateral accelerations on a vehicle reach a level beyond that which can be compensated by lateral weight shift on the tires. Cross-slope of the road (or off-road) surface may contribute along with disturbances to the lateral forces arising from curb impacts, soft ground, or other obstructions that may "trip" the vehicle.

The rollover process is one that involves a complex interaction of forces acting on and within the vehicle, as influenced by the maneuver and roadway. The process has been investigated analytically and empirically using models that cover a range of complexities. The process is most easily understood by starting with the fundamental mechanics involved in a quasi-static case

(neglecting the inertial terms and accelerations in the roll plane), and progressing to the more complex models.

QUASI-STATIC ROLLOVER OF A RIGID VEHICLE

The most rudimentary mechanics involved in rollover of a motor vehicle can be seen by considering the balance of forces on a rigid vehicle in cornering. By rigid vehicle it is meant that the deflections of the suspensions and tires will be neglected in the analysis.

In a cornering maneuver the lateral forces act in the ground plane to counterbalance the lateral acceleration acting at the CG of the vehicle, as shown in Figure 9.1. The difference in the position at which these forces act creates a moment on the vehicle, which attempts to roll it toward the outside of the turn.

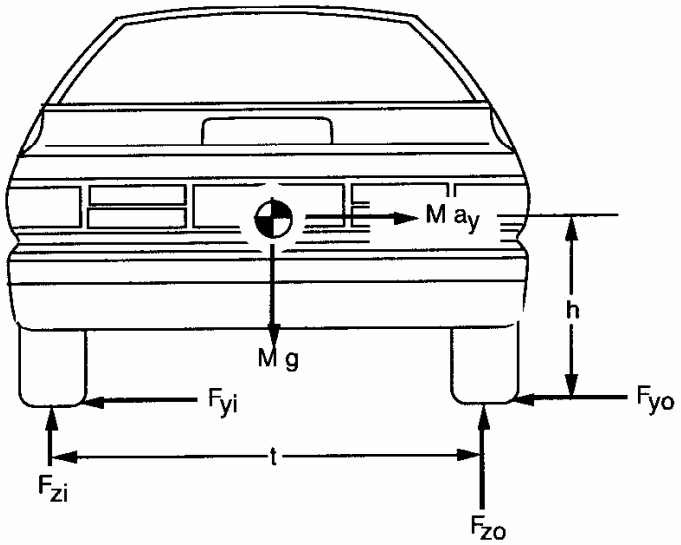

Fig. 9.1 Forces acting to roll over a vehicle.

For the purpose of analyzing the behavior, assume the vehicle is in a steady turn so that there is no roll acceleration, and let the tire forces shown in the figure represent the total for both the front and rear wheels. In many highway situations it is also appropriate to consider a transverse slope, known as cross-

slope or superelevation. For the analysis, the angle will be denoted by the symbol "φ," with a slope downward to the left representing a positive angle. A cross-slope in this direction helps to counterbalance the lateral acceleration. Cross-slope angles are normally quite small, justifying the use of small angle approximations ($\sin\varphi = \varphi$, $\cos\varphi = 1$) in the analysis that follows. Taking moments about the center of contact for the outside tires yields:

$$M a_y h - M \varphi h + F_{zi} t - M g t/2 = 0 \qquad (9\text{-}1)$$

from which we can solve for a_y to get:

$$\frac{a_y}{g} = \frac{t/2 + \varphi h - \frac{F_{zi}}{M g} t}{h} \qquad (9\text{-}2)$$

On a level road ($\varphi = 0$) with no lateral acceleration, this equation is satisfied when the load on the inside wheels, F_{zi}, is one-half of the weight of the vehicle (M g). Further, F_{zi} can be maintained at half the weight of the vehicle in the presence of lateral acceleration by judicious choice of the cross-slope angle. That is, by choosing:

$$\varphi = \frac{a_y}{g} \qquad (9\text{-}3)$$

In highway design, cross-slope is used in curves exactly for this purpose. Given the radius of turn and an intended travel (design) speed, the cross-slope will be chosen to produce a lateral acceleration in the range of zero to 0.1 g's. The speed at which zero lateral acceleration is experienced on a superelevated curve is called the "neutral speed."

Returning again to Eq. (9-2), as the lateral acceleration builds up, the load on the inside wheels must diminish. It is through this process that the vehicle acts to resist, or counterbalance, the roll moment in cornering. The limit cornering condition will occur when the load on the inside wheels reaches zero (all the load has been transferred to the outside wheels). At that point, rollover will begin because the vehicle can no longer maintain equilibrium in the roll plane. The lateral acceleration at which rollover begins is the "rollover threshold" and is given by:

$$\frac{a_y}{g} = \frac{t/2 + \varphi h}{h} \qquad (9\text{-}4)$$

With no cross-slope the lateral acceleration that constitutes the "rollover threshold" is simply "t over 2h." This simple measure of rollover threshold is

often used for a first-order estimate of a vehicle's resistance to rollover. It is especially attractive because it requires knowledge of only two vehicle parameters—the tread and the CG height. However, the estimates are very conservative (predicting a threshold that is greater than the actual) and are more useful for comparing vehicles rather than predicting absolute levels of performance. (Some dynamicists use the inverse form of this threshold, "h over t/2" as a measure of rollover propensity, in which case a higher value corresponds to a lower rollover threshold.)

The rollover threshold differs distinctively among the various types of vehicles on the road. As examples, typical values fall in the following ranges [1]:

Vehicle Type	CG Height	Tread	Rollover Threshold
Sports car	18-20 inches	50-60 inches	1.2-1.7 g
Compact car	20-23	50-60	1.1-1.5
Luxury car	20-24	60-65	1.2-1.6
Pickup truck	30-35	65-70	0.9-1.1
Passenger van	30-40	65-70	0.8-1.1
Medium truck	45-55	65-75	0.6-0.8
Heavy truck	60-85	70-72	0.4-0.6

The rigid-vehicle model suggests that the lateral acceleration necessary to reach the rollover of passenger cars and light trucks exceeds the cornering capabilities arising from the friction limits of the tires (typical peak coefficients of friction are on the order of 0.8). That being the case, it is possible for the car to spin out on a flat surface without rolling over. From that one might conclude that rollover with these types of vehicles should be rare; however, the accident statistics [2] prove otherwise and motivate the more in-depth analysis of rollover phenomena that will be addressed later in this chapter. In the case of heavy trucks it is equally obvious that it is possible to reach the rollover threshold within the friction limits of the tires [3]. As a consequence, a heavy vehicle is at risk of rollover if the driver allows the vehicle to spin out on a dry road surface.

Rigid-body rollover can be illustrated more fully by way of a plot of the lateral acceleration as a function of roll angle, ϕ, for equilibrium of the vehicle, as shown in Figure 9.2. Because of the rigid vehicle assumption, while at zero

roll angle the lateral acceleration can be any value up to the rollover threshold. Once this threshold is reached, the inside wheels lift. The vehicle begins to roll and the equilibrium lateral acceleration decreases with angle because the center of gravity is lifting and shifting toward the outside wheels.

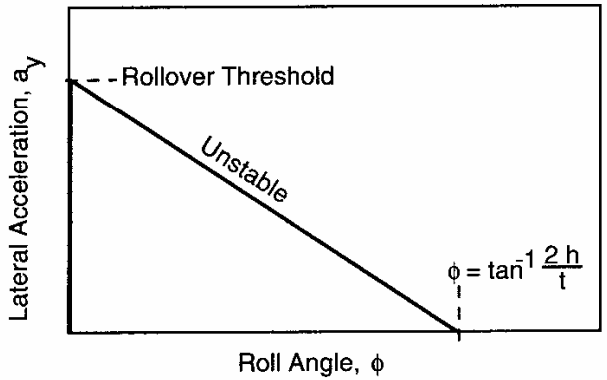

Fig. 9.2 Equilibrium lateral acceleration in rollover of a rigid vehicle.

This region is an inherently unstable roll condition. Consider a vehicle tipped up on two wheels in a turn. In order to be in equilibrium, the vehicle roll angle must be at the precise value on the above curve where the equilibrium lateral acceleration matches the actual. Any slight disturbance that increases the roll angle reduces the equilibrium lateral acceleration, and the excess lateral acceleration produces a roll acceleration that further increases the angle driving away from the equilibrium point. If left to continue, the vehicle roll attitude accelerates rapidly to complete the rollover in a matter of a second or two.

This brings up the issue of defining when rollover begins. Because of the inherent instability of the vehicle when the inside wheels leave the ground, it is appropriate to consider wheel lift-off as the beginning of rollover. Nevertheless, it is possible for a driver to halt the action by quickly steering out of the turn, thereby reducing the lateral acceleration to a level that will return the vehicle to an upright position. Quick response (within a fraction of a second) is necessary because of the speed with which rollover proceeds. Theoretically, rollover becomes irrecoverable only when the roll angle becomes so large that the center of gravity of the vehicle passes outboard of the line of contact of the outside wheels. This limit corresponds to the point in the figure where the equilibrium lateral acceleration reaches zero ($\phi = \tan^{-1}(2h/t)$).

It is well recognized that "stunt" drivers can take a vehicle up to this point and drive on two wheels for extended distances despite the instability. Yet, it is a rare event for a typical motorist to avoid rollover if the vehicle should inadvertently roll to this extreme position. Taking a conservative viewpoint, the automotive engineer should assume that the great majority of drivers will not have the reflexes or skills to deal with the instability once the wheels on one side of the vehicle leave the ground, and should focus on optimizing behavior of the vehicle up to that point.

QUASI-STATIC ROLLOVER OF A SUSPENDED VEHICLE

Neglecting the compliances in the tires and suspensions, as was done in the previous analysis, overestimates the rollover threshold of a vehicle [4]. In cornering, the lateral load transfer unloads the inside wheels of the vehicle and increases load on the outside wheels. Concurrently the body rolls with a lateral shift of the center of gravity toward the outside of the turn. The offset of the center of gravity reduces the moment arm on which the gravity force acts to resist the rollover.

Figure 9.3 illustrates these mechanisms on a vehicle with a suspension system. The body is represented by its mass, M_s, connected to the axle at an imaginary point known as the roll center. The roll center is the pivot around which body roll occurs, and is also the point at which lateral forces are transferred from the axle to the sprung mass.

A simple analytical solution for the rollover threshold is possible if the mass and roll of the axles are neglected [4, 5]. Taking moments about the point where the right wheel contacts the ground, and assuming the left wheel load has gone to zero gives:

$$\Sigma M_o = 0 = M_S a_y h - M_S g[t/2 - \phi (h - h_r)] \qquad (9\text{-}5)$$

Now the roll angle of the sprung mass, ϕ, is simply the roll rate, R_ϕ, times the lateral acceleration, a_y. The roll rate is the rate of change of roll angle with lateral acceleration expressed in units of radians per g. Substituting to eliminate the roll angle and solving for lateral acceleration yields:

$$\frac{a_y}{g} = \frac{t}{2h} \frac{1}{[1 + R_\phi(1 - h_r/h)]} \qquad (9\text{-}6)$$

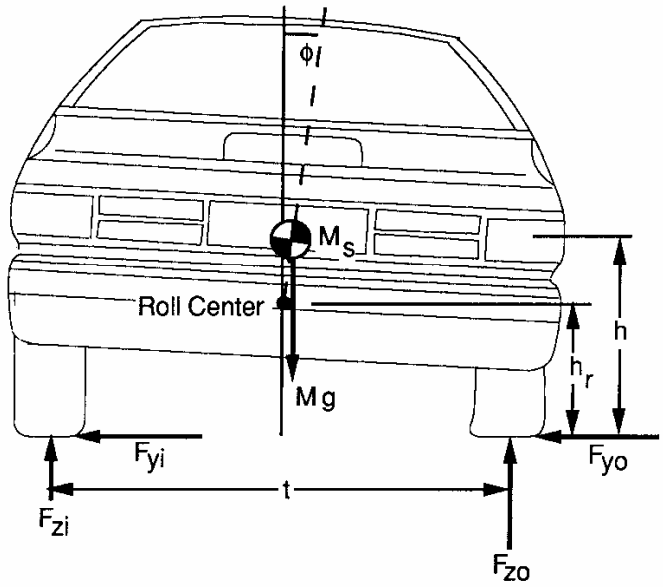

Fig. 9.3 Roll reactions on a suspended vehicle.

where:

- h = Height of the center of gravity above the ground
- h_r = Height of the roll center above the ground at the longitudinal CG location
- t = Tread
- R_ϕ = Roll rate (radians/g)

Thus taking into account the lateral shift of the CG, the rollover threshold is "t over 2h" reduced by the second term on the right-hand side of the above equation. For a passenger car with $h_r/h = 0.5$ and a roll rate of 6 degrees per g (0.1 radians/g), the second term evaluates to approximately 0.95. That is, the rollover threshold is reduced approximately 5 percent due to this mechanism. Sports vehicles with a low roll rate and low center of gravity experience less of these effects, whereas luxury cars with a higher roll rate and higher center of gravity will experience more. Solid axles (which tend to have a high roll center) also reduce the effect of lateral shift compared to independent suspensions (which have low roll centers) due to the reduced distance from the CG to the roll center.

A similar mechanism arises from lateral deflections of the outside tires, which allows the load center under the tires to move inboard during cornering, effectively reducing the tread. For typical passenger cars the lateral shift of the tire contact point may contribute another 5 percent reduction to the threshold.

A more precise analysis of the lateral shift and the effect on the rollover threshold requires detailed modeling of the tire and suspension systems. Among the mechanisms that must be considered are:

- Lateral shift of the sprung mass center of gravity caused directly by roll about the suspension roll center.
- Lateral shift of the suspension roll center with respect to the tread, due to roll of a solid axle or camber of independently sprung wheels.
- Lateral movement of the action point of the tire vertical force due to cornering forces and deflections (these factors being reflected in changes to the overturning moment under combined cornering and camber).
- Differences in behavior of the front and rear suspensions and wheels.

Taking into account all of these effects is less amenable to analytical solution. Particularly, if the front and rear suspensions are much different in load or roll stiffness, it is necessary to model simultaneous behavior of both front and rear suspensions. Computer programs [6] are the normal approach to calculating quasi-static rollover threshold when these effects are to be included.

When these mechanisms are precisely modeled, the quasi-static roll response of a motor vehicle will take the form shown in Figure 9.4. At low levels of lateral acceleration the vehicle roll response increases linearly with a slope equal to the roll rate. This proceeds until one of the inside wheels lifts off. (Both the front and rear wheels will not necessarily leave the ground at precisely the same instant on an actual vehicle due to differences between the front and rear suspensions and their loads. In the case of multi-axle trucks, the slope will change with the lift-off of each inside wheel, resulting in a curve with three or four line segments in this area.) At this point the response changes to a lower slope because the roll rate is reduced to that provided by the one suspension that remains in contact with the ground. When the second inside wheel lifts, the rollover threshold has been reached. Thereafter, the roll response follows the downward sloping line, closely equivalent to that discussed in the case of the rigid vehicle.

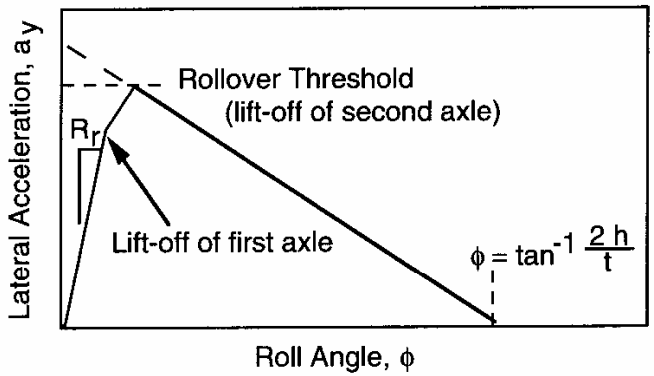

Fig. 9.4 Equilibrium lateral acceleration in rollover of a suspended vehicle.

The plot indicates that for a vehicle with a given tread and CG height, the highest rollover threshold will be achieved by maintaining the sprung mass roll rate at the highest possible level (using suspensions with high roll stiffness), and by designing the front and rear suspensions so as to have the inside wheels lift off at the same roll angle condition.

Experimental methods have been developed to measure the quasi-static rollover threshold by use of a "tilt-table." As suggested by the name, the table tilts the vehicle in the lateral, or roll, plane and, from measurement of the angle at which rollover occurs, the threshold is determined. The method is reasonably accurate for heavy trucks which have a high center of gravity and experience rollover at small angles (on the order of 20 to 25 degrees).

For passenger cars, however, the rollover threshold may well be on the order of 45 degrees. At high angles the component of the vehicle weight acting downward in the vehicle plane is reduced substantially (30 percent at 45 degrees). The reduced loading on the suspensions and tires raises the body above its normal ride position causing premature rollover and invalidating the test. In order to avoid these errors, test procedures must be devised which impose a lateral force at the center of gravity location (the "cable pull" test [5]) or by applying a pure moment to the body of the vehicle.

TRANSIENT ROLLOVER

Heretofore, the analyses have been quasi-static, and model rollover only when the vehicle is in a steady turn. (The quasi-static assumption is reasonable

only when the lateral acceleration is changing much more slowly than the vehicle responds in roll.) In order to examine vehicle response to rapidly changing lateral acceleration conditions, a transient model is necessary. A transient response model attempts to represent the way the vehicle roll varies with time. At the most elementary level, a simple roll model may be used to examine response to analytically simple examples of time-varying lateral accelerations. Alternately, more comprehensive models combining motions in the yaw and roll planes have been developed to examine roll response associated with specific maneuvering conditions.

Simple Roll Models

The first and simplest approach for investigating transient roll response is with a model similar to the suspended vehicle discussed previously, to which is added a roll moment of inertia for the sprung mass as shown in Figure 9.5. The body is represented by its mass, M_S, and roll moment of inertia, I_{xxs}. Not shown is the suspension stiffness and damping on the left and right side of the vehicle. Again, the properties of the front and rear tires and suspensions may be combined to simplify the analysis.

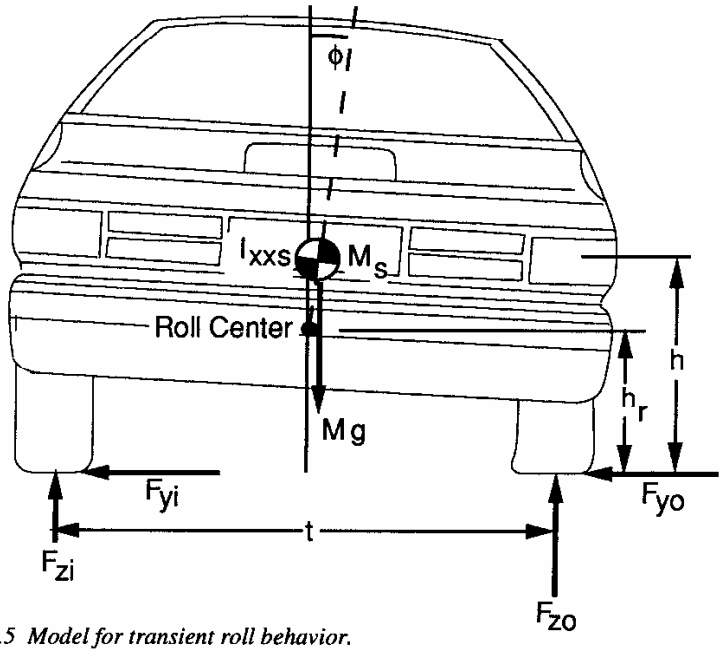

Fig. 9.5 Model for transient roll behavior.

This model can be useful for examining vehicle response to suddenly applied lateral accelerations in the nature of a step input. It is also representative of the transient that occurs when a vehicle goes into a slide with the brakes locked up and then experiences a sudden return of the cornering forces when the brakes are released. Or, it may simulate the effect of sliding from a low-friction surface onto one of a high-friction level.

The differential equations for motion in the roll plane can be written and solved analytically for the case of a step input [4]. The response of the system will be similar to that of a damped single-degree-of-freedom system exposed to a step input as shown in Figure 9.6.

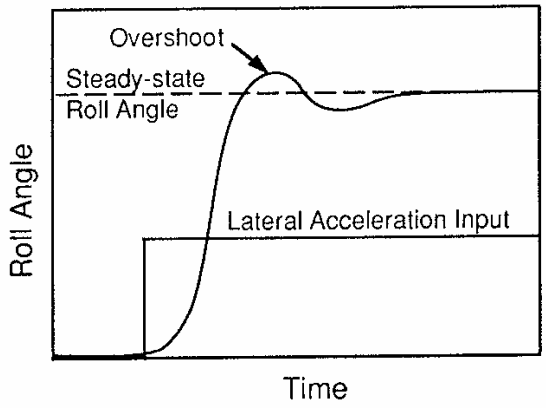

Fig. 9.6 Roll response to a step input.

With the sudden acceleration input the roll angle responds like a second-order system. With less than critical damping the angle rises toward the equilibrium point, but because it has roll velocity when it reaches equilibrium, it overshoots. Thereafter it reverses and may oscillate before settling to a steady-state angle at the equilibrium position.

The fact that the roll angle can overshoot means that wheel lift-off may occur at lower levels of lateral acceleration input in transient maneuvers than for the quasi-static case. A step steer maneuver that produces a lateral acceleration level just below the quasi-static threshold can result in rollover in the transient case because of the overshoot. Thus the rollover threshold is lower in transient maneuvers.

The extent to which overshoot occurs is dependent on roll damping. Figure 9.7 shows the calculated rollover threshold as a function of the damping ratio for a passenger car, utility vehicle,[1] and a heavy truck. The lowest rollover threshold occurs when there is no damping. It rises with the damping ratio but at a diminishing rate. Even so, the benefits of roll damping are evident. The rollover threshold of the automobile increases by nearly one-third in going from zero to 50 percent of critical damping. For the automobile and the utility vehicle, the transient in a step steer will reduce the rollover threshold by about 30 percent from the "t over 2h" value, compared to only about 10 percent for the quasi-static suspended vehicle. For the heavy truck the reduction is nearly 50 percent [4].

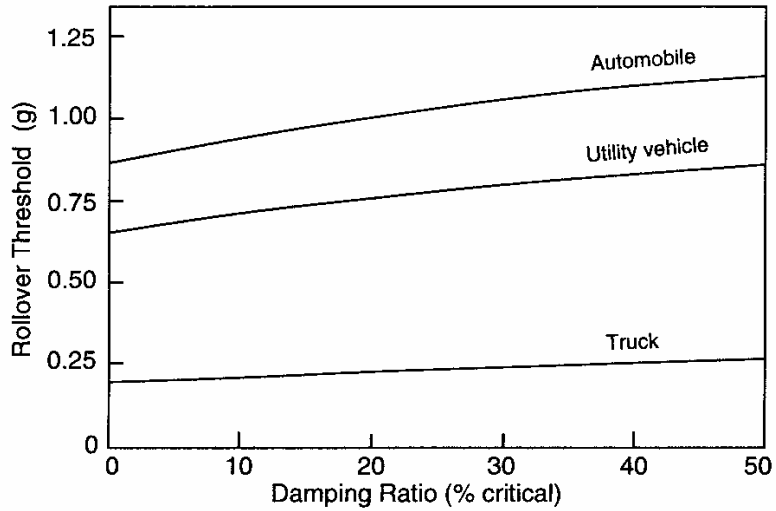

Fig. 9.7 Effect of damping ratio on rollover threshold in a step steer [4].

Exercising this model with a sinusoidal acceleration input illustrates the effect of roll resonance on the rollover threshold. A sinusoidal acceleration is similar to the input that would be experienced in a slalom course.

[1] Utility vehicles are defined as multipurpose passenger vehicles (other than passenger cars) which have a wheelbase of 110 inches or less and special features for occasional off-road operation.

Under a sinusoidal lateral acceleration the response of the vehicle will be dependent on the frequency of the input. Figure 9.8 shows the frequency dependence of the lateral acceleration threshold at which rollover (wheel lift-off) occurs for an automobile, utility vehicle and a heavy truck. At zero frequency the thresholds approach the steady-state values that would be obtained from the quasi-static model of the suspended vehicle. With increasing frequency the thresholds drop, going through a minimum which corresponds to the roll resonant frequency.

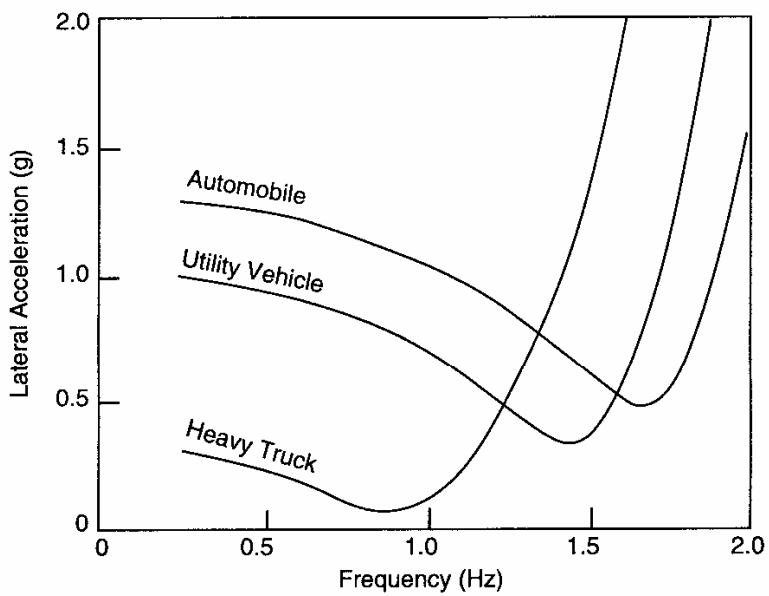

Fig. 9.8 Rollover threshold as a function of frequency in a sinusoidal steer [4].

The roll resonant frequency for a heavy truck, which is less than one cycle per second because of its high center of gravity, makes it especially vulnerable to these dynamics. Experience has shown that "lane-change type" maneuvers executed over two seconds (one-half Hz) are well capable of exciting roll dynamics that can precipitate rollover of heavy trucks [7]. The two-second timing is easily accomplished by the driver [8] and corresponds to the steering frequency necessary to move 8 to 10 feet laterally to avoid a road obstacle at normal highway speeds. As a result, lane change maneuvers have been identified as a common cause of heavy-truck rollover accidents [7].

The utility vehicle and automobile, which by comparison have a lower CG height to tread width ratio, have roll resonant frequencies of 1.5 Hz and greater. In order to tune into roll resonance, a very rapid steer oscillation is necessary. Studies of driver behavior show that steering inputs at these frequencies are normally of low amplitude [8]. Further, they produce only minor deviations in lateral position because of the attenuation of yaw response at these frequencies. (Even a relatively high-amplitude steer oscillation at 2 Hz will only cause the vehicle to move about one foot laterally.) Thus a logical conclusion is that simple roll resonance is of less significance to rollover with passenger cars and utility vehicles. In order to perform lane change maneuvers or negotiate slalom courses the timing of side-to-side oscillations is much slower (on the order of 4 seconds). Exciting frequencies below 1 Hz elicits vehicle roll response that is close to the quasi-static behavior. Therefore, from the rollover perspective, the step steer actually represents a more challenging maneuver to these vehicles than the sinusoidal steer.

Yaw-Roll Models

To develop the most complete and accurate picture of vehicle roll behavior, it is necessary to rely on more comprehensive vehicle models which simulate both yaw and roll response. Yaw motions produce the lateral accelerations causing roll motions, and roll motion in turn alters yaw response through the modification of tire cornering forces arising from lateral load transfer and suspension action. A number of computer models have been developed by the vehicle dynamics community to investigate this behavior [9, 10, 11].

Using a more comprehensive model to examine sinusoidal steer reveals an additional phenomenon of importance to vehicle roll response—the phasing of front and rear tire forces. On vehicles steered by the front wheels only, a steering action causes the front wheels to develop lateral force rather immediately (delayed only by the relaxation length of the tires), but the rear wheels do not develop a force until a sideslip angle builds up. As a result the rear wheel tire forces exhibit a phase lag in a sinusoidal steer. The phenomenon is illustrated for a passenger car in Figure 9.9.

In the one-cycle-per-second sinusoidal steer shown, the lateral forces on the rear wheels lag the fronts by approximately 0.2 seconds, corresponding to about a 70-degree phase lag. The lateral acceleration, which depends on the sum of the forces, is diminished by the phase lag. If the lateral force from both front and rear tires peaked simultaneously, the lateral acceleration would reach

0.8 g rather than 0.5 g in this maneuver. At higher frequencies the attenuation is even greater.

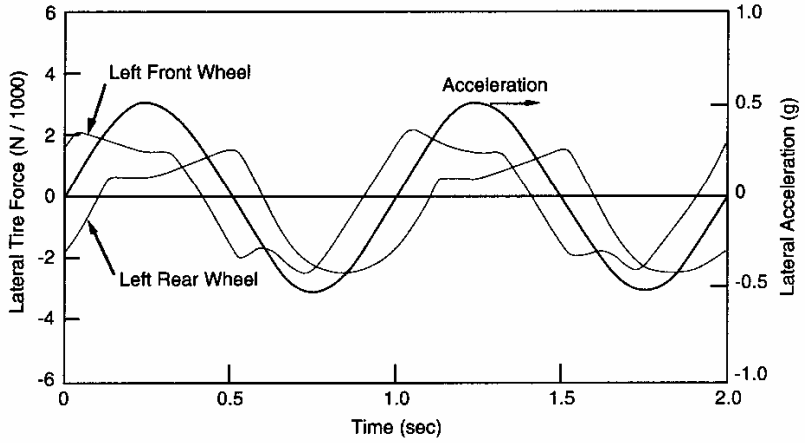

Fig. 9.9 Phasing of tire forces and lateral acceleration in a sinusoidal steer [4].

The effect of the phase lag is to allow the vehicle to yaw and change direction while moderating the level of lateral acceleration by spreading the acceleration over a longer time period. With passenger cars this effect contributes to a perception of lack of responsiveness (or sluggishness) in transient cornering. Since the time lag increases with the wheelbase of the vehicle, large cars do not feel as responsive in these maneuvers as small cars. Four-wheel-steer cars invariably steer the rear wheels in the same direction as the front wheels (albeit at a lesser steer angle) to eliminate the phase lag, thereby improving responsiveness in transient cornering. It could be argued that four-wheel steer—like any other feature that enhances cornering response—may therefore contribute to behavior that increases the potential for rollover. Keeping in mind that the roll resonance frequency of passenger cars is in the range of 1.5 to 2 Hz, the absence of the phase lag with four-wheel steer makes it easier for a motorist to inadvertently excite roll resonance in an evasive maneuver.

On very long vehicles like school buses, trucks and tractor-trailers, the phase lag may be very pronounced. Figure 9.10 shows the lateral accelerations experienced on the tractor and full trailer of a doubles combination. (A "doubles" is a tractor-semitrailer pulling a full trailer.)

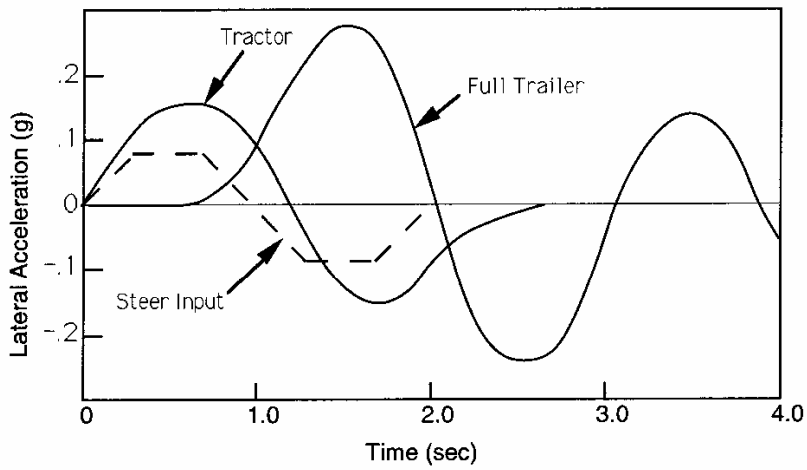

Fig. 9.10 Lateral accelerations on a tractor and full trailer [3].

A sinusoidal steer two seconds in duration excites both a rearward amplification of the yaw response and roll resonance of the full trailer, such that the full trailer experiences a much larger lateral acceleration than the tractor. Because of the vehicle length, the lateral acceleration on the full trailer is almost exactly 180 degrees out of phase with the tractor. The rearward amplification, which amounts to "cracking the whip," is recognized as very detrimental to safety performance of doubles combinations because low-level maneuvers on the tractor are amplified and can cause the full trailer to roll over. One way to prevent this is to use a hitch arrangement between the tractor-semitrailer and the full trailer which provides roll coupling. With roll coupling the out-of-phase lateral acceleration allows the full trailer to help the tractor-semitrailer resist rollover during the beginning of the maneuver, and the tractor-semitrailer helps the full trailer during the end of the maneuver. This feature is being used in the new generation of hitches for doubles combinations that are being developed at this time.

Tripping

A final class of rollover accidents that requires special modeling is the case where a vehicle skids laterally impacting an object, such as a curb or soft ground, which trips the vehicle into rollover. Engineering models for this phenomenon have been developed [12], although the understanding of the

phenomenon is in the embryonic stage. A nonlinear eight-degree-of-freedom simulation model was developed which utilizes simple linear sub-systems to model tires, suspension and impact forces. The vehicle is represented by a sprung mass and an unsprung mass (combining the front and rear suspensions), as shown in Figure 9.11. The masses have degrees of freedom in roll, lateral and vertical translation, while vehicle yaw and pitch are analyzed using a single lumped mass. The impact force for lateral wheel/curb impact is modeled using both plastic and elastic deformations. Damping effects are included through energy dissipative forces in the tires, the lateral bushing between the sprung and unsprung masses, the shock absorbers in the suspension, and the wheel/curb impact force. This model was developed for the National Highway Traffic Safety Administration with public funds, and therefore should be available to any user by request to the Administration.

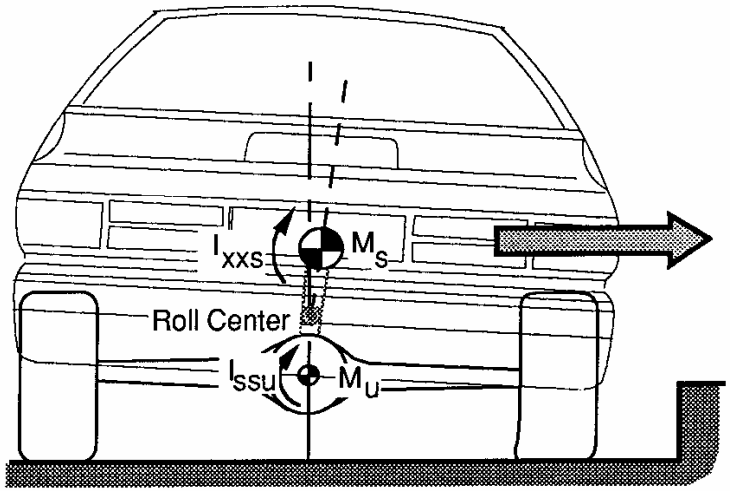

Fig. 9.11 Vehicle approaching a tripped rollover.

Models of this type have been used to investigate the conditions under which vehicles can experience tripped rollover, focusing on whether sufficient energy is developed in the curb impact to raise the CG of the vehicle to the rollover point [13]. At impact with the curb, rotation of the vehicle produces kinetic energy equal to one-half times the moments of inertia of the sprung and unsprung masses about their rotation points, times their respective rotational velocities squared. Concurrently, the lifting of the vehicle CG adds potential

energy equal to the mass times the increase in CG height. If the total of these two exceeds the potential energy necessary to lift the CG over the outside wheels, rollover is predicted.

From an engineering viewpoint this energy approach has many weaknesses because of the assumption that all of the kinetic energy is transformed to potential energy, raising the CG to the rollover point. It neglects additional energy input or dissipation from wheel contact with the ground during the process, and energy storage or dissipation in the tires and suspensions.

Figure 9.12 shows typical examples of the results from an energy analysis of the curb impact process. The vertical axis plots the net rollover energy, which is the instantaneous total of the rotational kinetic energy plus the potential energy of the elevated CG. The rollover threshold is the potential energy level associated with the CG passing over the outside wheels. If the rollover energy exceeds the threshold, rollover will occur.

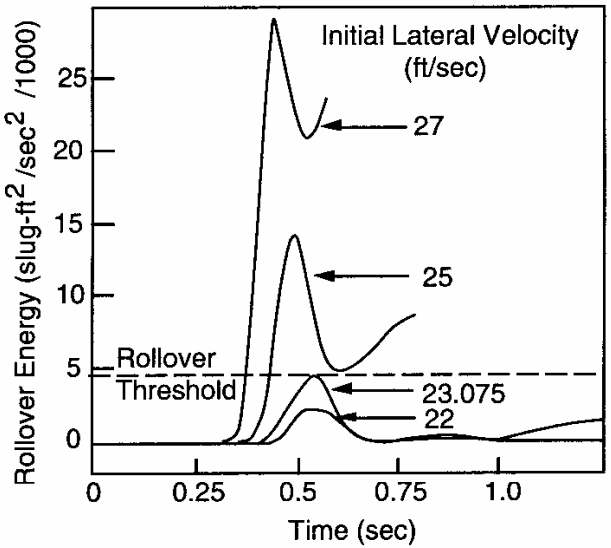

Fig. 9.12 Rotational energy during curb impact.

In the analysis, the simulated vehicle is given an initial lateral velocity while still 7.5 feet from the curb. With a 22 ft/sec initial velocity, the impact causes a brief rise in the rollover energy level due to the kinetic energy of

rotation and potential energy from elevation of the CG. However, the net energy always remains well below the threshold, so rollover does not occur. With time the energy is damped out by the suspension system.

The velocity of 23.075 ft/sec represents the case just sufficient to take the vehicle to rollover. The rollover energy rises to the rollover point, where the kinetic energy component nearly reaches zero. Thereafter, the energy drops as the vehicle completes the rollover. At the higher initial speeds of 25 and 27 ft/sec, rollover occurs.

This methodology was used to examine the effect of vehicle parameters on the propensity for rollover. Not surprisingly, the geometric parameters of track width and CG height are found to be most influential. The second most important variable is the deformation characteristics of the vehicle at impact. By spreading the impact deformation over a large distance, the energy dissipated in crush reduces the amount of energy which can contribute to the vehicle's rolling motion. The weight of the vehicle appears to have little effect except as it affects the ride height—greater weight lowering the CG height. Likewise, the suspension stiffness and damping properties were found to be of little influence.

ACCIDENT EXPERIENCE

The primary motivation for giving attention to the mechanics of rollover in vehicle design is to reduce or prevent rollover accidents. In recent years, analysts have examined the accident records in an effort to identify those characteristics of vehicles that appear to be most closely correlated with rollover experience—the presumption being that the frequency of rollover accidents can be reduced by altering those correlated properties of the vehicles.

It is common practice in these studies to stratify the analyses both in the types of accidents and the types of vehicle. In the simplest treatment, the frequency of rollover in all accidents of a given make of vehicle might be considered on the assumption that all vehicles are exposed to the same general spectrum of accident types. Therefore, any atypical characteristics of those vehicles are potential causes of rollover and good design practice would argue that they should be eliminated. A flaw in this approach, however, becomes evident when it is recognized that utility vehicles experience more off-road rollover accidents than passenger cars, in part because they operate more frequently in this environment. Improving their rollover experience by making them lower and wider can only be achieved with a penalty in off-road mobility.

In the interest of normalizing accident statistics, it is then necessary to distinguish between on-road and off-road accidents, rollovers as the first or only event of an accident, rollovers as a subsequent event, and the use or exposure factors for the class of vehicle. With regard to vehicle types, they are often classified as passenger cars, utility vehicles (high CG four-wheel-drive vehicles used for personal transport), light trucks (used for personal transport and light hauling) and heavy trucks.

Systems Technology, Inc., in the work they have done for the NHTSA [14], examined the rollover accident experience of small cars as a function of the rollover potential. A replot of some of their data is shown in Figure 9.13. The rollover rate (fatal accidents per 100,000 new car years) is plotted against rollover threshold for accidents where rollover was the first event or a subsequent event in the accident. The data show a trend of decreasing rollover involvement as the threshold increases. However, the degree of scatter in the plot suggests that more than just the rollover threshold is needed to explain the accident experience. For example, the Mercury Capri has three times as many rollover accidents as the Vega, even though they both have the same rollover threshold. Because of this broad disparity in behavior, there is no guarantee to the automotive designer that good rollover experience is assured by increasing the rollover threshold.

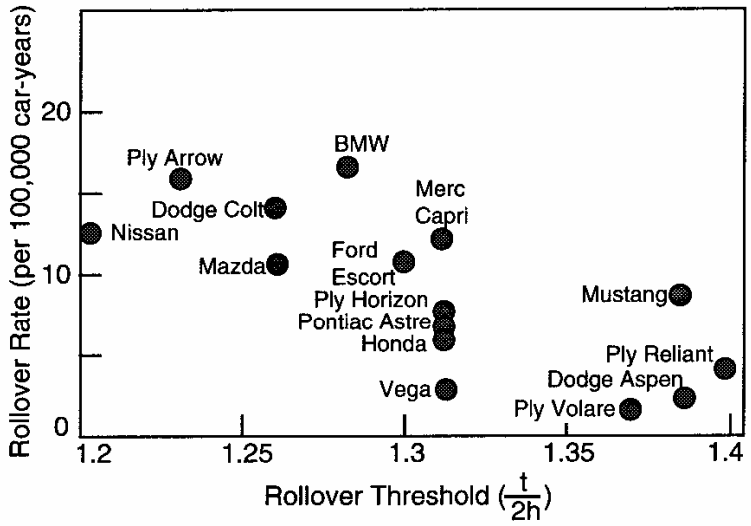

Fig. 9.13 Rollover accident rates of small cars [14].

Observations of this nature are common when examining rollover accident rates and prompt analysts to hypothesize explanations for the differences in behavior between vehicle makes. A methodical analysis of rollover accident experience for passenger cars and utility vehicles was recently conducted by Robertson and Kelley [15] in which some of the potential explanatory factors were examined. In their work, a broader range of vehicles was considered. Figure 9.14 shows their data for number of accidents per 100,000 vehicle-years in which rollover was the "first harmful event."

As plotted here the data would appear to show a much more direct relationship between rollover threshold and accident rates. This impression comes about because of the inclusion of the utility vehicles (CJ-5, CJ-7, Blazer, and Bronco) which have much higher accident rates. Among the automobiles, which have thresholds ranging from 1.25 to 1.6, there is no trend evident. The high involvement of the utility vehicles has prompted proposals for Federal Motor Vehicle Safety Standards (FMVSS) requiring new vehicles to have a minimum rollover threshold of 1.2. Over-involvement of utility vehicles is not unique to this study, but has been found in other studies [16, 17] as well.

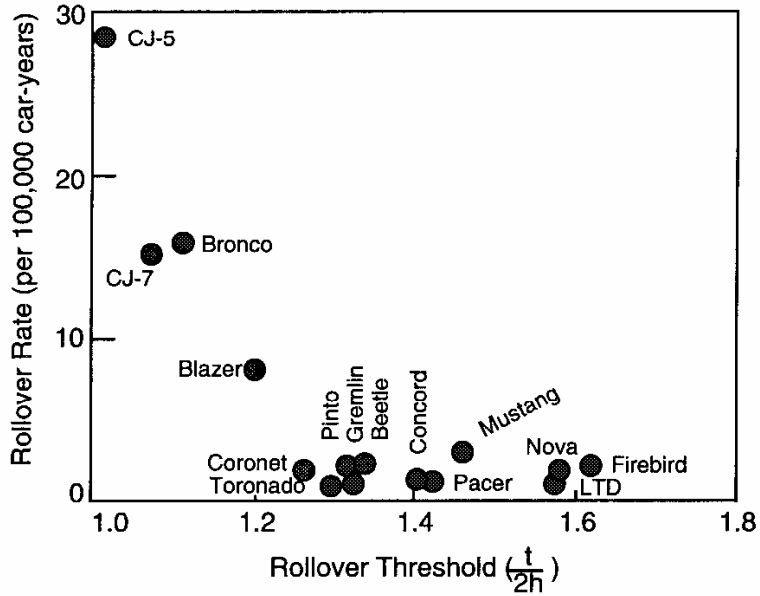

Fig. 9.14 Rollover rates of cars and utility vehicles [15].

The authors used the accident records to examine other factors which might be peculiar to the use of the different kinds of vehicles, to determine if they might be correlated to the accident experience, thereby providing other potential explanations for the high frequency of rollover accidents with utility vehicles. For example, it might be argued that the type of driver most attracted to utility vehicles is one willing to take more risks and therefore is more likely to have accidents. However, when the non-rollover fatal accident rates are compared, the utility vehicle rates are seen to be no higher than the passenger cars. When driver characteristics—suspended licenses, history of traffic violations, DWI convictions, or blood alcohol level at the time of the accident—were examined, no explanations were found.

Similarly, the road environment—urban vs. rural, interstate vs. other roads, straight vs. curved, dry vs. wet, etc.—had no correlation. The only significant environmental factor was whether the vehicle crashed on the road or after leaving it. The ratio of rollover fatal crashes on the road relative to those that left the road was substantially higher among the utility vehicles. Finally, the possibility that utility vehicles accumulate higher mileage as a potential explanation of higher rollover accident rates was examined, but with the conclusion that the usage rates necessary to account for the higher accident rates were unreasonable.

In general, other reviews of accident experience confirm the conclusions reached above, even though the Robertson study is easily criticized. Numerous studies show conflicting results and interpretations [16, 17, 18] because of the uncertainty in identifying rollover threshold as the most significant variable related to rollover frequency for these classes of vehicles. In particular, the concern that other vehicle factors play a significant role appears justified. Vehicle control and handling stability are identified as important associated variables. Likewise, vehicle wheelbase can be shown to be correlated with rollover experience, suggesting that it is a combination of factors that must be controlled before effective action to reduce rollovers can be taken. Until those factors and interactions are known, it is considered premature to impose an arbitrary limit on rollover threshold on the industry.

Another class of vehicle that has received special attention for rollover accident experience is the heavy truck. For tractor-semitrailer vehicles, the frequency of rollover in single-vehicle accidents has been related to rollover threshold as shown in Figure 9.15. This curve is derived from accident data for three-axle tractors pulling two-axle van-type semitrailers reported to the Bureau of Motor Carrier Safety (BMCS) of the U.S. Department of Transportation. The data were resolved into the illustrated format assuming a rollover

threshold for each vehicle combination based on the gross vehicle weight reported to BMCS with each accident. Knowing the gross vehicle weight, the analysis assumed that payload was placed in a fashion representing medium-density freight. Typical values for tire, spring, and geometric properties were then employed to calculate rollover threshold for each increment of gross weight in the accident file. The relationship shown here has proved very useful in heavy truck design for assessing the potential benefits of design alternatives which can reduce rollover experience.

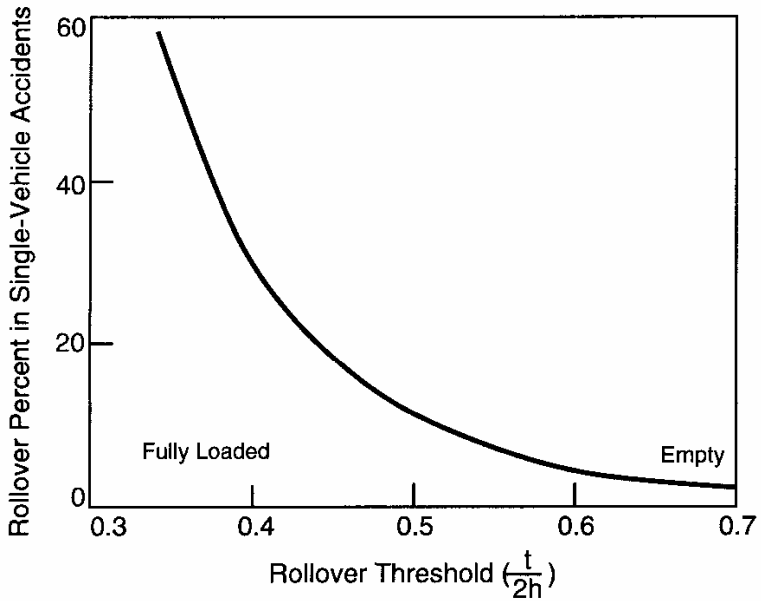

Fig. 9.15 Rollover frequency of tractor-semitrailers in single-vehicle accidents [3].

REFERENCES

1. Gillespie, T.D., and Ervin, R.D., "Comparative Study of Vehicle Roll Stability," The University of Michigan Transportation Research Institute, Report No. UMTRI-83-25, May 1983, 42 p.

2. "NCSS for Passenger Cars, January 1977-March 1979," Leda Ricci, Editor, The University of Michigan, Report No. UM-HSRI-80-36, 1980, 102 p.

3. Ervin, R.D., "The Influence of Size and Weight Variables on the Roll Stability of Heavy Duty Trucks," SAE Paper No. 831163, 1983, 26 p.

4. Bernard, J., Shannan, J., and Vanderploeg, M., "Vehicle Rollover on Smooth Surfaces," SAE Paper No. 891991, 1989, 10 p.

5. Bickerstaff, D., "The Handling Properties of Light Trucks," SAE Paper No. 760710, 1976, 29 p.

6. Gillespie, T.D., *et al.*, "Roll Dynamics of Commercial Vehicles," *Vehicle Systems Dynamics,* Vol. 9, 1980, pp. 1-17.

7. Ervin, R.D., *et al.*, "Ad Hoc Study of Certain Safety-Related Aspects of Double Bottom Tankers," The University of Michigan Transportation Research Institute, Report No. UM-HSRI-78-18, 1978, 78 p.

8. McLean, J.R., and Hoffman, E.R., "The Effects of Restricted Preview on Driver Steering Control and Performance," *Human Factors,* Vol. 15, No. 4, 1973, pp. 421-30.

9. Gillespie, T.D., and MacAdam, C.C., "Constant Velocity Yaw/Roll Program: User's Manual," The University of Michigan Transportation Research Institute, Report No. UM-HSRI-82-139, October 1982, 119 p.

10. McHenry, R.R., "Research in Automobile Dynamics—Computer Simulation of General Three-Dimensional Motions," SAE Paper No. 710361, 1971, 20 p.

11. Orlandea, N.V., "ADAMS Theory and Applications," Proceedings of Advanced Vehicle Systems Dynamics Seminar, Swets and Zeitlanger, 1987, pp. 121-166.

12. Rosenthal, R.J., *et al.*, "User's Guide and Program Description for a Tripped Roll Over Vehicle Simulation," Report No. DOT HS 807140, Systems Technology Inc., 1987, 76 p.

13. Nalecz, A. G., Bindemann, A.C., and Bare, C., "Sensitivity Analysis of Vehicle Tripped Rollover Model," Final Report, Contract No. DTNH22-8-Z-07621, University of Missouri-Columbia, July 1988, 100 p.

14. Wade Allen, R., *et al.*, "Validation of Tire Side Force Coefficient and Dynamic Response Analysis Procedures: Field Test and Analysis Comparison of a Front Wheel vs. a Rear Wheel Drive Subcompact,"

Systems Technology Inc., Working Paper No. 1216-6, Contract No. DTNH22-84-D-17080 - Task 4, 17 February 1986, 50 p.

15. Robertson, L.S., and Kelley, A.B., "Static Stability as a Predictor of Overturn in Fatal Motor Vehicle Crashes," *Journal of Trauma,* Vol. 29, No. 3, 1988, pp. 313-319.

16. Terhune, K.W., "A Comparison of Light Truck and Passenger Car Occupant Protection in Single Vehicle Crashes (MVMA)," Calspan Corporation, Report No. 7438-1, September 1986, 58 p.

17. Ajluni, K.K., "Rollover Potential of Vehicles on Embankments, Sideslopes, and Other Roadside Features," *Public Roads,* Vol. 52, No. 4, March 1989, pp. 107-113

18. Malliaris, A.C., Discerning the State of Crash Avoidance in the Accident Experience, Proceedings, Tenth International Technical Conference on Experimental Safety Vehicles, Technical Session No. 2, Crash Avoidance, July 1985, pp. 199-220.

CHAPTER 10
TIRES

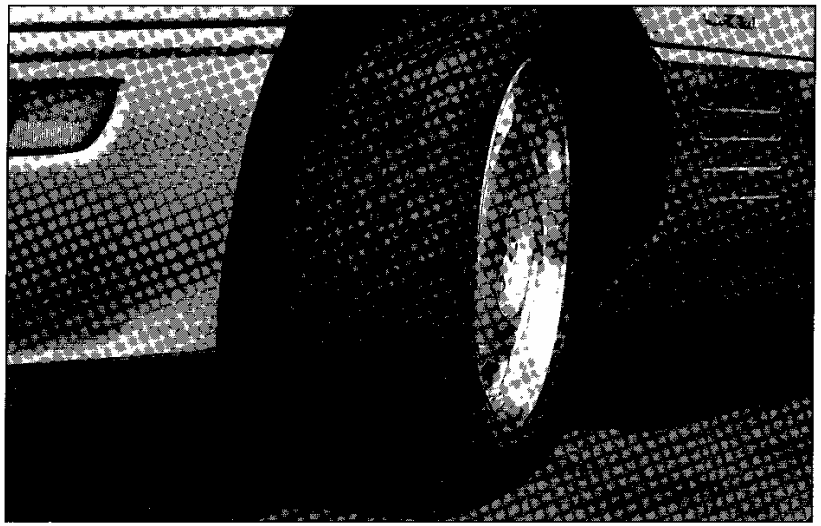

Eagle CS-C. (Photo courtesy of Goodyear Tire & Rubber Co.)

In modern highway vehicles all the primary control and disturbance forces which are applied to the vehicle, with the exception of aerodynamic forces, are generated in the tire-road contact patch. Thus it has been said that "the critical control forces that determine how a vehicle turns, brakes and accelerates are developed in four contact patches no bigger than a man's hand." A thorough understanding of the relationship between tires, their operating conditions, and the resulting forces and moments developed at the contact patch is an essential aspect of the dynamics of the total vehicle.

The tire serves essentially three basic functions:

1) It supports the vertical load, while cushioning against road shocks.
2) It develops longitudinal forces for acceleration and braking.
3) It develops lateral forces for cornering.

While the tire is a simple visco-elastic toroid, with modern refinement and optimization of its properties it is a very complex nonlinear system which is

difficult and complex to quantify [1]. Numerous simplified tire models have been developed in the past to approximate various performance properties [2, 3], but for the purposes of understanding their role in vehicle dynamics it is sufficient to look to empirical data to quantify essential properties.

As a mechanical structure, the elastic torus of a tire is composed of a flexible carcass of high-tensile-strength cords fastened to steel-cable beads that firmly anchor the assembly to the rim. The internal (inflation) pressure stresses the structure in such a way that any external force causing deformation in the carcass results in a tire reaction force. The behavioral characteristics of the tire depend not only on the operating conditions, but on the type of construction as well.

TIRE CONSTRUCTION

Two basic types of tire construction are broadly used—radial- and bias-ply tires. The two types are illustrated in Figure 10.1. Bias-ply tires were the standard in the early years of the American automotive industry until about the 1960s when the advantages of radial tires (developed in Europe) became recognized. Over several decades radial tires gradually displaced bias-ply tires on passenger cars, such that they are the standard today. The acceptance on trucks has lagged that of passenger cars, such that radial and bias tires see about equal use today. Bias-belted tires had a brief life as a cross between radial and bias tires during the transition period, but are seen very little today.

Radial construction is characterized by parallel plies (rubberized fabric reinforced by cords of nylon, rayon, polyester or fiberglass) running directly across the tire from one bead to the other at a nominal 90-degree angle to the circumference. These plies are referred to as the "carcass." This type of construction makes for an extremely flexible sidewall and a soft ride but provides little or no directional stability. Directional stability is supplied by a stiff belt of fabric or steel wire that runs around the circumference of the tire between the carcass and the tread. The cord angle in the belts is normally within about 20 degrees of the tread. In cornering, the belts help to "stabilize" the tread, keeping it flat on the road despite lateral deflection of the tire. Most radial passenger-car tires have a two-ply fabric sidewall, and either one or two steel belts, or two to six fabric belts.

In bias tire construction the carcass is made up of two or more plies extending from bead to bead with the cords at high angles (35 to 40 degrees to the circumference) and alternating in direction from ply to ply. High angles

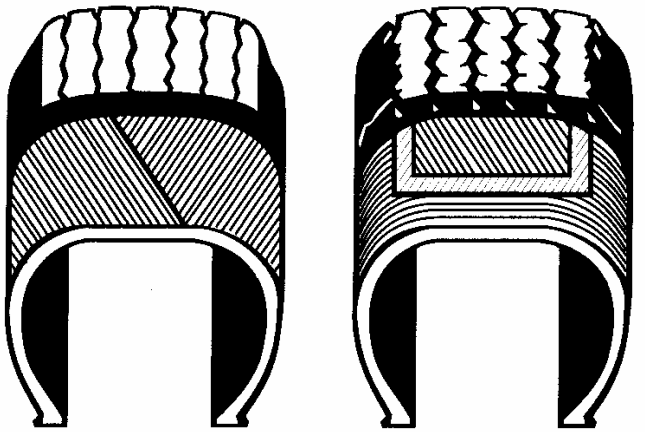

Fig. 10.1 Illustrations of bias and radial tire construction. (Courtesy of Goodyear Tire & Rubber Co.)

result in tires which are soft for ride comfort, but low angles are best for directional stability. Although a bias-ply carcass is laterally much stiffer than a radial-ply tire, in cornering, the bias plies allow the tread to roll under, putting more load on the outer ribs. Bias construction also causes more distortion in the contact patch as the toroid deforms into a flat shape, causing the tread to squirm in the contact patch [4] when rolling, as seen in Figure 10.2.

SIZE AND LOAD RATING

Tire size is denoted by one of several methods, variously including the section height (distance from the bead seat to the outer extreme of the tread), section width (maximum width across the shoulder), aspect ratio (ratio of height to width) and rim diameter [5]. The Tire & Rim Association [6] defines the method of designating tire sizes and the load range for which they should be designed by the manufacturers. Bias tire size (e.g., 6.95-14) denotes the section width with the first number and the rim size with the second, both in inch units. Radial tire size (e.g., 175R14) denotes the section width in millimeters and the rim diameter in inches. The more recent P-metric designation method (e.g., P175/70R14) denotes passenger car (P), 175-mm section width, 70 aspect ratio, radial (R-radial, B-belted, D-bias), and 14-inch rim.

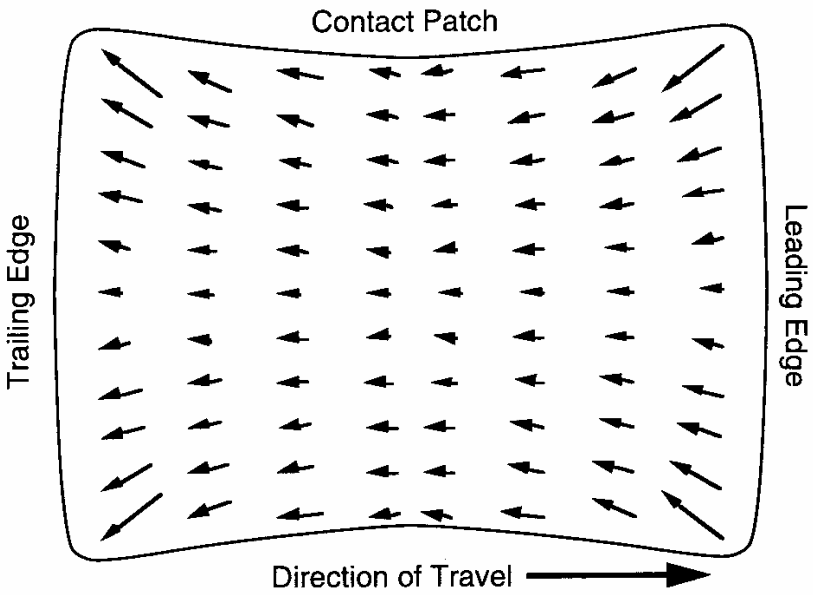

Fig. 10.2 Squirm in the contact patch of a bias-ply tire.

TERMINOLOGY AND AXIS SYSTEM

To facilitate precise description of the operating conditions, forces, and moments experienced by a tire, the SAE [5] has defined the axis system shown in Figure 10.3. The X-axis is the intersection of the wheel plane and the road plane with the positive direction forward. The Z-axis is perpendicular to the road plane with a positive direction downward. The Y-axis is in the road plane, its direction being chosen to make the axis system orthogonal and right-hand.

The following definitions are of importance in describing the tire and its axis system.

- Wheel Plane—central plane of the tire normal to the axis of rotation.
- Wheel Center—intersection of the spin axis and the wheel plane.
- Center of Tire Contact—intersection of the wheel plane and projection of the spin axis onto the road plane.

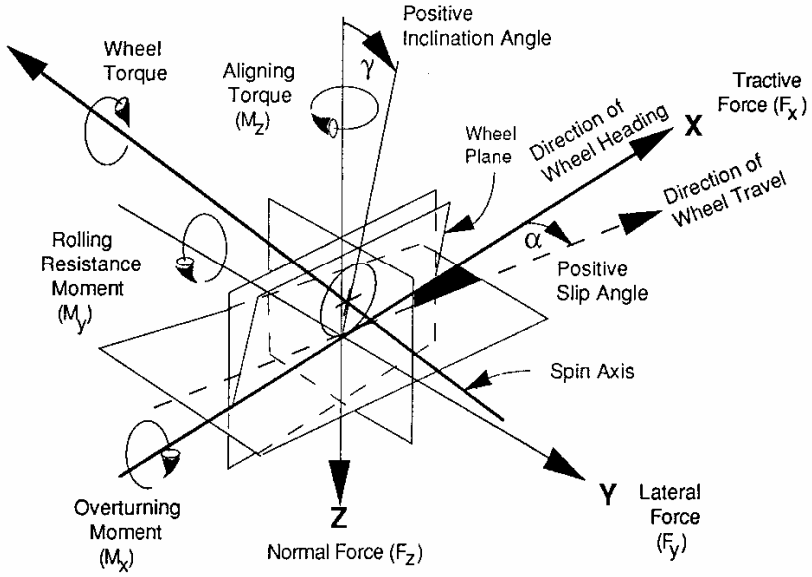

Fig. 10.3 SAE tire axis system.

- Loaded Radius—distance from center of tire contact to the wheel center in the wheel plane.
- Longitudinal Force (F_X)—component of the force acting on the tire by the road in the plane of the road and parallel to the intersection of the wheel plane with the road plane. The force component in the direction of wheel travel (sine component of the lateral force plus cosine component of the longitudinal force) is called tractive force.
- Lateral Force (F_Y)—component of the force acting on the tire by the road in the plane of the road and normal to the intersection of the wheel plane with the road plane.
- Normal Force (F_Z)—component of the force acting on the tire by the road which is normal to the plane of the road. The normal force is negative in magnitude. The term vertical load is defined as the negative of the normal force, and is thus positive in magnitude.
- Overturning Moment (M_X)—moment acting on the tire by the road in

the plane of the road and parallel to the intersection of the wheel plane with the road plane.

- Rolling Resistance Moment (M_y)—moment acting on the tire by the road in the plane of the road and normal to the intersection of the wheel plane with the road plane.
- Aligning Moment (M_z)—moment acting on the tire by the road which is normal to the plane of the road.
- Slip Angle (α)—angle between the direction of wheel heading and the direction of travel. Positive slip angle corresponds to a tire moving to the right as it advances in the forward direction.
- Camber Angle (γ)—angle between the wheel plane and the vertical. Positive camber corresponds to the top of the tire leaned outward from the vehicle.

MECHANICS OF FORCE GENERATION

The forces on a tire are not applied at a point, but are the resultant from normal and shear stresses distributed in the contact patch. The pressure distribution under a tire is not uniform but will vary in the X and Y directions. When rolling, it is generally not symmetrical about the Y-axis but tends to be higher in the forward region of the contact patch. Both of these phenomena are shown in Figure 10.4.

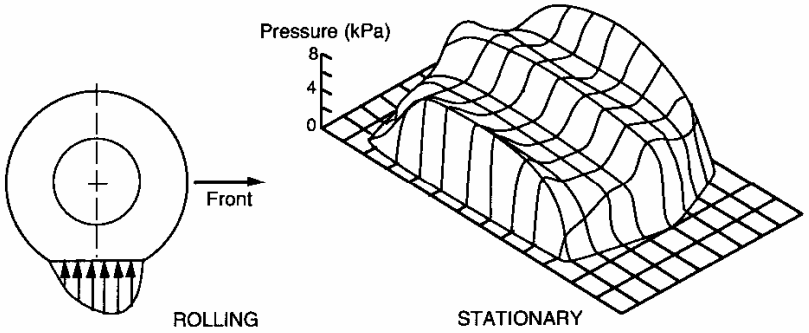

Fig. 10.4 Pressure distributions under a rolling and non-rolling tire.

Because of the tire's visco-elasticity, deformation in the leading portion of the contact patch causes the vertical pressure to be shifted forward. The centroid of the vertical force does not pass through the spin axis and therefore generates rolling resistance. With a tire rolling on a road, both tractive and lateral forces are developed by a shear mechanism. Each element of the tire tread passing through the tire contact patch exerts a shear stress which, if integrated over the contact area, is equal to the tractive and/or lateral forces developed by the tire.

There are two primary mechanisms responsible for the friction coupling between the tire and the road [4] as illustrated in Figure 10.5.

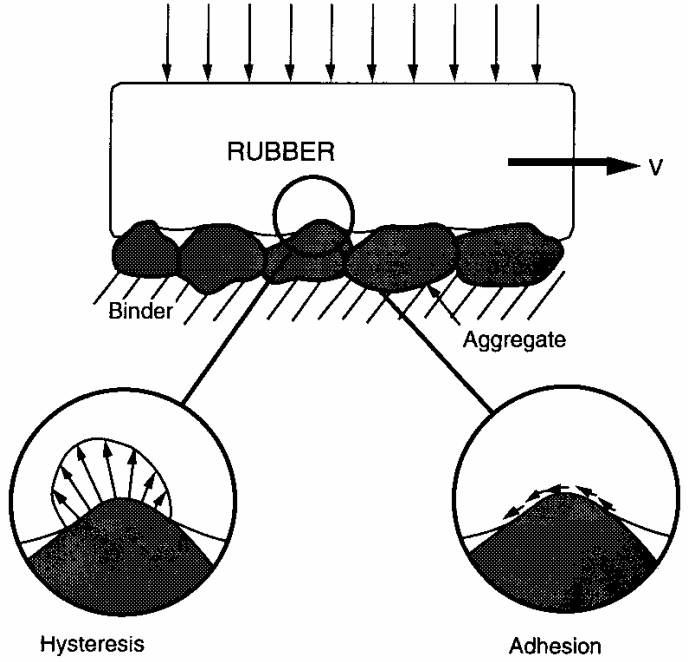

Fig. 10.5 Mechanisms of tire-road friction.

Surface adhesion arises from the intermolecular bonds between the rubber and the aggregate in the road surface. The adhesion component is the larger of the two mechanisms on dry roads, but is reduced substantially when the road surface is contaminated with water; hence, the loss of friction on wet roads.

The hysteresis mechanism represents energy loss in the rubber as it deforms when sliding over the aggregate in the road. Hysteresis friction is not so affected by water on the road surface, thus better wet traction is achieved with tires that have high-hysteresis rubber in the tread. Both adhesion and hysteresis friction depend on some small amount of slip occurring at the tire-road interface.

TRACTIVE PROPERTIES

Under acceleration and braking, additional slip is observed as a result of the deformation of the rubber elements in the tire tread as they deflect to develop and sustain the friction force. Figure 10.6 illustrates the deformation mechanism in the contact patch under braking conditions.

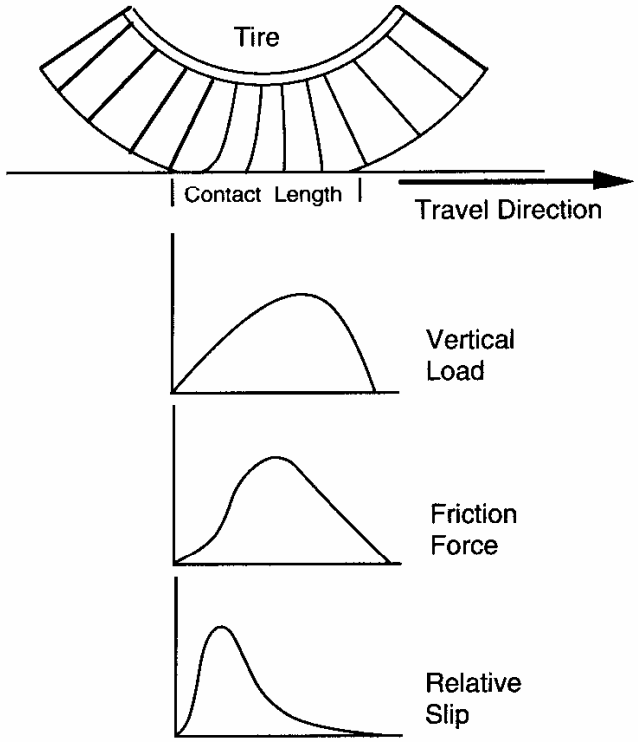

Fig. 10.6 Braking deformation in the contact patch.

As the tread elements first enter the contact patch they cannot develop a friction force because of their compliance—they must bend to sustain a force. This can happen only if the tire is moving faster than the circumference of the tread. As the tread element proceeds back through the contact patch its deflection builds up concurrently with vertical load and it develops even more friction force. However, approaching the rear of the contact patch the load diminishes and there comes a point where the tread element begins to slip noticeably on the surface such that the friction force drops off, reaching zero as it leaves the road.

Thus acceleration and braking forces are generated by producing a differential between the tire rolling speed and its speed of travel. The consequence is production of slip in the contact patch. Slip is defined non-dimensionally, as a percentage of the forward speed, as:

$$\text{Slip}\ (\%) = \left(1 - \frac{r\,\omega}{V}\right) \times 100 \qquad (10\text{-}1)$$

where:

r = Tire effective rolling radius
ω = Wheel angular velocity
V = Forward velocity

Under typical braking conditions the longitudinal force produced by a tire will vary with slip as shown in Figure 10.7. As slip is applied (e.g., by brake application) the friction force rises with slip along an initial slope that defines a longitudinal stiffness property of the tire. In general, this property is not directly critical to braking performance, except at the detailed level of the design of anti-lock systems where the cycling efficiency may be affected by this property. Longitudinal stiffness tends to be low when the tire is new and has full tread depth, increasing as the tire wears. For the same reasons, rib-type treads produce a higher stiffness than lug (traction) tires.

On a dry road, when the slip approaches approximately 15-20 percent, the friction force will reach a maximum (typically in the range of 70 to 90 percent of the load) as the majority of tread elements are worked most effectively without significant slip. Beyond this point friction force begins to drop off as the slip region in the rear of the contact patch extends further forward. The force continues to diminish as the tire goes to lockup (100% slip).

Performance on slippery roads is qualitatively similar to dry roads, differing primarily in the peak level of friction force that can be achieved. Since

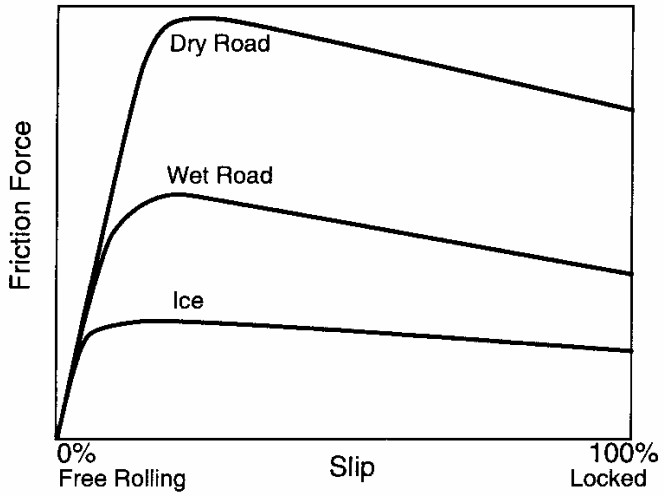

Fig. 10.7 Brake force versus slip.

the initial rate at which friction force builds up with slip is dependent on tire stiffness properties, the initial slope is the same. On wet roads the peak friction force will typically be in the range of 25 to 50 percent of the vertical load. On ice-covered roads the peak friction will be only 10 to 15 percent of the vertical load and will be reached at only a few percent slip. A part of the treachery of driving on ice is that not only is the friction level low, but the tire is very quick to brake through its maximum friction level.

For purposes of characterizing the traction properties of tires it is common to refer to the coefficient of friction (traction force divided by load) at the peak and slide conditions. These are referred to as μ_p and μ_s. The peak and slide coefficients will be dependent on a number of variables.

Vertical Load

Increasing vertical load is known categorically to reduce friction coefficients under both wet and dry conditions [7]. That is, as load increases, the peak and slide friction forces do not increase proportionately. Typically, in the vicinity of a tire's rated load, both coefficients will decrease on the order of 0.01 for a 10% increase in load. The general range of the coefficients of friction for passenger-car tires on dry roads as a function of load is shown in Figure 10.8.

Truck tires generally exhibit lower coefficient values because of their higher unit loading in the contact patch and different tread rubber compounds.

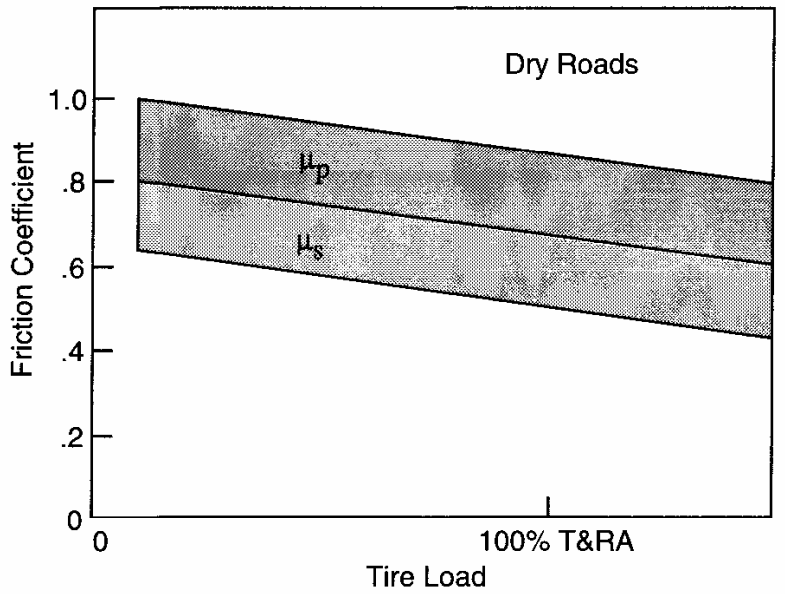

Fig. 10.8 Typical variation of friction coefficient with tire load.

Inflation Pressure

On dry roads, peak and slide coefficients are only mildly affected by inflation pressure. On wet surfaces, inflation pressure increases are known to significantly improve both coefficients.

Surface Friction

The road surface and its condition have a direct effect on the friction coefficient that can be achieved. Strictly speaking, a tire alone does not have a coefficient of friction; it is only the tire-road friction pair that has friction properties. But in the interest of characterizing the relative friction qualities of road surfaces, the highway community has developed a test method in which a "standard" tire is dragged at lockup over the surface.

This method has been standardized by the American Society for Testing and Materials as ASTM Standard Method E-274 using an ASTM Standard E-501 test tire [8]. Equipment for making these measurements is generically referred to as a "skid tester." The testers are typically configured as a trailer pulled behind a light truck with the capability to brake one wheel of the trailer while measuring the friction force and load. The ratio of friction force to load is a coefficient of friction, which is typically less than 1. For convenience, the coefficient is multiplied by 100 and given the name Skid Number. Thus the Skid Number of 81, which is specified for dry surfaces in government braking regulations, means that the surface should exhibit a 0.81 coefficient of friction when measured with the ASTM E-274 test method. Most clean, dry roads have a Skid Number close to this value.

Skid testers also have the capability to distribute water in front of the locked wheel in a controlled fashion, such that a wet road skid number can be measured. The 30 Skid Number specification for wet road friction in government braking regulations then means that the surface should exhibit a 0.3 coefficient of friction when measured with the ASTM E-274 method under wet conditions. Bituminous asphalt roads with smooth, polished aggregate generally fall in this range when lightly wetted. Portland Cement concrete road surfaces with good texture will have a higher wet Skid Number, in the range of 45 to 50. Road surfaces coated with a bitumen material like driveway sealer (e.g., Jennite) will have Skid Numbers in the range of 20 to 25.

Speed

On dry roads, both peak and slide coefficients decrease with velocity as illustrated in Figure 10.9. Under wet conditions, even greater speed sensitivity prevails because of the difficulty of displacing water in the contact patch at high speeds. When the speed and water film thickness are sufficient, the tire tread will lift from the road creating a condition known as hydroplaning.

Relevance to Vehicle Performance

Longitudinal traction properties are the properties of the tire/vehicle system that determine braking performance and stopping distance. The peak coefficient, μ_p, determines the limit for braking when the wheels do not lock up. Because of the weight transfer during deceleration, all wheels cannot be brought to the peak traction condition except by careful design of the braking system so as to proportion the front and rear braking forces in accordance with

the prevailing loads under these dynamic conditions. In situations where one or more wheels lock up, the sliding coefficient of friction, μ_s, determines the braking contributions from those wheels. Since it is practically impossible to design a conventional braking system that can achieve exact proportioning under all conditions of load, center of gravity location, and road condition, it is inevitable that the driver will experience occasions of lockup. Therefore, the sliding coefficient of friction is an important tire performance property. With the use of anti-lock braking systems (ABS) the brake system maintains the wheels near the peak of the traction curve and does not allow lockup. Thus with ABS the dominant tire performance parameter is the peak coefficient.

Longitudinal traction properties may also determine limiting acceleration or hill-climbing performance of a vehicle. Again, the peak coefficient is of primary importance and can be effectively utilized by the skilled driver or a traction control system. The sliding coefficient is only related in an uncontrolled attempt at acceleration. Even then the sliding coefficient of friction (defined for the wheels-locked condition) is only an approximate indicator of the traction level that can be achieved when uncontrolled wheel spin occurs.

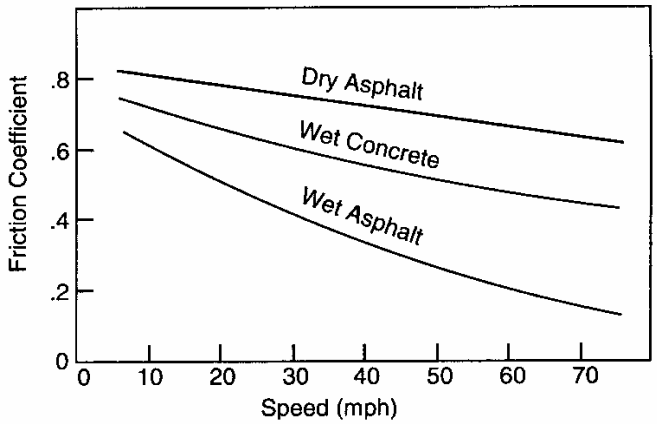

Fig. 10.9 Sliding coefficient as a function of speed on various surfaces.

CORNERING PROPERTIES

One of the very important functions of a tire is to develop the lateral forces necessary to control the direction of the vehicle, generate lateral acceleration in corners or for lane changes, and resist external forces such as wind gusts and

road cross-slope. These forces are generated either by lateral slip of the tire (slip angle), by lateral inclination (camber angle), or a combination of the two.

Slip Angle

When a rolling pneumatic tire is subjected to a lateral force, the tire will drift to the side. An angle will be created between the direction of tire heading and the direction of travel. This angle is known as slip angle. The mechanisms responsible can be appreciated by considering the simplified illustration of the tire's behavior as shown in Figure 10.10.

As the tire advances and tread elements come into contact with the road, they are undeflected from their normal position and therefore can sustain no lateral force. But as the tire advances further at the angle of its direction of travel, the tread elements remain in the position of their original contact with the road and are therefore deflected sideways with respect to the tire. By this process the lateral force builds up as the element moves rearward in the contact patch up to the point where the lateral force acting on the element overcomes the friction available and slip occurs. Thus the profile of the lateral force developed throughout the contact patch takes the form shown in Figure 10.10.

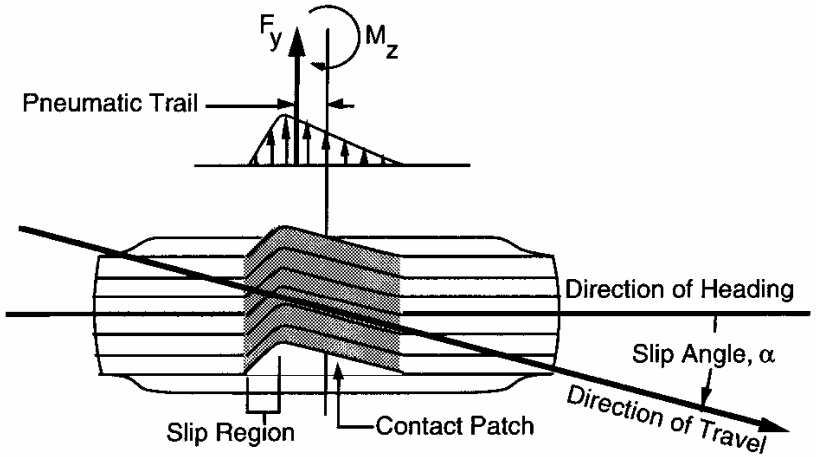

Fig. 10.10 Rolling tire deformation under a lateral force.

The integration of the forces over the contact patch yields the net lateral force with a point of action at the centroid. The asymmetry of the force buildup in the contact patch causes the force resultant to be positioned toward the rear of the contact patch by a distance known as the pneumatic trail. By SAE convention the lateral force is taken to act at the center of tire contact. At this position the net resultant is a lateral force, F_y, and an aligning moment, M_z. The magnitude of the aligning moment is equal to the lateral force times the pneumatic trail.

The mechanism is not an instantaneous phenomenon, but lags the actual development of slip angle because of the necessity of deflecting the tire sidewalls in the lateral direction [9]. The lag is closely related to the rotation of the tire, typically taking between one-half and one full revolution of the tire to effectively reach the steady-state force condition. The phenomenon is seen under low-speed test conditions when the tire is given a step change in steer angle. The lateral force response is then similar to that shown in Figure 10.11. With the change in steer angle the tire must roll through a half-turn or more for the lateral deflection and force to build up. This distance is often referred to as the "relaxation length." The time lag in development of lateral force necessarily depends on the speed of rotation of the tire. At a highway speed corresponding to 10 revolutions per second of the tire, the time lag will be only about 0.05 (1/20) second, which is imperceptible to many motorists. The effect, however, may be perceptible to expert drivers as a lag or sluggishness in turning response.

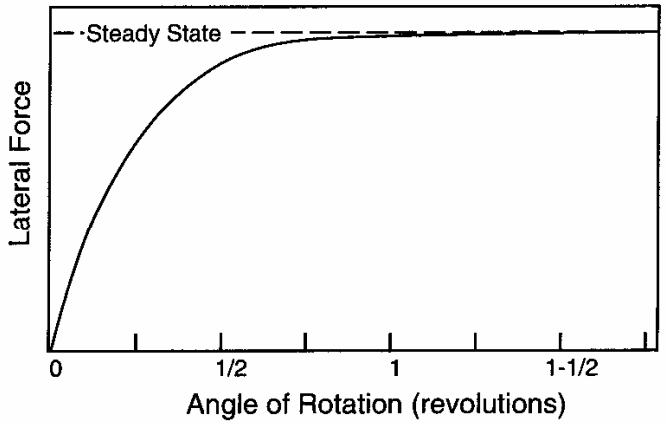

Fig. 10.11 Lateral force response to a step steer.

The relaxation effect is instrumental in the loss of cornering force when a tire operates on a rough road surface and experiences variations in its vertical load. When the load diminishes, slip occurs over the entire length of the contact patch and the tire sidewalls straighten out. The tire must then roll through its relaxation length in order to again build up a lateral force. As a consequence the tire is observed to have lower lateral force capability on rough roads. To achieve the best road-holding performance, the suspension should be designed to minimize tire load variations under rough road conditions.

Most commonly, the lateral force behavior of rolling tires is characterized only in the steady state (constant load and slip angle). Experimental measurements invariably exhibit the characteristic relationship to slip angle like that shown in Figure 10.12. When the slip angle is zero (the tire is pointed in its direction of travel) the lateral force is zero. With the first 5 to 10 degrees of slip angle the lateral force builds rapidly and linearly as the mechanisms shown in the previous figures take effect. In the range of 15 to 20 degrees the lateral force reaches a maximum (nominally equal to $\mu_p \cdot F_z$) and begins to diminish as the slip region grows in the contact area. At large angles it approaches the behavior of a locked wheel, which has a lateral force equal to the sine angle resultant of the sliding coefficient of friction, μ_s, times the vertical load, F_z.

A property of primary importance to the turning and stability behavior of a motor vehicle is the initial slope of the lateral force curve. The slope of the curve evaluated at zero slip angle is known as the "cornering stiffness," usually denoted by the symbol C_α.

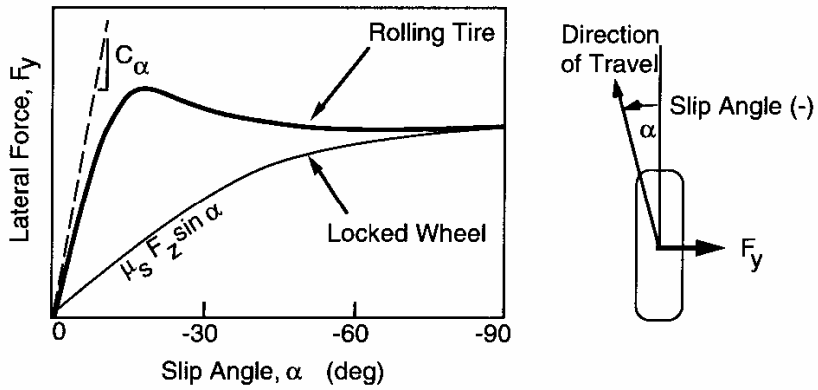

Fig. 10.12 Tire lateral force properties.

$$C_\alpha = -\left.\frac{\partial F_y}{\partial \alpha}\right|_{\alpha = 0} \qquad (10\text{-}2)$$

It should be noted that by the SAE convention, a positive slip angle produces a negative force (to the left) on the tire, implying that C_α must be negative. For that reason the slip angles in the figure are labeled with negative angles. In order to get around this problem, the SAE defines cornering stiffness as the negative of the slope, such that C_α takes on a positive value. A positive convention for C_α is used throughout this text.

Tire cornering properties as a function of load and slip angle are often shown in the form of a carpet plot as seen in Figure 10.13.

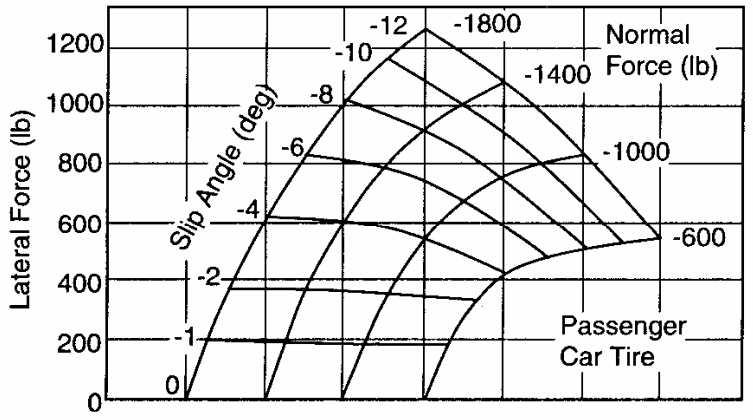

Fig. 10.13 Carpet plot of lateral force due to slip angle for a bias-ply tire.

The vertical axis is the scale of lateral force. The horizontal axis is a scale for both the slip angle and normal force. Note that both the slip angle and normal force are shown as negative numbers—negative slip angle produces a positive lateral force, and negative normal force is a positive vertical load. The load can be shown as positive if it is labeled "vertical load." The carpet plot provides a convenient format for mapping the properties of a tire.

The cornering stiffness is dependent on many variables. Tire size and type (radial versus bias construction), number of plies, cord angles, wheel width, and tread design are significant variables. For a given tire, the load and inflation pressure are the main variables.

Tire Type

On average, radial tires have a higher cornering stiffness than bias-ply tires. This is illustrated in Figure 10.14, which shows the cornering coefficient for the population of radial, bias, and bias-belted tires used on passenger cars.

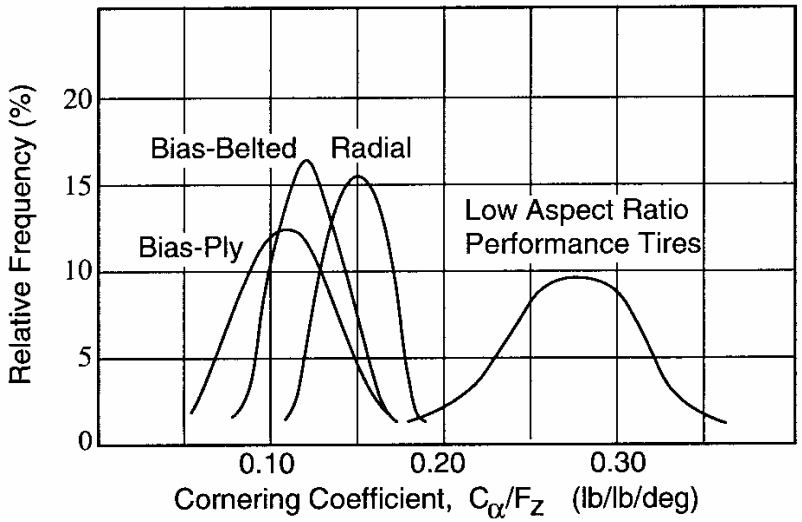

Fig. 10.14 Frequency distribution of cornering coefficient for passenger-car tires.

The cornering coefficient is the cornering stiffness normalized by the vertical load. For bias-ply tires the cornering coefficient is just about 0.12 lb/lb/deg. This means that at 1 degree of slip angle the average bias tire will produce a lateral force that is 10 percent of the vertical load. Radial tires of similar aspect ratio on average are stiffer, producing a lateral force at the same condition that is approximately 15 percent of the vertical load. As seen in Figure 10.14, the properties of bias-belted tires fall between those of radial and bias-ply tires. Although it is a general rule that radial tires have greater cornering stiffness than bias tires, as the distribution illustrates, the opposite may be true among some tires in the population.

By far one of the greatest influences on tire cornering properties is the aspect ratio—the ratio of section height to section width. For years the more

common passenger-car tires have had aspect ratios from 0.78 down to 0.70, yielding the cornering coefficient properties just described. The trends toward lower-aspect-ratio performance tires (0.60 and lower) on passenger cars have resulted in tires with much higher cornering coefficients. These tires with cornering coefficients in the range of 0.25 to 0.30 and above have given passenger cars much quicker and precise cornering behavior.

Load

Although cornering force at a given slip angle rises with vertical load on the tire, it does not rise proportionately with load. By and large, the maximum cornering force per unit load occurs at the lightest loads. The effect of load can be seen in Figure 10.15 as it affects both the cornering stiffness and the cornering coefficient. Characteristically, the stiffness versus load curve is always concave down, a property that has some significance to the understeer gradient.

Load also decreases the peak coefficient of friction that can be achieved in cornering. Over the range of 50 percent to 125 percent of rated load, the peak friction level may decrease by more than 20 percent.

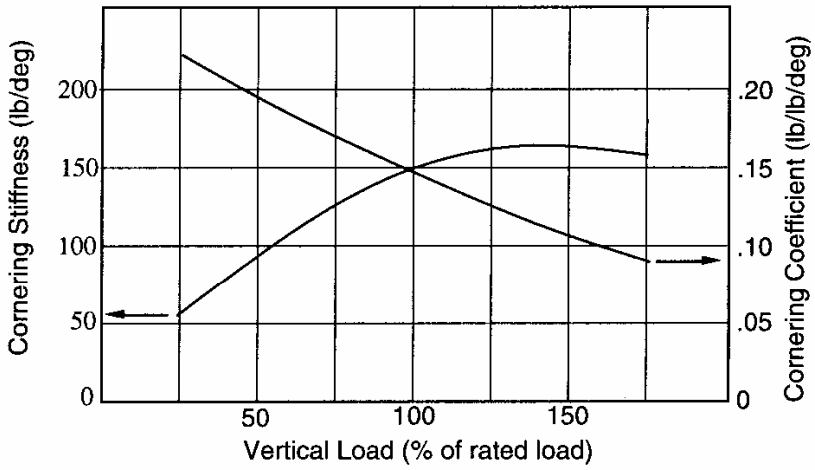

Fig. 10.15 Effect of load on cornering performance.

Inflation Pressure

Since inflation pressure increases carcass stiffness but reduces contact length, the net influence on cornering stiffness cannot be generalized across all types of tires [7]. It is generally accepted that increasing inflation pressure results in increasing cornering stiffness for passenger-car tires. Because of the monotonic and rather strong relationship between cornering stiffness and inflation pressure, it was common practice in the past to control the low-g directional behavior of passenger cars through the specification of different inflation pressures for front and rear tires. This practice is no longer common. In the case of truck tires, the influence of inflation pressure on cornering stiffness is varied and dependent on obscure sensitivities to details of the tire carcass design.

Inflation pressure also has a strong influence on the peak traction level that can be achieved under slip angle conditions. The pressure most influences lateral force production at high loads, and tires at reduced inflation pressures arrive at lateral force saturation at substantially higher values of slip angle.

Size and Width

For a given load condition, larger or wider tires exhibit a greater cornering stiffness. This effect is attributable to the contribution of carcass stiffness to cornering stiffness. Larger tires generally have a higher load capacity. Thus at the same load as a smaller tire, the larger tire will be operating at a lower percentage of its rated load and will effect greater cornering stiffness. For tires of the same nominal size but greater width (lower aspect ratio), that with the greater width will generally have a higher carcass stiffness resulting in greater cornering stiffness. The same effect can be accomplished by increasing rim width for a given tire.

Tread Design

The lateral compliance of the tread rubber acts as a series spring in the generation of lateral force response to slip angle; therefore, tread design has a potential influence on cornering stiffness. Among bias-ply tires it is generally recognized that snow-type tread designs produce lower cornering stiffness levels than do rib-tread designs. It is not clear that this trend holds true for radial tires. At best one can only be confident that all other things being held fixed, changes in tread design producing a more open pattern with deeper grooves and

less support from one tread block or rib element to another will effect greater lateral compliance in the tread, and thus a reduction in cornering stiffness.

It is not known that sensitivities of cornering stiffness to tread compound have been demonstrated. Presumably, increases in durometer produce higher stiffness. Accordingly, one could expect a stiffness increase with rubber durometer, although the sensitivity would be expected to be small.

Other Factors

Velocity does not significantly affect cornering stiffness of tires in the normal range of highway speeds. This basic insensitivity is due to the kinematic nature of the mechanisms determining cornering stiffness. Surface properties also have little effect on cornering stiffness, as long as the surface itself is sufficiently rigid to react the shear forces without appreciable shear deflection of its own. This is also true of wet surfaces as well. The surface effects have their strongest influence on the peak traction that can be achieved in cornering under wet conditions. Harsh, gritty textures which can penetrate the water film provide much higher friction levels than smooth, polished surfaces.

Relevance to Vehicle Performance

Cornering stiffness is one of the primary variables affecting steady-state and transient cornering properties of vehicles in the normal driving regime. Understeer gradient, the characteristic commonly used to quantify turning behavior, is directly influenced by the balance of cornering stiffness on front and rear tires, as normalized by their loads. A higher relative cornering stiffness on the rear wheels is necessary to achieve understeer. Higher stiffness on the front wheels will produce oversteer, unless compensated by other factors, and results in a vehicle that has a critical speed above which it becomes unstable.

CAMBER THRUST

A second means of lateral force generation in a tire derives from rolling at a non-vertical orientation, the inclination angle being known as camber angle. With camber, a lateral force known as "camber thrust" is produced. The inclination angle is defined with respect to the perpendicular from the ground

plane, positive corresponding to an orientation with the top of the wheel tipped to the right when looking forward along its direction of travel. (Note that on a vehicle, positive camber occurs when the wheel leans outward at the top. Thus the direction of positive camber differs from side-to-side on a vehicle, and the relationship to a positive lateral force is complicated by that fact. For discussion it is sufficient to recognize that the force is always oriented in the direction the tire is inclined.)

As with slip angle the lateral force due to camber angle is characterized by the initial slope of the curve, termed the camber stiffness, C_γ, and is defined as in the equation:

$$C_\gamma = \left.\frac{\partial F_y}{\partial \gamma}\right|_{\gamma = 0} \tag{10-3}$$

In absolute value, the camber stiffness of a tire is typically in the range of 10 to 20 percent of the cornering stiffness. Figure 10.16 provides a carpet plot of lateral force as a function of camber and load for a typical passenger-car tire.

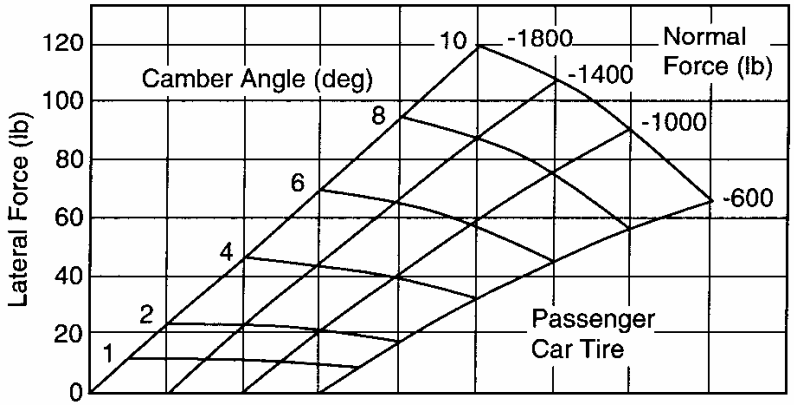

Fig. 10.16 Carpet plot of lateral force due to camber angle for a bias-ply tire.

Tire Type

Large changes in camber stiffness are known to accompany differences in tire construction. Figure 10.17 shows the camber stiffness distributions for a population of radial, bias, and bias-belted tires. The camber stiffness for low-

aspect-ratio performance tires is in the same range as other radial tires shown. The stiffness for radial passenger-car tires is generally only about 40 to 50 percent of that for bias-ply tires.

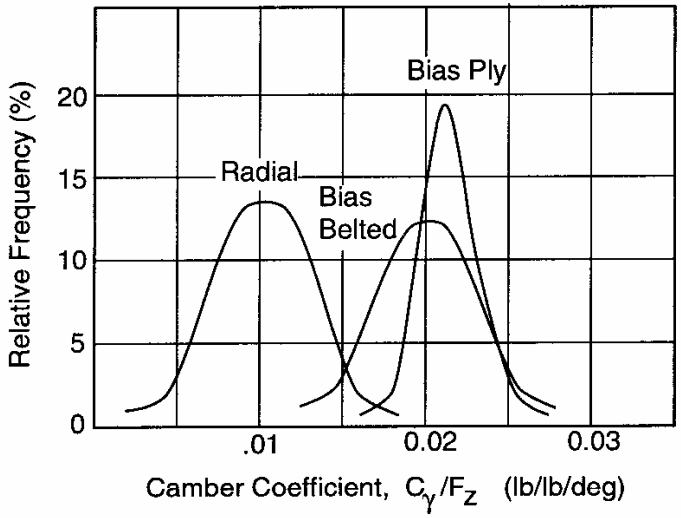

Fig. 10.17 Frequency distribution of camber coefficient for passenger-car tires.

The camber coefficient is a particularly important tire property with regard to how a tire responds to surface discontinuities oriented along the direction of travel, such as ruts in the wheelpath, faulting between lanes, shoulder dropoffs, railroad tracks, etc. When a vertically oriented tire operates on a surface with a cross-slope (such as the side of a rut in the wheelpath), the horizontal component of its load acts to push the wheel toward the lowest part of the rut as shown in Figure 10.18.

The lateral force per unit load is:

$$\frac{F_y}{W} = \sin \gamma' \cong \gamma' \tag{10-4}$$

where:

W = Weight on the tire
γ' = Inclination angle of the road surface

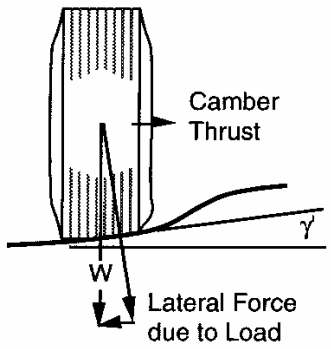

Fig. 10.18 Forces acting on a tire on a cross-slope surface.

Thus at 1 degree of surface cross-slope angle, a lateral force of 1/57.3 = 0.0175 lb/lb is produced in the "downhill" direction by the gravitational component. On the other hand, the camber thrust from the tire acts to push the tire "up" the slope in proportion to its camber coefficient. If the camber coefficient is greater than 0.0175 lb/lb/deg, the tire will try to climb out of the rut. If it is less it will tend to run down in the bottom of the rut and track in that position.

As seen from Figure 10.17, radial and bias-ply tires fall on opposite sides of that boundary, such that radial tires will tend to run in a rut, but bias-ply tires will tend to climb out of the rut. With the high proportion of radial tires being used on modern trucks, it has been postulated that this tracking tendency may be one of the primary factors responsible for the dual wheel ruts that frequently develop on asphalt roads.

Load

As indicated by the typical bias-ply car tire in Figure 10.16, camber stiffness is only slightly affected by vertical load in the vicinity of the design load. Over the range of 600 to 1800 lb load, the stiffness increases only about 20 percent.

Inflation Pressure

There is no general rule concerning the sensitivity of camber stiffness to inflation pressure. Limited data available tend to show some increase in

camber stiffness with inflation pressure for bias-ply tires (0.25 lb/deg per psi), whereas radial tires are relatively insensitive to changes in pressure [7].

Tread Design

Camber stiffness is sensitive to the gross compliance properties of the tire tread, increasing substantially with tread stiffness. Thus more compliant treads as is often true of open pattern snow traction treads will be lower in camber stiffness by factors of 20 to 40 percent. For the same reasons, camber stiffness will go up as the tread wears.

Other Factors

Surface texture has no effect on camber stiffness except as it affects the limiting level of the frictional coupling. Likewise, the presence of water on the surface should have no significant effect. Because of the mechanisms involved, speed should have negligible effect on camber stiffness, except at very high values where centrifugal loading may act to stiffen the tire.

Relevance to Vehicle Performance

Camber thrust is the primary cornering force by which motorcycles and other two-wheeled vehicles are controlled. On passenger cars and trucks, camber thrust contributes to understeer behavior, but normally as a secondary source. On vehicles with independent suspensions where significant camber angles may be achieved, this mechanism may contribute up to about 25 percent of the understeer gradient. On vehicles with solid axles, little camber can occur, such that its contribution to turning performance is even less.

ALIGNING MOMENT

Because the shear forces in the contact patch of a tire operating at a slip angle develop with their centroid aft of the tire centerline, an aligning moment or torque is generated about the vertical axis. Although this moment is only a small contribution to the total yaw moments on a vehicle, it contributes to reactions in the steering system which may have a more substantial effect. It should be noted that positive aligning moment always attempts to steer the tire in the direction it is traveling, thus it has a stabilizing influence on a vehicle.

Slip Angle

A typical carpet plot showing the influence of both slip angle and vertical load on aligning moment is given in Figure 10.19. Both radial and bias-ply tires possess aligning moment characteristics similar to those shown, although on average the moment is larger with radial tires. Typically, bias-ply tires will have an aligning moment coefficient (aligning moment per pound load) of approximately 0.033 ft-lb/lb/deg, whereas radial tires have a coefficient on the order of 0.043 ft-lb/lb/deg.

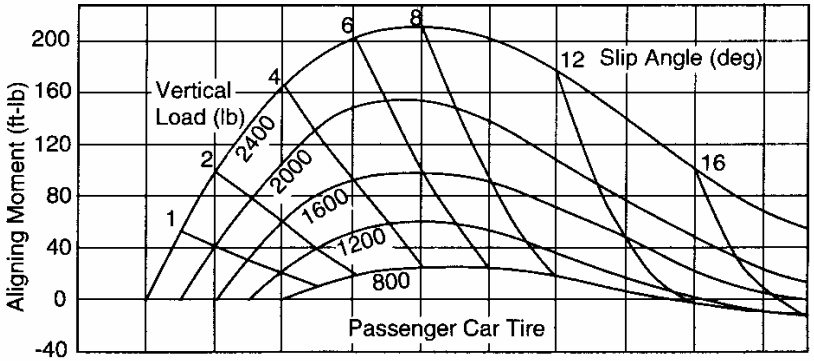

Fig. 10.19 Carpet plot of aligning moment versus slip angle and load.

The aligning moment is very sensitive to the size of the contact patch and the growth of the slip region. The shear stress and the torque arm responsible for the moment are both proportional to the distance from the tire center. Thus the major contributors to aligning moment are the tread elements at the extremes of the contact patch. The moment rises with the increasing shear forces up to about 8 degrees of slip angle. At greater angles, however, the growing slip region erodes the extremities and causes a decrease in the aligning moment. At very high slip angles the slip region advances forward such a distance that the aligning moment can actually become negative.

A high sensitivity to vertical load is seen in the plots. This sensitivity arises from the influence of contact area on the moment. Although doubling the load nominally doubles the contact area, all the increase in area occurs at the extreme regions of the contact patch—the regions that most affect the aligning moment. As a result, aligning moment increases in an accelerated fashion with load.

An aligning moment is also produced when a tire rolls at a non-zero camber angle. As shown in Figure 10.20, a bias-ply tire produces aligning moments due to camber which are on the order of 10 percent of the magnitude produced in response to slip angle. For radial tires, aligning moments due to camber angle are substantially lower than those measured for bias tires. The aligning moment coefficient (aligning moment per pound load) due to camber will be approximately 0.003 ft-lb/lb/deg for bias-ply tires, versus 0.001 ft-lb/lb/deg for radial tires. With regard to sensitivity to operating variables, as a general rule, influences which increase side force level also tend to increase aligning moment due to camber.

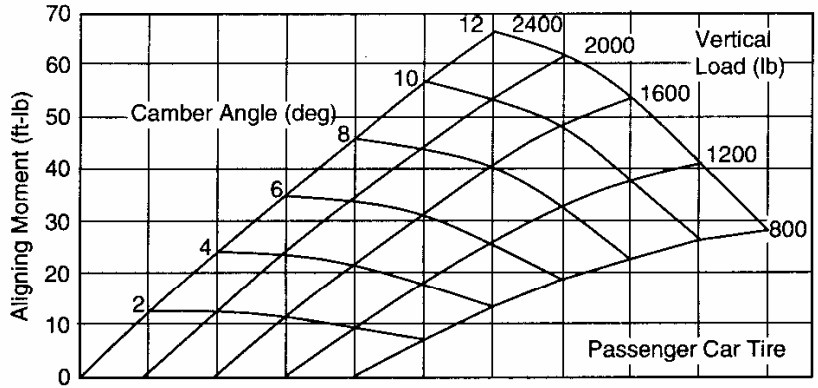

Fig. 10.20 Carpet plot of aligning moment versus camber angle and load.

Path Curvature

Whereas the aligning moments discussed thus far arise from a tire generating lateral force by traveling in a straight line with either slip or camber angle, aligning moments are also created when a tire is forced to roll on a curved path, even though not generating a lateral force. In effect, a torque must be applied to the tire about the vertical axis to force it to roll on a curve when under load. Such conditions are seen when a vehicle is turned at low speed, or when the wheels are steered with the vehicle stationary such that they are forced to roll on the small-radius path of the scrub radius. Little experimental data is available to quantify behavior under this condition, but Figure 10.21 shows the aligning moment generated by a truck tire on a dry road surface [10]. At zero radius, large torques are required to rotate the tire about the steer axis. The